DOI: 10.1070/RCR4665

Organic electroluminescent materials and devices emitting in UV and NIR regions

Anatoly P. Pushkarev,[a] Mikhail N. Bochkarev [a, b]

[a] G.A.Razuvaev Institute of Organometallic Chemistry, Russian Academy of Sciences ul. Tropinina 49, 603950 Nizhny Novgorod, Russian Federation
[b] National Research Lobachevsky State University of Nizhni Novgorod prosp. Gagarina 23, 603950 Nizhny Novgorod, Russian Federation

Literature data on organic materials capable of generating electroluminescence in the UV (200 – 400 nm) and near-IR (700 – 2000 nm) spectral ranges are summarized and systematized. Organic, organometallic and coordination compounds are considered. Comparative analysis of materials is performed, and the composition and operating characteristics of light-emitting diodes based on them and possible mechanisms of electroluminescence generation are discussed.
The bibliography includes 173 references.

Contents

I. Introduction 1338
II. UV emitters 1339
III. NIR emitters 1345
IV. Conclusion 1364

I. Introduction

Organic light-emitting diodes (OLEDs) represent one of the most striking examples of extremely rapid development of high technology. Just five years after the first prototype of an efficient light-emitting device was created in 1987 on the basis of the organic emitter aluminium tris(8-hydroxyquinolate) (**1**, Alq_3, see below),[1] Samsung company launched the production of full-colour OLED displays for mobile applications. Nowadays, Samsung Electronics and LG Electronics companies produce 55-inch OLED television sets. Philips and Panasonic have announced their intention to enter the market of OLED television. Research and development activities for the production of large-area and flexible thin-film light-emitting devices are close to completion. According to the prognosis of HIS company, the production of OLED TVs will reach 1 million units in 2016. All the above achievements pertain to full-colour or monochromic devices emitting in the visible range (400 – 700 nm). Technologies of production and functional materials for such devices have been well developed and described in hundreds of monographs,[2 – 7] reviews[8] and original papers. In contrast, organic materials and corresponding devices where OLEDs are capable of emitting light at a wavelength < 400 nm, *i.e.*, in the UV range, or > 700 nm, *i.e.*, in the IR range, have so far received much less attention of researchers and engineers. At the same time, possible applications of such electron-to-photon converters are as important and diverse as those of visible emitters. This review surveys data on luminescent materials used for producing UV and IR LEDs. Taking into account that blue emitters are in great demand, we have also considered compounds emitting beyond the UV range (below 430 nm). Molecular and polymeric organic compounds, organometallic and coordination compounds have been scrutinized, structures of electroluminophore molecules, configurations of heterojunctions, their operating characteristics and electroluminescence mechanisms have been described. The review covers papers published before March 2016.

A.P.Pushkarev. Candidate of Chemical Sciences, Researcher at the IOMC RAS.
Telephone: +7(813)435 – 4021, e-mail: pushkarev@iomc.ras.ru
Current research interests: photophysical and optoelectronic properties of main-group metal, transition metal and lanthanide complexes with organic ligands.
M.N.Bochkarev. Doctor of Chemical Sciences, Professor, Head of Laboratory at the same Institute, Professor at NNSU.
Telephone: +7(813)435 – 4021, e-mail: mboch@iomc.ras.ru
Current research interests: synthesis, reactivity and photophysical and optoelectronic properties of organometallic and coordination compounds of main-group and d and f transition metals; hyperbranched polymers.

Received 16 May 2016
Translation: G.A.Kirakosyan

© 2016 Russian Academy of Sciences and Turpion Ltd.

II. UV emitters

The key advantage of UV OLEDs, as compared with inorganic analogues, mercury gas discharge lamps and excimer lasers, is that they can give strong and uniform UV light from large surfaces, including flexible devices. Similar emitters can be used for excitation of visible fluorescence of phosphors in lighting devices and for carrying out photochemical reactions. UV-emitting molecular and polymeric compounds are applicable as luminescent labels with high contrast in biomedical assays. Electroluminescent materials emitting in the range 400 – 450 nm, *i.e.*, blue emitters, are equally in demand since they serve not only as a basic component of red-green-blue full-colour displays but also as a key luminescent component for generation of white light by mixing blue and orange colours. It should be noted that the number of compounds capable of emitting in the blue spectral range is significantly smaller and their stability is considerably lower than those for red and green phosphors. There is an even smaller number of organic materials with UV luminescence.

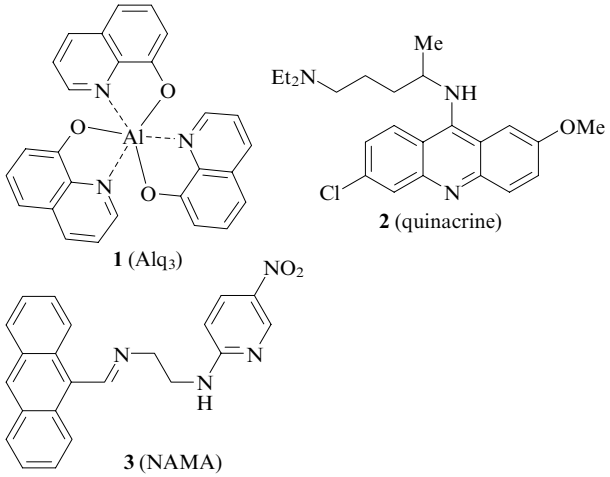
Organic UV/blue emitters (like visible-light- and UV-emitting phosphors) can be divided into two major groups differing in the mechanism of radiation generation. The first, more numerous, group comprises compounds where emission is due to electron transitions from singlet and triplet excited levels to the ground state. This type of luminescence is exhibited by organic compounds and organometallic derivatives of main-group and transition metals. Since the emission wavelength decreases with an increase in the energy difference (gap) between the highest occupied (HOMO) and lowest unoccupied (LUMO) molecular orbitals of the emitting compound, the gap width for all UV/blue emitters is larger than for green and red emitters. Owing to this specific feature, blue luminescent materials are often used as a matrix for visible-light phosphors that have higher HOMO and lower LUMO energies, which is essential for efficient excitation energy transfer from the matrix to the emitter molecule.

The second group of UV/blue emitters contains organic complexes of lanthanides: Ce^{III}, Gd^{III}, Eu^{II} and Yb^{II}. In this case, the luminescence centres are metal ions that emit light through intraatomic electronic f – f (Gd^{III}) or f – d transitions (Ce^{III}, Eu^{II}, Yb^{II}). All transitions are comparable in energy, being in the range 30 000 – 32 000 cm^{-1} (Refs 9 and 10). The photoluminescence (PL) and electroluminescence (EL) spectra often show, in addition to metal-centred luminescence bands, ligand luminescence bands, which can arise from intraligand $\pi - \pi^*$ transitions and formation of excimers, exciplexes, electroplexes (intra- or intermolecular associates of planar ligand moieties) or excited states with ligand-to-metal (LMCT) and metal-to-ligand (MLCT) charge transfer. For complexes of the above lanthanides, the ligand-centred emission bands usually have longer wavelengths than the f – f and f – d transitions, which is often responsible for their visible luminescence.

II.1. Organic fluorophores

Almost all compounds with fused aromatic rings exhibit fluorescence in the blue and near-UV regions, which is caused by the wide HOMO – LUMO gap (2.5 – 3.6 eV). The excimers and exciplexes formed by aromatic molecules give rise to emission bands in the same range. In most cases, the luminescence properties of these derivatives were studied upon photoexcitation in solutions. The electroluminescence of UV/blue organic phosphors has been studied to a much less extent, although it was precisely quinacrine (**2**) that was the first organic compound for which luminescence was detected when electric current was applied.[11]

Structures 1 – 3



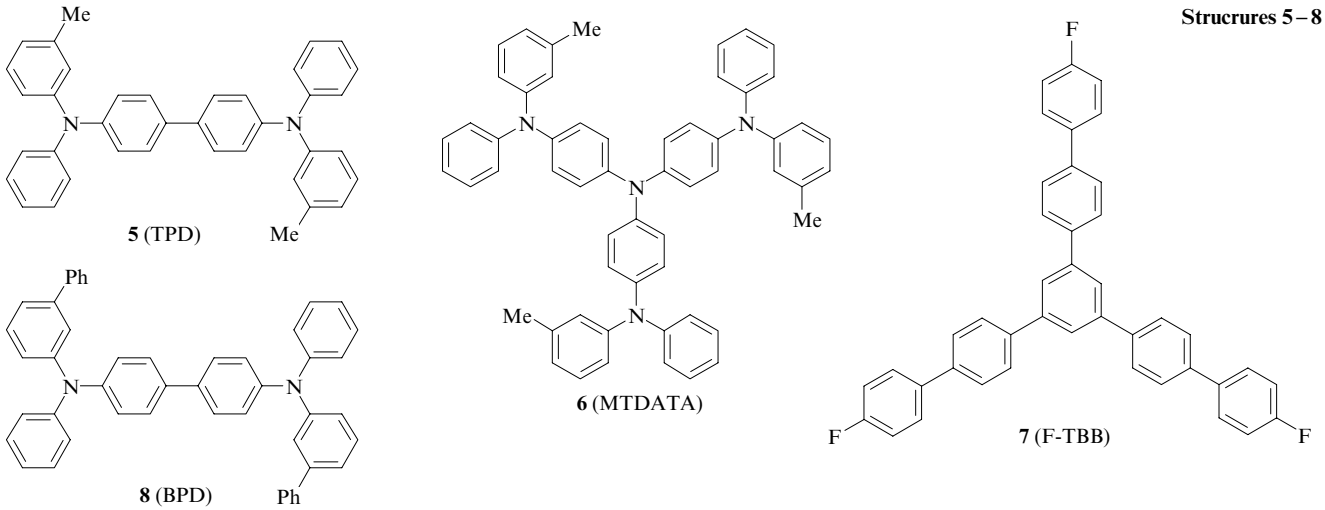
Polycyclic arylenes attracted no attention as efficient short-wavelength emitters for a long time; however, iminoanthracene **3** (NAMA) has been recently synthesized,† which, being incorporated in a four-layer diode, shows bright violet-blue emission with λ_{max} = 410 nm (CIE 1931 chromaticity diagram coordinates $x = 0.14$, $y = 0.10$).[12]

One of the first short-wavelength organic LEDs was designed by Romero *et al.*[13] on the basis of *N*,*N*′-diethyl-3,3′-bicarbazole (Cz-ethyl, **4**). The EL spectrum of the single-layer undoped device showed a band at 420 nm and a small shoulder at 650 nm. The luminescence intensity did not exceed 18 cd m^{-2} at a very low efficiency. The addition of the second emission layer composed of 9,9′-di-n-octyl-3,3′-bicarbazole-6,6′-dicarboxylic acid did not enhance the efficiency but led to the narrowing of the band. Strong blue emission with a wavelength of 400 – 420 nm was observed upon electroexcitation of 1,1′-biphenyl-4,4′-diamine derivatives, the best-known among them is *N*,*N*′-bis(3-methylphenyl)-*N*,*N*′-diphenyl-1,1′-biphenyl-4,4′-diamine (TPD, **5**), often used in OLED devices as a hole-conducting material. In the four-layer device ITO/MTDATA/TPD/F-TBB/Alq_3/MgAg (ITO/**6**/**5**/**7**/**1**/MgAg, ITO is indium tin oxide), this compound exhibited luminescence with λ_{max} = 404 nm and an intensity of 3960 cd m^{-2} at 15 V with a quantum yield of 1.4%.[14] The LED in which diamine **8** (BPD) is used instead of diamine **5** had almost the same characteristics.

Another 'classical' hole-conducting compound — dinaphthyldiamine **9** (NPB) — in combination with the hole-blocking layer based on perylene-3,4,9,10-tetracarboxylic diimide (PTCDI, **10**) was responsible for the UV luminescence of the PEDOT:PSS/NPB/PTCDI/TPBI/LiF/Al/Ag (**11**:**12**/**9**/**10**/**13**/LiF/Al/Ag) LED, the luminescence

† In the review, abbreviations of compounds from original works are used. It should be noted that sometimes quite different structures have the same designations (see, for example, compounds **20** and **39a**), whereas in other cases, the same compound has several designations (see compound **9**).

Strucrures 5 – 8



intensity at a wavelength of 370 nm being 300 W cm^{-2} at 13 V.[15]

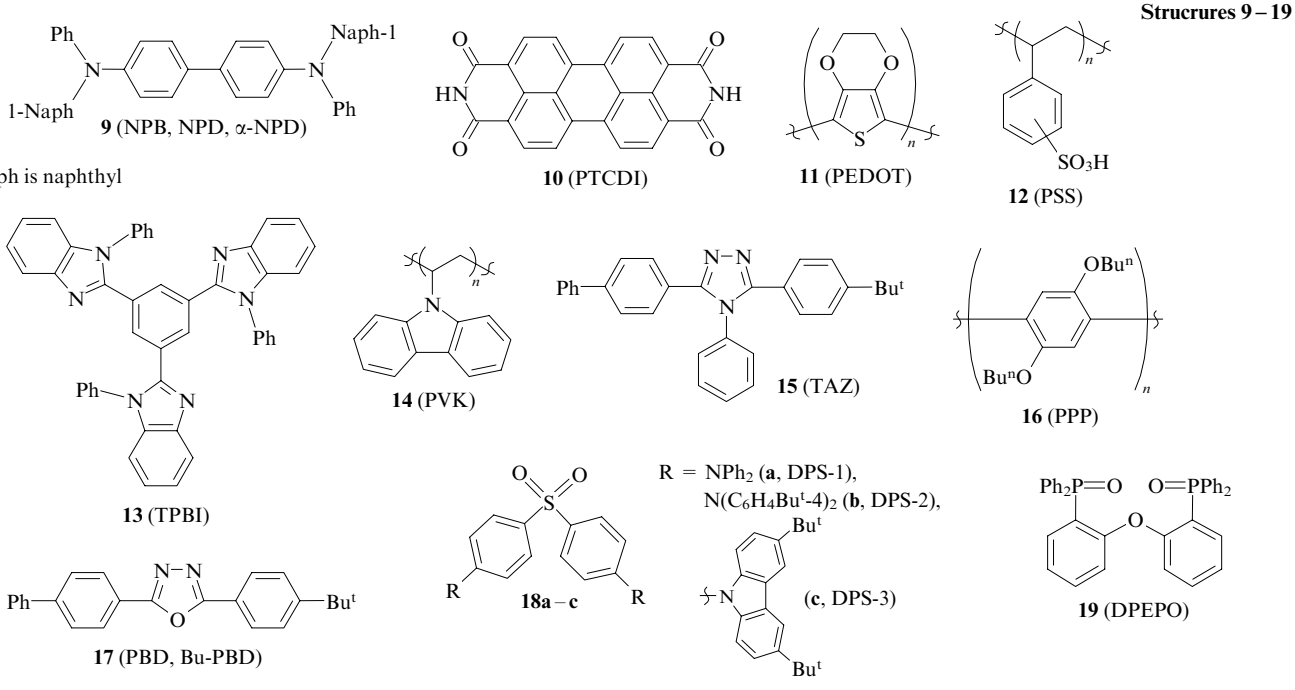
The frequently used matrix in doped LED cells is polyvinylcarbazole (PVK, **14**), which exhibits good charge-conducting properties.[7] However, this compound often generates its own short-wavelength luminescence, which is used in some LEDs for producing white light by mixing with orange or red and green emitters. The ITO/PVK/TAZ/Alq_3/Mg:Al (ITO/**14**/**15**/**1**/Mg:Al) cell exhibited luminescence at λ_{max} = 410 nm of moderate intensity, attributed by the authors to the EL of PVK excimers.[16]

One of the first LED cells with blue luminescence (λ_{max} = 424 nm) was designed on the basis of poly(2,5-dibutoxy-*p*-phenylene) (PPP, **16**).[17] The luminescent layer in this case consisted of three components: PPP (**16**), PBD (**17**) and PVK (**14**).

Diaryl sulfone phosphors DPS-1 – DPS-3 (**18a** – **c**) doped into the DPEPO (**19**) matrix exhibited stable blue luminescence for which the CIE coordinates (0.15, 0.07) are almost the same as the pure blue colour coordinates according to the NTSC scale (National Television Standards Committee, United States) (0.14, 0.08).[18] It is assumed that a narrow gap between the triplet and singlet levels in DPS-1 – DPS-3 (**18a** – **c**) molecules is responsible for thermally induced back intrasystem energy transfer $^3T_1 \rightarrow {}^1S_1$, which leads in the case of sulfone DPS-3 (**18c**) to the largest-ever quantum yield 9.9% among blue organic fluorophores. When carbazole moieties in compound DPS-3 are replaced by diphenylamine (DPS-1) or bis(*tert*-butylphenyl)amine (DPS-2) moieties, the LED characteristics somewhat decrease, while the emission wavelength remains almost unaltered (~420 nm).

Characteristics close to the highest-ever values for UV LEDs have been obtained by a team of Taiwan researchers.[19] Using bifluorene [T2 (**20**) and TB2 (**21**)] and bis(spirobifluorene) derivatives (B2, **22**) as emissive undoped materials in four-layer OLED devices, the authors observed short-wavelength luminescence at 374 nm with an efficiency of 3.6%. It is worth noting that the FL and EL spectra of these compounds are nearly the same (Fig. 1). Although the

Strucrures 9 – 19



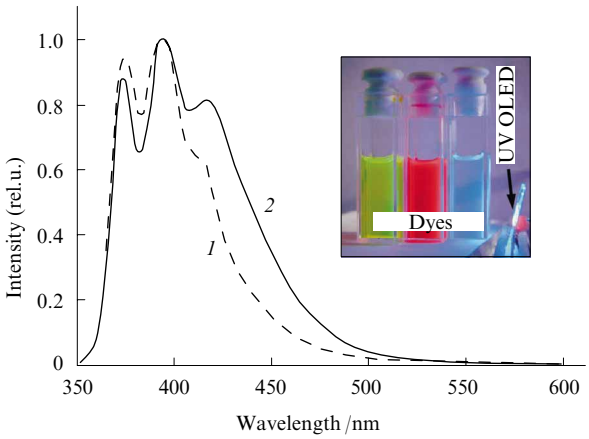


Figure 1. Photoluminescence (*1*) and electroluminescence (*2*) spectra of bis(spirobifluorene) B2 (**22**) and luminescence of organic dyes under excitation with the light of the OLED with the structure ITO/PEDOT:PSS/TCTA/B2/TPBI/LiF/Al/Ag (ITO/**11**:**12**/**23**/**22**/**13**/LiF/Al/Ag).[19]

emission is beyond the visible range, the light intensity is expressed in cd m^{-2}, which renders correct comparison with other UV-emitting devices difficult. Nevertheless, the achieved light intensity — almost 5000 cd m^{-2} — is evidence of the very high intensity, which is confirmed by the bright luminescence of the dyes irradiated with an LED based on derivative B2 (see Fig. 1).

In their search for efficient short-wavelength electroluminophores among oligomeric spirofluorenes, the same authors [20] have synthesized spirobifluorene trimers SSS (**24**) and TST (**25**).

New materials showed noticeably higher (as compared with B2 and T2) glass transition and decomposition temperatures, enhanced emission intensity and a certain hypsochromic shift of the emission band. These characteristics and a wide HOMO – LUMO gap made it possible to use the SSS and TST trimers as a matrix for iridium phosphors in design of red LEDs.

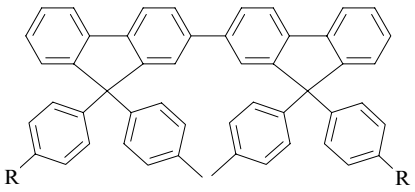
A series of analogous derivatives where the spirobifluorene moieties are combined through the benzene ring [compounds **26** (TSBFB), **27** (BSBFB)] or contain naphthyl substituents in the 2-position [compounds **28** (1SBFN), **29** (2SBFN)], have been synthesized by Tsutsui with co-workers by the Pd-catalyzed reaction of corresponding haloaryls with boron-substituted bifluorenes.[21] When used as emissive layers in the ITO/PEDOT:PSS/PVK/fluorene/PBD/LiF/Al (ITO/**11**:**12**/**14**/fluorene/**17**/LiF/Al, fluorene = **26** – **29**) LEDs, all these compounds exhibited UV luminescence in the range 382 – 395 nm. The emission intensity has not been reported; however, judging from the quantum yield (up to 2.9%), the devices were rather efficient.

As a development of this approach, French researchers [22] synthesized dispiroxanthene-indenofluorene **30** (DSX-IF) and determined its EL properties. In the three-layer diode ITO/PEDOT:PSS/NPB/DSX-IF/Ca (ITO/**11**:**12**/**9**/**30**/Ca), the compound showed blue emission with chromaticity coordinates 0.19, 0.08 and luminosity 2800 cd m^{-2}, which increased to 3800 cd m^{-2} when an electron-conducting layer made of 2,9-dimethyl-4,7-diphenyl-1,10-phenanthroline (BCP, **31**) was introduced. The efficiency was as large as 1 cd A^{-1} and 0.3 lm W^{-1} (Ref. 1).

A series of efficient fluorophores emitting at 382 – 390 nm in methylene chloride were synthesized by modifying a 7-diphenylamino-9,9-diethylfluorene molecule with various alkyl and aryl substituents.[23] However, upon photo- and electroexcitation of solid samples, the emission band shifted to the range 440 – 480 nm, which is typical of many organic phosphors.

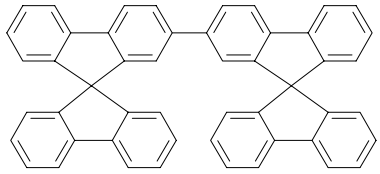
It is likely that the shortest wavelength emission among OLEDs was observed when studying the luminescence properties of modified poly(*m*-phenylene) **32** (EHO-PMP).[24] It has been found that the ITO/PEDOT:PSS/EHO-PMP/OXD-7/LiF/Al OLED (ITO/**11**:**12**/**32**/**33**/LiF/Al) has luminescence with a wavelength of 362 nm caused by the formation of exciplexes at the EHO-PMP/OXD-7 (**32**/**33**) interface, while the LED without the polyphenylene layer generates emission with the shortest-ever wavelength λ_{max} = 352 nm.[24] Unfortunately, the efficiency and other characteristics of these devices have not been reported. In an attempt to combine the high blue emission efficiency and

Structures 20 – 25

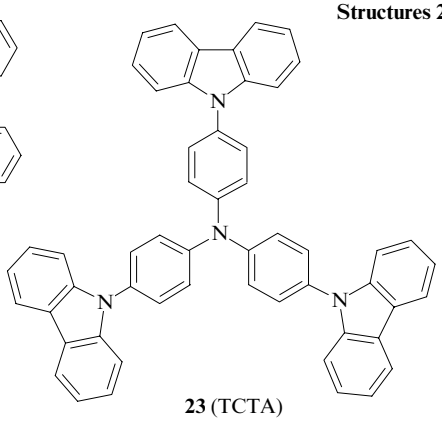


20 (T2), **21** (TB2)

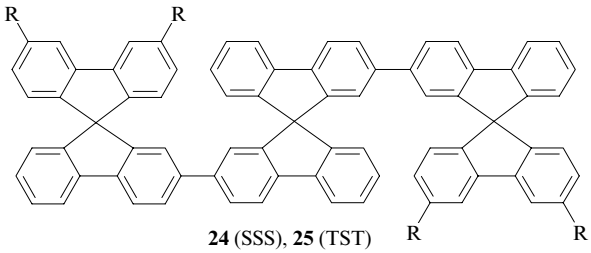
R = Me (**20**), Ph (**21**)



22 (B2)



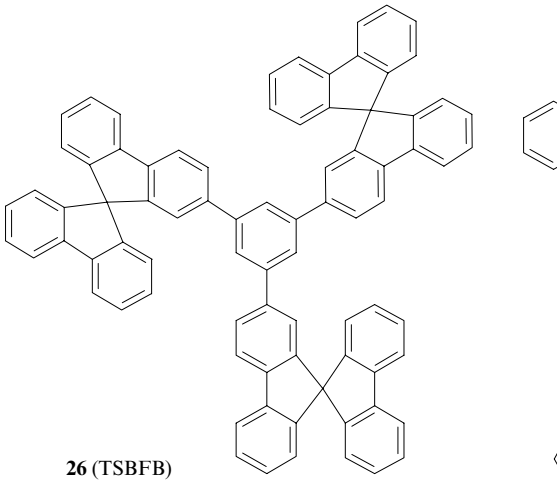
23 (TCTA)



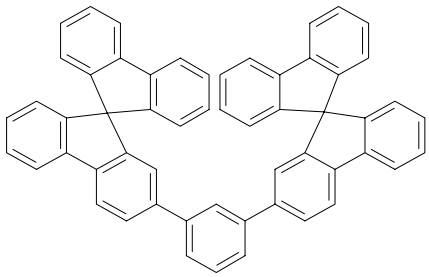
24 (SSS), **25** (TST)

R = H (**24**), Me (**25**)

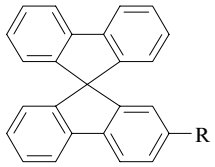
Structures 26 – 30, 32 – 34



26 (TSBFB)

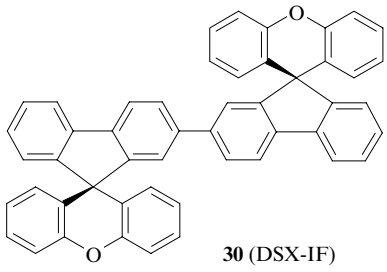


27 (BSBFB)

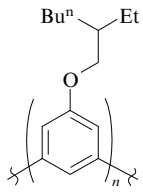


28 (1SBFN),
29 (2SBFN)

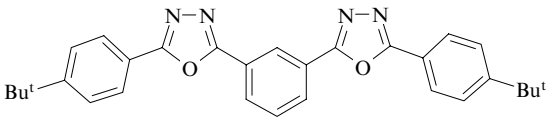
R = 1-Naph (**28**), 2-Naph (**29**)



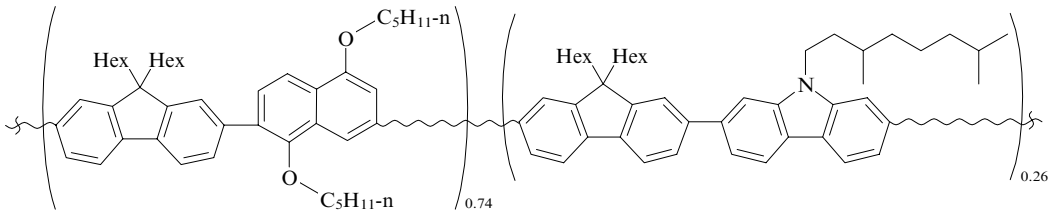
30 (DSX-IF)



32 (EHO-PMP)



33 (OXD-7, OXA)



Hex = n-C_6H_{13}

34 (NCF)

good charge transport properties in one molecule, Korean researchers [25] synthesized a terpolymer of dialkoxynaphthalene, *N*-alkylcarbazole and dialkylfluorene (NCF, **34**) by the Pd-catalyzed Suzuki reaction. The LED based on this material actually showed strong blue emission with chromaticity coordinates $x = 0.15$, $y = 0.12$ at 11 V.

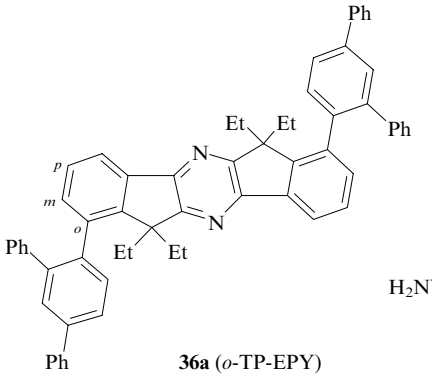
Varying the thickness of the hole-injecting layer composed of copper phthalocyanine (CuPc) and the thickness of the hole-blocking layer composed of 2-(4-biphenylyl)-5-(4-*tert*-butylphenyl)-1,3,4-oxadiazole (Bu-PBD, **17**), Zou *et al.*[26] observed the UV luminescence of 4,4′-bis(9-carbazolyl)biphenyl (CBP, **35**) at 390 nm with an external quantum yield of 1.25% and a radiance of 0.38 mW cm^{-2} at a current density of 10 mA cm^{-2}; at 100 mA cm^{-2}, the radiance increased to 1.2 mW cm^{-2}. The same fluorophore **35** (CBP) incorporated into another device gave EL with a wavelength of 405 nm.[27]

Diindenopyrazines **36a – c** (*o*-, *m*- and *p*-TP-EPY) showed violet emission upon electric excitation.[28] The emission wavelength shifted from 419 to 440 nm when going from the *ortho* to *para* and *meta* derivatives.

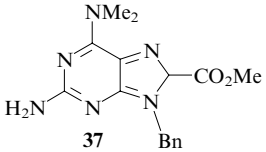
A new type of UV emission material — purine derivative **37** — was suggested by researchers from the University of Florida.[29] When used as a luminescent dopant (5%) into the *N*,*N*′-*m*-dicarbazolobenzene (mCP, **38**) layer in a three-layer OLED, this compound generated emission with a wavelength of 393 nm and an intensity of 5 mW cm^{-2}. It turns out that the emission wavelength and efficiency noticeably depend on the materials of the adjacent hole-transport and electron-transport layers.

The addition of several fluorenyl units to tris(carbazolo)triphenylamine (TCTA, **23**), often used as a hole-transporting material, leads to starburst oligomers T2, T3 and T4 (**39a – c**) displaying short-wavelength luminescence.[30] In a multilayer diode, these compounds displayed fluorescence with a wavelength of 408, 414 and 416 nm, respectively. The highest luminance 1014 cd m^{-2} at 11 V and luminous efficiency 0.47 cd A^{-1} were observed for oligomer **39a** ($n = 2$). It should be noted that in the PL spectra, the shortest wavelength emission is generated by amine with $n = 1$; however, its EL has not been studied. All tris(carbazolophenyl)amines have large HOMO – LUMO gaps at a

Structures 36a, 37

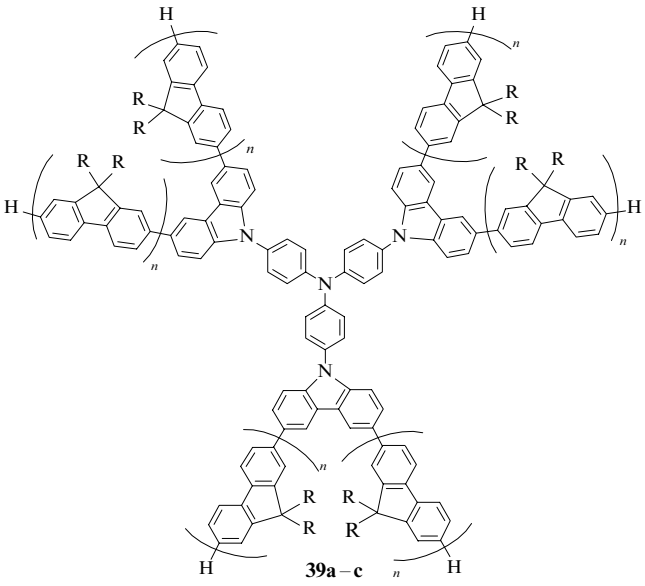


36a (*o*-TP-EPY)



37

Structures 39



39a – c

R = n-C_8H_{17}; n = 2 (**a**, T2), 3 (**b**, T3), 4 (**c**, T4)

rather high morphological and thermal stability. This fact makes it possible to use these compounds as a matrix for green emitters for the formation of host – guest systems. This prediction was supported by the OLED with the luminescent layer of **39a** doped with an osmium complex, which showed the luminance twice as high as that of an analogous diode based on a traditional host – guest system.[30]

Key operating characteristics of LEDs generating luminescence with a wavelength < 430 nm, are summarized in Table 1.

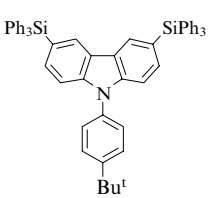
II.2. Organometallic and coordination emitters

A search for short-wavelength EL materials among organometallic derivatives was begun in the late 1990s when the first UV light-emitting diode was designed using poly(methylphenylsilane), which exhibited weak emission at λ = 353 nm.[31] Other poly(organosilanes) synthesized later also gave UV/blue luminescence, but very weak.[32–34] In particular, poly[bis(*p*-butylphenyl)silane] (PBPS, **43**) in the simplest single-layer cell ITO/PBPS/Al generated weak violet EL. The emission band maximum was at 406 nm.[35] The introduction of a cathode substrate electron-transport layer made of a PBD (**17**): PMMA or BND:PMMA mixture [BND is 2,5-bis(1-naphthyl)-1,3,4-oxadiazole, PMMA is

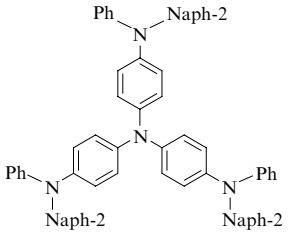
Table 1. Operating characteristics of OLED devices based on organic compounds emitting in the range below 430 nm.

Device	V_0 /V	λ_{max} /nm	R_{max}/ cd m^{-2}	η_{ext}^{EL} (%)	Ref.
CuPc/α-NPD/NAMA/Alq_3/LiF/Al (CuPc/**9**/**3**/**1**/LiF/Al)	–	410	7735 (10.4)	0.07	12
Cz-ethyl/Mg:Ag (**4**/Mg:Ag)	–	420	18	0.07	13
MTDATA/TPD/F-TBB/Alq_3/MgAg (**6**/**5**/**7**/**1**/MgAg)	–	404	3960 (15)	1.4	14
PVK/TAZ/Alq_3/Mg:Al (**14**/**15**/**1**/Mg:Al)	–	410	700 (14)	–	16
PPP:PBD:PVK/Al (**16**:**17**:**14**/Al)	20	424	50 (35)	1.2	17
PEDOT:PSS/NPB/PTCDI/TPBI/LiF/Al/Ag (**11**:**12**/**9**/**10**/**13**/LiF/Al/Ag)	4.5	370	0.3 [a] (13)	–	15
α-NPD/TCTA/CzSi/DPS-3:DPEPO/TPBI/LiF/Al (**9**/**23**/**40**/**18c**:**19**/**13**/LiF/Al)	–	423	–	9.9	18
PEDOT:PSS/TCTA/B2/TPBI/LiF/Al/Ag (**11**:**12**/**23**/**22**/**13**/LiF/Al/Ag)	2.5	374, 392	4890 (11)	3.6	19
PEDOT:PSS/TCTA/T2/TPBI/LiF/Al/Ag (**11**:**12**/**23**/**20**/**13**/LiF/Al/Ag)	2.5	402	3183 (11)	2.8	19
PEDOT:PSS/TCTA/TB2/TPBI/LiF/Al/Ag (**11**:**12**/**23**/**21**/**13**/LiF/Al/Ag)	2.5	374, 396	2894 (11)	2.7	19
PEDOT:PSS/PVK/2SBFN/PBD/LiF/Al (**11**:**12**/**14**/**29**/**17**/LiF/Al)	7	382	–	2.2	21
CuPc/CBP/Bu-PBD/CsF/Al (CuPc/**35**/**17**/CsF/Al)	6	390	380	1.25	26
MoO_3/CBP/Bath/Alq_3/LiF/Al (MoO_3)/**35**/Bath/**1**/LiF/Al)	–	405	–	–	27
2-TNATA/NPB/TCTA/*o*-TP-EPY/Alq_3/LiF/Al (**41**/**9**/**23**/**36a**/**1**/LiF/Al)	8.8	419	–	1.27	28
PEDOT:PSS/OXD-7/LiF/Al (**11**:**12**/**33**/LiF/Al)	–	352	–	–	24
PEDOT/NCF/LiF/Al (**11**/**34**/LiF/Al)	8.2	422	180	–	25
PEDOT:PSS/TCTA/SSS/TPBI/LiF/Al (**11**:**12**/**23**/**24**/**13**/LiF/Al)	3	373, 393	4020 (13.5)	2.6	20
PEDOT:PSS/TCTA/TST/TPBI/LiF/Al (**11**:**12**/**23**/**25**/**13**/LiF/Al)	3	373, 393	3600 (12)	3.1	20
TAPC/mCP:**37**/OXD-7/LiF/Al (**42**/**38**:**37**/**33**/LiF/Al)	3.2	393	5 [a] (16)	1.6	29
PEDOT:PSS/T2/F-TBB/Alq_3/LiF/Al (**11**:**12**/**39a**/**7**/**1**/LiF/Al)	5	408	625 (15)	1.4	30
PEDOT:PSS / NPB/DSX-IF/BCP/Ca (**11**:**12**/**9**/**30**/**31**/Ca)	10	414, 435	3800 (12.5)	–	22

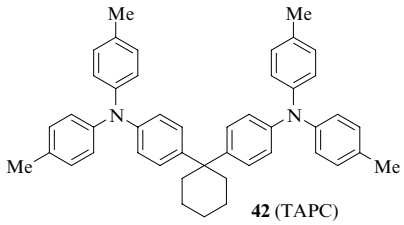
Note. CzSi = **40**, Bath is 4,7-diphenyl-1,10-phenanthroline, 2-TNATA = **41**, TAPC = **42**. Here and in Tables 2 – 4, the anode is indium tin oxide (ITO); V_0 is switch-on voltage; R_{max} is maximum EL radiance, the voltage at a given intensity (V) is parenthesized; η_{ext}^{EL} is external quantum yield.
[a] In mW cm^{-2}.



40 (CzSi)



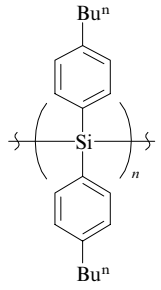
41 (2-TNATA)



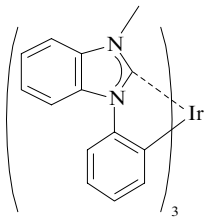
42 (TAPC)

poly(methyl methacrylate)] did not change the emission wavelength but increased twice the efficiency of the device.[36]

Structures 43, 44



43 (PBPS)



44 (Ir(pmb)$_3$)

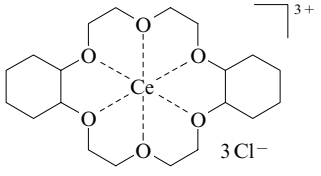
One of a few UV-emitting OLEDs based on d-transition metal complexes has been fabricated using tris(2-methyl-3-phenylbenzimidazolyl)iridium [Ir(pmb)$_3$, **44**] doped into a *p*-bis(triphenylsilyl)benzene (UGH2) matrix as an emitter.[37] It is worth noting that in the ITO/NPD/Ir(ppz)$_3$/Ir(pmb)$_3$:UGH2/BCP/LiF/Al [ITO/**9**/Ir(ppz)$_3$/**44**:UGH2/**31**/LiF/Al] OLED device, also an iridium complex — tris(1-phenylpyrazolyl)iridium [Ir(ppz)$_3$] — was used as the electron-blocking layer. The facial and meridional isomers of the Ir(pmb)$_3$ complex displayed emission at 389 and 395 nm, respectively; the efficiency of the latter was noticeably higher (5.8% against 2.6%).

As already mentioned, a special place among short-wavelength phosphors is held by some lanthanide complexes able to generate at room temperature metal-centred luminescence due to f – f or f – d transitions. The former (f – f) luminescence was detected only for gadolinium compounds. The $^6P_{7/2}$ resonance level (31 940 cm^{-1}) of Gd^{3+} ion, corresponding to emission at 312 nm,[10] is considerably higher in energy than the triplet level of the vast majority of organic ligands. As a result, such ligands cannot act as sensitizers and provide the metal-centred luminescence of gadolinium complexes. An exception are polycarboxylate anions,[38] including 1,1,4,7,7-diethylenetriaminepentaacetate widely used as a contrast reagent in magnetic resonance imaging.[39] These ligands do not contain π-conjugates groups absorbing at wavelengths > 260 nm and, hence, do not prevent the photoexcitation of gadolinium at 275 nm and subsequent emission at 312 nm caused by the f – f transition $^6P_{7/2} \rightarrow {}^8S_{7/2}$. Electroluminescence of carboxylates has not been studied.

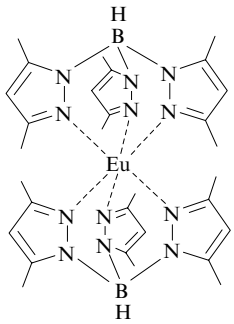
All the other lanthanide UV emitters (Ce^{3+}, Eu^{2+}, Yb^{2+}) generate emission due to f – d transitions. For two compounds, not only photo- but also electroluminescence was observed. One of them — cerium trichloride complex with dicyclohexano-18-crown-6 **45** — in a three-layer cell ITO/CuPc/**45**:CBP/Bu-PBD/LiF/Al (CBP = **35**, Bu-PBD = **17**) exhibited UV emission at λ = 376 nm.[40] The radiance power was as large as 13 W cm^{-2} at 22 V. It is worth noting that a 3% **45**:CBP mixture was used in the device, since the single-component layer of the cerium complex did not exhibit sufficient conductivity. Inasmuch as the PL of complex **45** turned out to be twice as large as that of free $CeCl_3$, the authors have suggested that crown ether sensitizes the cerium luminescence through excitation energy transfer from the singlet level to the excited 5d level of the Ce^{3+} ion, so that emission occurs due to the allowed 5d – 4f transition.

The second lanthanide complex exhibiting short-wavelength luminescence caused by a d – f transition is bis[tris(dimethylpyrazolyl)borato]europium (Eu1, **46**), synthesized by Shipley *et al.*[41] by the reaction of europium diiodide with potassium tris(pyrazolyl)borate. The PL spectrum of the complex shows two bands: a strong band at 597 nm and a weak band at 430 nm. The former has been assigned to the LMCT state and the latter, to the d – f transition in the Eu^{2+} ion. Sublimability of complex **46** in vacuum, uncommon for divalent lanthanide compounds, made it possible to fabricate the ITO/TPD/Eu1/TAZ/Al OLED device (ITO/**5**/**46**/**15**/Al), which showed orange luminescence with moderate luminance (10 cd m^{-2} at 20 V, η_{ext}^{EL} = 0.01%); the spectrum turned out to be similar to the PL spectrum of the EuI_2 salt.

Structures 45, 46



45



46 (Eu1)

Although the band at 430 nm in the spectrum is weak, this device deserves attention as a first example of an organic LED based on a divalent lanthanide complex.

Attempts to synthesize lanthanide complexes with polyfluorinated β-diketonate and alkoxide ligands for fabrication of UV OLED devices have been unsuccessful.[42, 43] Complexes have been synthesized, including Ce^{III}, Gd^{III}, Eu^{II} and Yb^{II} isopropoxides, *tert*-butoxides and hexafluoroisopropoxides, the europium and cerium compounds exhibiting the expected UV luminescence; however, their low thermal and hydrolytic stability has prevented the fabrication of diode cells.

Analysis of the above data demonstrates that hydrocarbons containing no metal atoms represent the major part of short-wavelength organic electrophosphors. Similar compounds have been used in design of devices with the shortest-ever wavelength (352 nm)[24] and the highest quantum efficiency (9.9%)[18] and luminescence intensity in the violet (7735 cd m^{-2})[12] and UV (5 mW cm^{-2})[29] ranges recorded to date. It is likely that these values are not limiting and can be improved by optimizing devices and using new materials. A special challenge is to synthesize phosphors emitting in a shorter wavelength UV range. The question arises whether there is an in-principle limit on the luminescence wavelength of organic emitters. For lanthanide complexes generating metal-centred emission, this limit is evident since it is determined by the highest-lying resonance level of the metal (the $^6P_{7/2}$ level of Gd^{3+} ion); however, for pure organic compounds or d-metal complexes, this question is still open. The shift of emission band in such emitters toward vacuum UV can be achieved by increasing the HOMO – LUMO gap (mainly, by lowering the LUMO

level);[44] however, taking into account the infinite diversity of organic compounds, it is difficult to determine the limiting gap width.

III. NIR emitters

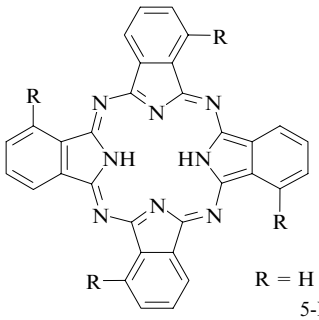
As compared with the materials and devices emitting in the short-wavelength range of electromagnetic spectrum, organic compounds generating emission in the near-IR range (NIR, 700 – 2500 nm) have been studied in much more detail. Great interest in these compounds is caused by wide possibilities of their practical application, including telecommunication (for transmission of a signal by fibre lines, wavelengths of 1310 and 1550 nm), wireless communication, sensors, probes, night vision devices, targeting devices, security systems, watermarks on banknotes, documents, *etc*. Recent special interest is related to the use of NIR-emitting materials in biomedicine, which is primarily caused by the transparency of biological tissues to NIR light with a wavelength of 650 – 900 nm (the so-called transparency window where radiation penetrates tissue to a depth up to 1.5 cm).[45] In addition, since the natural luminescence of biological fluids and tissues in the IR range is extremely low, NIR-emitting phosphors have essential advantages for use as biomarkers of the damaged cells and drugs and for visualization of internal organs. These biomedical applications are based on photoexcitation of materials, which is beyond the scope of this review; however, general mechanisms and principles of PL and EL justify their mention. Yet another extremely important application of materials absorbing and emitting in the NIR range, which promises significant progress, is noteworthy: this is solar power generation. As is known, ~70% of solar radiation incident on Earth's surface is within the IR range and is almost not used by modern silicon-based solar cells.

III.1. Organic compounds

III.1.a. Molecular compounds

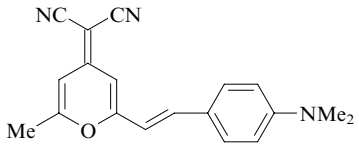
IR electroluminescence of organic derivatives was discovered in 1996 by Fujii *et al*.[46] for phthalocyanine (H_2Pc, **47a**) in a single-layer cell composed of ITO/H_2Pc/Mg:In. The EL spectrum of the device showed two peaks at 480 and 950 nm, which were assigned to the Soret B and Q bands, respectively. Later the same research team[47] studied the EL characteristics of devices based on phthalocyanine doped with 6-(4-dimethylaminostyryl)-4-(dicyanomethylene)-2-methyl-4*H*-pyran (DCM, **48**). Since the absorption spectrum of DCM overlaps with the B emission band of phthalocyanine, while the Q band overlaps with the emission band of DCM, efficient energy transfer occurs in the system from the B emission band of H_2Pc to the Q band. Thus, the authors designed a device producing only NIR emission. Further studies of the EL of phthalocyanine (H_2Pc) have shown that emission at 950 nm corresponds to the emission of aggregates formed *via* π – π interactions of conjugated systems of neighbouring molecules; in its turn, aggregation leads to significant quenching of the luminescence of the shorter wavelength Q band. The introduction of peripheral phenoxyl substituents induces steric hindrance that prevents intermolecular π – π interactions and, thus, reduces the probability of aggregation. Owing to this effect, the OLED cell with the tetra(2-isopropyl-5-methylphenoxy)phthalocyanine (Tetra-H_2Pc, **47b**) emitting layer produced NIR emission (λ_{max} = 910 nm) with intensity exceeding 14 times the emission of unsubstituted H_2Pc (**47a**).[48] It was found that the decrease in the Tetra-H_2Pc concentration in the Alq_3 (**1**) and PVK (**14**) matrices from 40% to 1% resulted in a short-wavelength shift of the long-wavelength emission band (to 730 nm), which is caused by predominant luminescence of non-associated molecules. Another compound — 4-methoxyphenoxy-substituted phthalocyanine **47c** (MPPc) — in the PVK matrix showed broadband electroluminescence (with λ_{max} = 891 nm), which suits well for information transfer through fibre-optic communication lines in the first transparency window.[49]

Structures 47, 48



47a – c

R = H (**a**, H_2Pc);
5-Me-2-Pr^{i}C$_6$H$_3$O (**b**, Tetra-H_2Pc);
4-MeOC$_6$H$_4$O (**c**, MPPc)

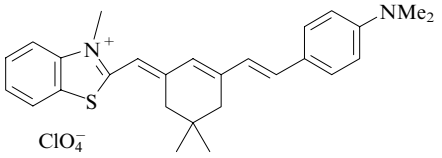


48 (DCM)

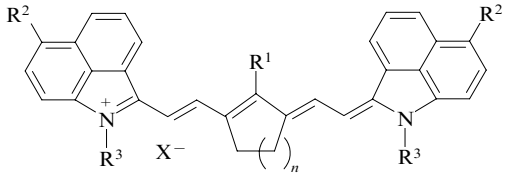
Some dyes exhibit strong NIR photoluminescence with high quantum yield (η_{ext}^{PL}); in most cases, this is a necessary (but not sufficient) criterion for potential NIR electrophosphors. Suzuki *et al*.[50 – 52] have designed devices containing a three-component host – guest system where the matrix was PVK (**14**), and guest molecules were PBD (**17**) (electron-transporting material) and ionic dye molecules. An LED based on 2-[6-(4-dimethylaminophenyl)-2,4-neopentylene-1,3,5-hexatrienyl]-3-methylbenzothiazolium perchlorate (LDS821, **49**) exhibited NIR luminescence with a maximum at 805 nm and efficiency η_{ext}^{EL} = 0.015%.[50] Longer wavelength EL was shown by IR1050 (**50a**) (1113 nm), IR1051 (**50b**) (990, 1116 nm), IR1061 (**51**) (1125 nm) and SO447 (**50c**) (1088 nm) dyes; however, the maximum efficiency of the corresponding devices was low, being η_{ext}^{EL} = 0.036% for the device with the SO447 dye.[51, 52]

Other cyanine dyes are also able to generate NIR emission. Among them are 3,3′-bis(γ-sulfopropyl)-4,5,4′,5′-dibenzo-12-methyl-11,13-(β,β-dimethyltrimethylene)thiacarbocyanine betaine triethylammonium salt (TCC, **52**) and dye ADS830AT (**53**).[53, 54] It has been found that the TCC molecules introduced into a matrix of polyamide **54** (PI), form J-aggregates exhibiting electroluminescence with λ_{max} = 815 nm and η_{ext}^{EL} = 0.01%.[53] The EL spectrum of compound ADS830AT (**53**) doped into the PVK matrix is a single band with a maximum at 890 nm.[54] The formation of J-aggregate responsible for the long-wavelength shift of the EL spectrum and for the quenching of emission of the monomer of squarine dye M (**55**), similar to cyanine dyes, has been described in detail for doped LEDs with the super yellow poly(phenylene vinylene) matrix (SY-PPV, **56**).[55] As

Structures 49 – 56

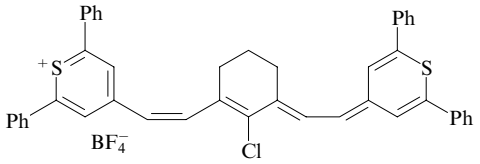


49 (LDS821)

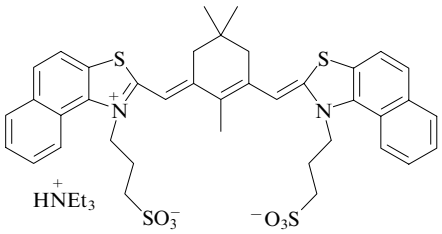


50a – c

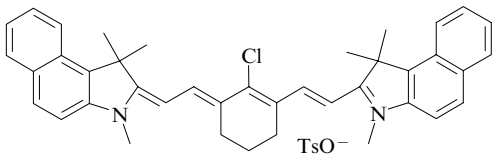
Compound	Code	R^1	R^2	R^3	n	X
a	IR1050	Cl	Cl	Bu^n	2	BF_4
b	IR1051	Ph	Cl	Et	1	BF_4
c	S0447	Cl	H	n-$C_{12}H_{25}$	2	Cl



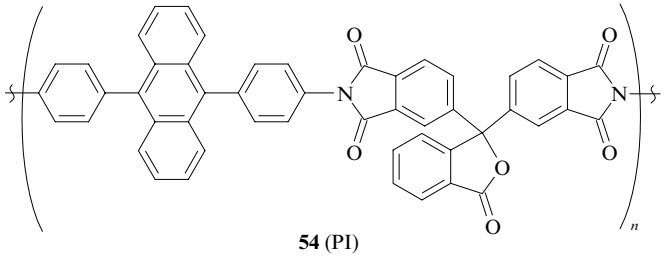
51 (IR1061)



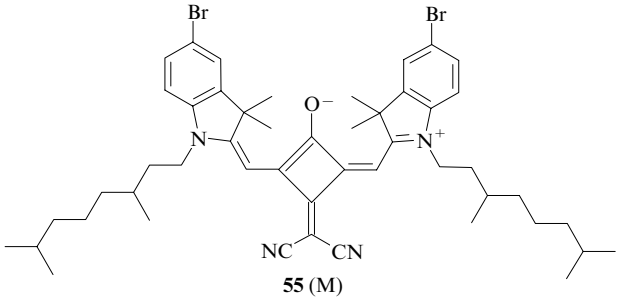
52 (TCC)



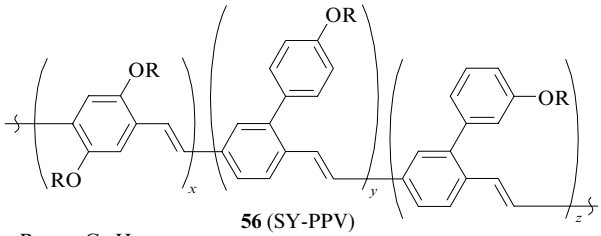
53 (ADS830AT) (Ts = 4-$MeC_6H_4SO_2$)



54 (PI)



55 (M)



56 (SY-PPV)

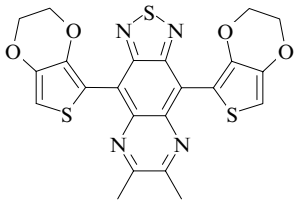
R = n-$C_{10}H_{21}$

a result of Förster resonance energy transfer,[56] an increase in the dopant concentration from 0.05% to 0.2% led to the vanishing of the luminescence band of SY-PPV in the visible range and to generation of exclusively NIR emission (λ_{max} = 743 nm). The turn-on voltage of this OLED device was 2.5 V, and the efficiency did not exceed 0.25%.

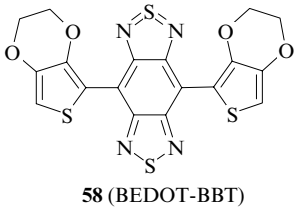
Promising emissive materials for NIR-emitting OLED devices are π-conjugated compounds containing both donor and acceptor moieties in the same molecule. The LUMO – HOMO energy gap for such compounds depends on the donor (D) and acceptor (A) strength and can be decreased by selecting appropriate groups to <1.24 eV, which corresponds to the wavelength 1000 nm. Noteworthy is the same luminescence intensity of these compounds in both solutions and the solid state, which is desirable for materials intended for use in OLED devices.[57, 58] When studying the EL properties of donor – acceptor conjugated oligomers BEDOT-$TQMe_2$ (**57**) and BEDOT-BBT (**58**), Yang *et al.*[59] observed luminescence at 692 and 815 nm, respectively. The initial luminescence intensity and LED efficiency were later increased 2 – 3-fild by introducing, into the luminescent layers CBP:BEDOT-$TQMe_2$(BEDOT-BBT) [**35**:**57**(**58**)], iridium complex molecules (phosphorescent centres), which sensitized NIR emission.[60]

Thiadiazoloquinoxaline derivatives **59a – c** are also classified with phosphors of the D – π – A – π – D type.[61] The luminescence band of OLED cells with the emission layer made of Alq_3 (**1**) doped with these compounds shifts to the IR range by 30 – 50 nm with increasing the dopant concentration from 2% to 100%. The authors explain this fact by the strong polarization effect typical of similar compounds.[62] Among these compounds, the highest EL intensity (R_{max} = 1.8 mW cm^{-2}) has been achieved for an LED with dopant **59a** at 15 V. The same research team[63 – 65] has synthesized other NIR chromophores of the D – π – A – π – D type with acceptor benzobis(thiadiazole) (BBTD) or thiadiazoloquinoxaline (TQ) moieties (compounds **60 – 64**) emitting in the range from 700 to 1220 nm. Maximal operating characteristics for these compounds have been observed for the undoped OLED devices ITO/NPB/**60b**/BCP/Alq_3/LiF/Al (ITO/**9**/**60b**/**31**/**1**/LiF/Al) (R_{max} = 0.125 mW cm^{-2}, η_{ext}^{EL} = 0.28%)[64] and ITO/NPB/**62a**/TPBI/Alq_3/LiF/Al (ITO/**9**/**62a**/**13**/**1**/LiF/Al) (R_{max} = 1.83 mW cm^{-2}, η_{ext}^{EL} = 0.89%).[65] Chinese researchers[66] used compound PTZ-BZP (**64**), which contains the donor

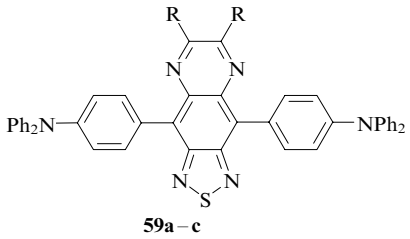
Structures 57 – 64



57 (BEDOT-TQMe$_2$)

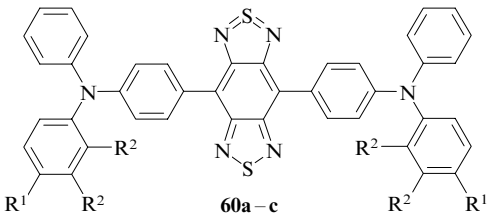


58 (BEDOT-BBT)



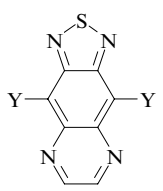
59a – c

R = H (**a**), Ph (**b**); R – R is biphenyl-2,2′-diyl (**c**)

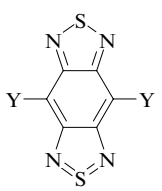


60a – c

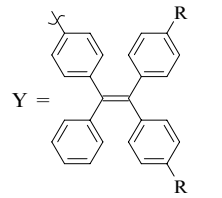
$R^1 = R^2 = H$ (**a**); R^1 = Me, R^2 = H (**b**);
R^1 = H, $R^2 – R^2$ is benzo (**c**)



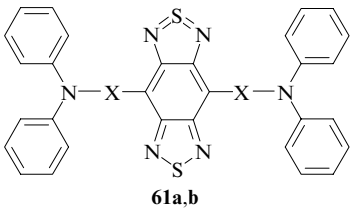
62a,**b**



63a,**b**

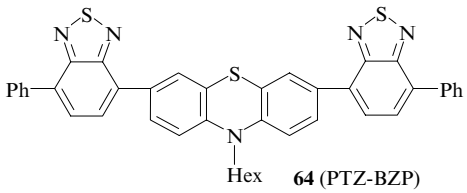


(R = H (**a**), OMe (**b**))



61a,**b**

X = (**a**), (**b**)



64 (PTZ-BZP)

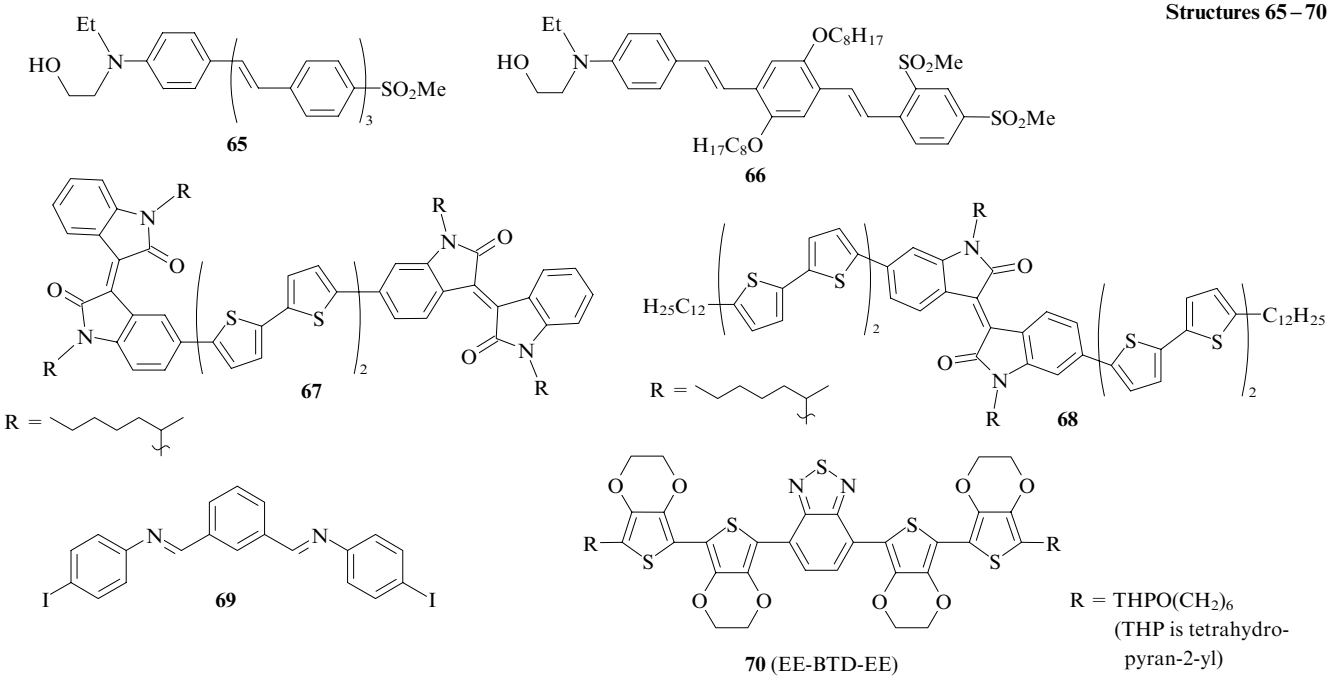
phenothiazine moiety and acceptor benzothiadiazole moieties, as an emission layer in an undoped OLED of the A – π – D – π – A type. This OLED demonstrated the external quantum efficiency of NIR emission of 1.54% (λ_{max} = 700 nm). It has been found that a fraction of excimers undergoing radiative recombination under electroexcitation is as large as 48% and considerably exceeds the limit of 25% in conventional fluorescent OLEDs owing to efficient intersystem crossing $^3T_3 \rightarrow {}^1S_1$.

III.1.b. Oligomeric compounds

In the course pf studying NIR electrophosphors, Iranian researchers [67 – 69] have synthesized oligomers exhibiting high emission and charge-transport characteristics. In particular, substituted distyrylstilbene **65**, containing the sulfone and amino groups in the 4-position of styryl moieties, showed a significant bathochromic shift of the absorption and luminescence band ($\Delta\lambda$ = 175 nm) as compared with an analogous distyrylbenzene derivative owing to the increase in the conjugation length. The polarizability of similar molecules can significantly change depending on the number of donor and acceptor groups located at different positions of styryl moieties. It has been shown that, in oligomer **66** with two sulfone groups and one amino group, intramolecular charge transfer is optimized owing to a decrease in the hyperpolarizability of the molecule.[70] The introduction of an extra sulfone group leads to the increase in the effective conjugation length of the oligomer and, as a result, reduces the HOMO – LUMO gap to 1.35 eV, while the bulky alkyl substituents in the *para*-positions of the central moiety hinder association. Multilayer OLED devices with the structure ITO/NPD/**65**(**66**)/BCP/Alq$_3$/LiF/Al [ITO/**9**/**65**(**66**)/**31**/**1**/LiF/Al] exhibited emission at 775 and 905 nm with maximal power efficiencies of 15.8 and 5.8 mW W^{-1}, respectively.[67] Higher power efficiencies (η_p = 16.7 and 6.6 mW W^{-1}) at longer emission wavelengths (λ_{max} = 900 and 1150 nm) have been observed for OLEDs with the emitting layer composed of Alq$_3$ doped with A – D – A- (compound **67**) or D – A – D-type (**68**) oligomers.[68] The NIR emission of compound **67** is caused by the formation of the common π-conjugated system involving two substituted isoindigo chromophores and connected by the oligothiophene spacer, whereas the acceptor component of isoindigo in derivative **68** links two donor oligothiophene moieties. The repulsion between 2-heptyl and dodecyl substituents is responsible for the almost planar geometry of molecules **67** and **68**, which facilitates the interaction of the π-systems of their donor and acceptor components. Yet another oligomer generating NIR EL in the structure of OLEDs is diiodo-substituted diimine **69**.[69] However, broadband emission of this compound at λ_{max} = 770 nm is observed not only in the NIR but also in the visible range (500 – 700 nm).

The most striking example of the influence of intramolecular donor – acceptor interactions on the optical characteristics of oligomers has been described by Ellinger *et al.*[71] Using thiophene, phenylene or 3,4-ethylenedioxythiophene units as donors along with benzothiadiazole (or its derivatives) units as acceptors, these researchers have synthesized ten compounds generating fluorescence with λ_{max} from 651 to 1088 nm depending on the number and strength of the donor and acceptor moieties in the oligomer. One of the products (EE-BTD-EE, **70**) has been selected for fab-

Structures 65 – 70



rication of polymeric EL devices with the poly[2-methoxy-5-(2-ethylhexyloxy)-1,4-phenylenevinylene] (MEH-PPV, **71**) or PVK (**14**) matrix. Measurements of radiance and voltage – current characteristics of the cells with the MEH-PPV:EE-BTD-EE layer have shown that an increase in the content of the oligomer in the polymeric matrix from 0% to 4% strongly deteriorates the LED efficiency: R_{max} decreases from 4.5 to 1.3 mW cm^{-2}, and η_{ext}^{EL} decreases from 0.87% to 0.28%. The weak efficiency of the diode has been explained by phase separation in a mixture of strongly polar EE-BTD-EE and weakly polar MEH-PPV, which leads to the formation of oligomeric aggregates quenching luminescence.

III.1.c. Polymeric compounds

As compared with molecular compounds, the electroluminescent properties of NIR-emitting polymers have been much less studied. Although the latter have a significant advantage — the possibility of fabrication of OLED devices on flexible substrates and of large area through solution processing (spin coating, spray deposition, vertical dipping, ink-jet printing). The first communication on the polymeric NIR LED based on poly[3-(4-octylphenyl)thiophene] (POPT, **72**) was reported by Berggren *et al.*[72] The emission peak (λ_{max} = 670 nm) of the ITO/POPT/Ca/Al device shifted toward longer wavelengths (to 800 nm) depending on heat treatment temperature and duration of the polymer

Structures 72 – 75, 77 – 79

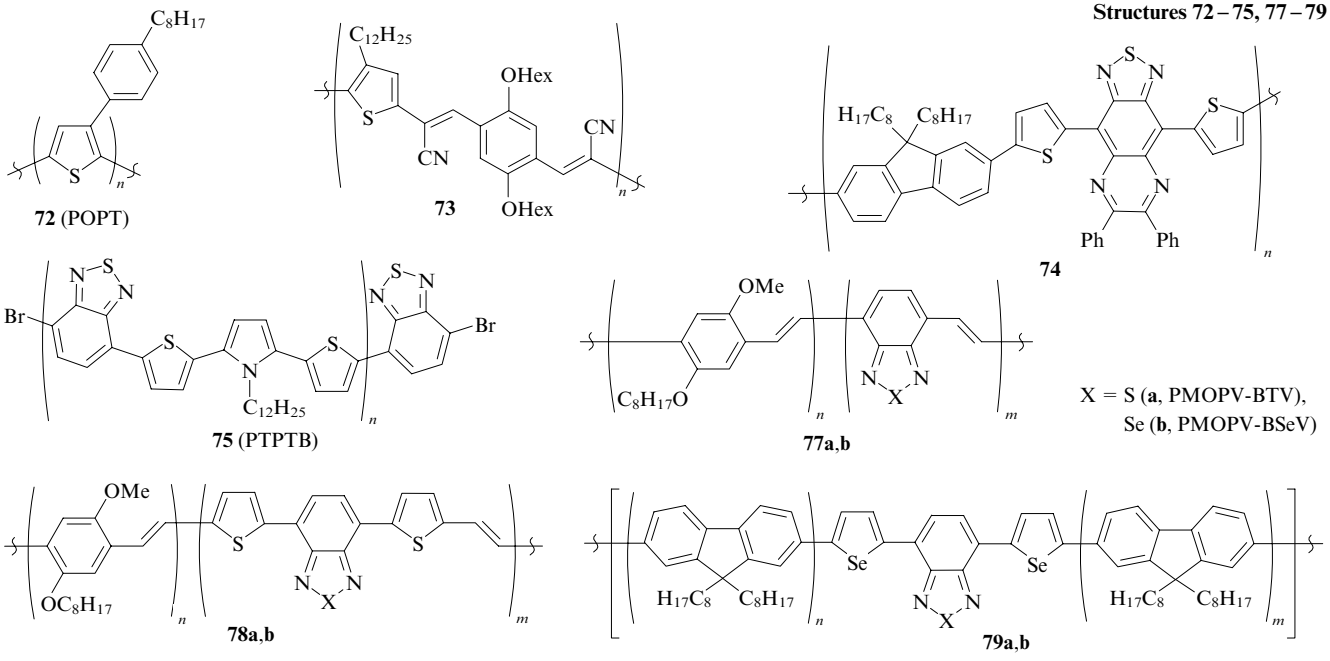


Table 2. Operating characteristics of IR-emitting OLED devices based on organic compounds.

Device	V_0 /V	λ_{max} /nm	R_{max} /mW cm^{-2}	η_{ext}^{EL} (%)	Ref.
H_2Pc/H_2Pc:DCM/Mg:In (**47a**/**47a**:**48**/Mg:In)	–	930	–	–	47
PVK:Tetra-H_2Pc/BCP/Alq_3/LiF/Al (**14**:**47b**/**31**/**1**/LiF/Al)	–	910	–	–	48
PVK:MPPc/BCP/Alq_3/Al (**14**:**47c**/**31**/**1**/Al)	–	891	–	–	49
PVK:PBD:LDS821/Al (**14**:**17**:**49**/Al)	7.0	805	–	0.015	50
PVK:PBD:IR1050/Al (**14**:**17**:**50a**/Al)	–	1113	–	–	52
PVK:PBD:IR1051/Al (**14**:**17**:**50b**/Al)	–	1116	–	–	52
PVK:PBD:IR1061/Al (**14**:**17**:**51**/Al)	–	1125	–	–	52
PVK:PBD:SO447/Al (**14**:**17**:**50c**/Al)	–	1088	–	0.036	52
PI:TCC(J-units)/Al (**53**:**52**(J-units)/Al)	–	815	–	0.01	53
PEDOT:PSS/PVK:ADS830AT/Al (**11**:**12**/**14**:**54**/Al)	9.0	890	0.36 (16)	0.015	54
PEDOT:PSS/SY-PPV:M/Ca/Al (**11**:**12**/**56**:**55**/Ca/Al)	2.5	743	–	0.25	55
α-NPD/Alq_3:BEDOT-$TQMe_2$/BCP/LiF/Al (**9**/**1**:**57**/**31**/LiF/Al)	2.7	692	6 (20)	1.6	59
α-NPD/CBP:Ir(ppy)$_3$, BEDOT-$TQMe_2$/BCP/LiF/Al [**9**/**35**:Ir(ppy)$_3$, **57**/**31**/LiF/Al]	3.4	692	19 (20)	3.1	60
α-NPD/Alq_3:BEDOT-BBT/BCP/LiF/Al (**9**/**1**:**58**/**31**/LiF/Al)	2.7	815	0.5 (20)	0.5	59
α-NPD/CBP:PQIr, BEDOT-BBT/BCP/LiF/Al (**9**/**35**:PQIr, **58**/**31**/LiF/Al)	3.4	815	2 (20)	1.5	60
MoO_3/NPB/Alq_3:**59a**/BCP/Alq_3/LiF/Al (MoO_3/**9**/**1**:**59a**/**31**/**1**/LiF/Al)	4.0	752	1.8 (15)	1.12	61
MoO_3/NPB/**59a**/BCP/Alq_3/LiF/Al (MoO_3/**9**/**59a**/**31**/**1**/LiF/Al)	5.8	784	0.007 (10)	0.02	61
MoO_3/NPB/Alq_3:**59b**/BCP/Alq_3/LiF/Al (MoO_3/**9**/**1**:**59b**/**31**/**1**/LiF/Al)	3.5	748	0.21 (8)	1.23	61
MoO_3/NPB/**59b**/BCP/Alq_3/LiF/Al (MoO_3/**9**/**59b**/**31**/**1**/LiF/Al)	4.1	788	0.015 (8)	0.03	61
MoO_3/NPB/Alq_3:**59c**/BCP/Alq_3/LiF/Al (MoO_3/**9**/**1**:**59c**/**31**/**1**/LiF/Al)	3.9	823	0.55 (15)	0.27	61
MoO_3/NPB/**59c**/BCP/Alq_3/LiF/Al (MoO_3/**9**/**59c**/**31**/**1**/LiF/Al)	4.5	870	0.006 (8)	0.02	61
MoO_3/NPB/**60a**/BCP/Alq_3/LiF/Al (MoO_3/**9**/**60a**/**31**/**1**/LiF/Al)	5.0	1050	0.025 (9.9)	0.08	64
MoO_3/NPB/**60b**/BCP/Alq_3/LiF/Al (MoO_3/**9**/**60b**/**31**/**1**/LiF/Al)	4.2	1080	0.125 (9.9)	0.28	64
MoO_3/NPB/**60c**/BCP/Alq_3/LiF/Al (MoO_3/**9**/**60c**/**31**/**1**/LiF/Al)	4.8	1050	0.06 (9.9)	0.12	64
MoO_3/NPB/**61a**/BCP/Alq_3/LiF/Al (MoO_3/**9**/**61a**/**31**/**1**/LiF/Al)	–	1220	–	–	64
MoO_3/NPB/Alq_3:**61b**/BAlq/LiF/Al (MoO_3/**9**/**1**:**61b**/BAlq/LiF/Al)	–	1115	–	–	63
MoO_3/NPB/**62a**/TPBI/Alq_3/LiF/Al (MoO_3/**9**/**62a**/**13**/**1**/LiF/Al)	5.5	706	1.83 (14)	0.89	65
MoO_3/NPB/**62b**/TPBI/Alq_3/LiF/Al (MoO_3/**9**/**62b**/**13**/**1**/LiF/Al)	4.6	749	0.99 (13.5)	0.29	65
MoO_3/NPB/**63a**/TPBI/Alq_3/LiF/Al (MoO_3/**9**/**63a**/**13**/**1**/LiF/Al)	4.5	802	1 (12.5)	0.43	65
MoO_3/NPB/**63b**/TPBI/Alq_3/LiF/Al (MoO_3/**9**/**63b**/**13**/**1**/LiF/Al)	4.4	864	0.63 (12.5)	0.2	65
PEDOT:PSS/NPB/TCTA/PTZ-BZP/TPBI/LiF/Al (**11**:**12**/**9**/**23**/**64**/**13**/LiF/Al)	–	700	780 [a]	1.54	66
NPD/**65**/BCP/Alq_3/LiF/Al (**9**/**65**/**31**/**1**/LiF/Al)	4.5	775	–	3.54	67
NPD/**66**/BCP/Alq_3/LiF/Al (**9**/**66**/**31**/**1**/LiF/Al)	4.5	910	–	1.32	67
CBP/Alq_3:**67**/HGH_2/Alq_3/LiF/Al (**35**/**1**:**67**/HGH_2/**1**/LiF/Al)	–	900	–	3.3	68
CBP/Alq_3:**68**/HGH_2/Alq_3/LiF/Al (**35**/**1**:**68**/HGH_2/**1**/LiF/Al)	–	1150	–	1.32	68
NPB/**69**/BCP/Alq_3/LiF/Al (**9**/**69**/**31**/**1**/LiF/Al)	2.3	761	–	1.9	69
MEH-PPV:EE-BTD-EE/LiF/Al (**71**:**70**/LiF/Al)	2	721	3.1 (14)	0.5	71
POPT/Ca/Al (**72**/Ca/Al)	1.8	800	–	0.3	72
73/Ca/Al	–	740	–	0.2	73
74/Ca/Al	1.1	970	–	0.04	74
PTPTB/LiF/Al (**75**/LiF/Al)	3	800	–	–	75
PEDOT:PSS/PMOPV-BTV5/Ba/Al (**11**:**12**/**77a**(5%)/Ba/Al)	–	702	19.4 [a] (8.6)	0.15	76
PEDOT:PSS/PMOPV-BTV30/Ba/Al (**11**:**12**/**77a**(30%)/Ba/Al)	–	724	1.66 [a] (5.2)	0.0047	76
PEDOT:PSS/PMOPV-BSeV1/Ba/Al (**11**:**12**/**77b**(1%)/Ba/Al)	–	705	21 [a] (11.4)	0.26	77
PEDOT:PSS/PMOPV-BSeV30/Ba/Al (**11**:**12**/**77b**(30%)/Ba/Al)	–	752	3 [a] (6.4)	0.02	77
PEDOT:PSS/PMOPV-DBTV1/Ba/Al (**11**:**12**/**78a**(1%)/Ba/Al)	–	715	62 [a] (6.4)	0.31	78
PEDOT:PSS/PMOPV-DBTV30/Ba/Al (**11**:**12**/**78a**(30%)/Ba/Al)	–	762	5 [a] (9.2)	0.04	78
PEDOT:PSS/PMOPV-TBSV1/Ba/Al (**11**:**12**/**78b**(1%)/Ba/Al)	–	763	3 [a] (11.8)	0.16	78
PEDOT:PSS/PMOPV-TBSV30/Ba/Al (**11**:**12**/**78b**(30%)/Ba/Al)	–	800	0.2 [a] (8.0)	0.01	78
PEDOT/PVK/PFO-SeBT30/Ba/Al (**11**/**14**/**79a**(30%)/Ba/Al)	–	708	17 [a] (7.8)	0.15	79
PEDOT/PFO-SeBT30/Ba/Al (**11**/**79a**(30%)/Ba/Al)	–	712	6 [a] (5.6)	0.05	79
PEDOT/PVK/PFO-SeBSe1/Ba/Al (**11**/**14**/**79b**(1%)/Ba/Al)	–	723	3.8 [a] (16.7)	0.3	79
PEDOT/PVK/PFO-SeBSe15/Ba/Al (**11**/**14**/**79b**(15%)/Ba/Al)	–	790	2 [a] (9.7)	0.02	79

Note. ppy is 2-phenylpyridine, PQIr = Ir(pq)$_3$acac (pq is 2-phenylquinoxaline, acac is acetylacetonate), BAlq is bis(2-methyl-8-hydroxyquinoline)(4-phenylphenoxy)aluminium, HGH_2 is 1,4-phenylenebis(triphenylsilane). [a] In cd m^{-2}.

film heat treatment before its was coated with the cathode. It has been suggested that the heating of the film leads to the formation of an ordered stable chain conformation generating NIR emission. The maximum efficiency of the device (η_{ext}^{EL}) was 0.3%.

A year later, Baigent *et al.*[73] designed a double-layer OLED cell ITO/PPV/**73**/Ca/Al [PPV is poly(phenylene vinylene)], containing copolymer **73** with alkylthiophene, dialkoxy-*p*-phenylene and cyanovinylene moieties. The cell showed electroluminescence of copolymer **73** with a peak at 730 nm with the efficiency $\eta_{ext}^{EL} = 0.2\%$. Adhering to the concept of narrow-gap donor – acceptor compounds, Swedish researchers[74] have synthesized polymer **74** in which thiophene rings are donors, and the [1,2,5]thiazolo[3,4-*g*]quinaxaline moiety is an acceptor. Such a polymer showed emission at 970 nm with the efficiency $\eta_{ext}^{EL} = 0.04\%$. More modest operating characteristics were exhibited by the OLED device based on the polymer PTPTB (**75**) containing *N*-dodecyl-2,5-bis(2-thienyl)pyrrole and 2,1,3-benzothiadiazole as a donor and acceptor moiety, respectively.[75] The emission intensity at 800 nm for this device increases with increasing voltage to 7 V and is saturated, while the low efficiency of the ITO/PEDOT/PTPTB/LiF/Al (ITO/**11**/**75**/LiF/Al) device can be significantly enhanced by introducing 1% – 5% of the polymer into the poly[5-(3,7-dimethyloctyloxy)-2-methyloxy-*p*-phenylene vinylene] matrix (MDMO-PPV, **76**).

Interesting results on the luminescence of polymeric NIR electrophosphors were obtained during the years 2004 – 2006 for copolymers containing, in different proportions, the host units — 2-methoxy-5-octyloxy-*p*-phenylenevinylene (MOPV) or 9,9-dioctylfluorene (FO) — and the guest units: 2,1,3-benzothiadiazolevinylene (PMOPV-BTV, **77a**),[76] 2,1,3-benzoselenadiazolevinylene (PMOPV-BSeV, **77b**),[77] 4,7-bis(2-thienyl)-2,1,3-benzothiadiazolevinylene (PMOPV-DBTV, **78a**), 4,7-bis(2-thienyl)-2,1,3-benzoselenadiazolevinylene (PMOPV-TBSV, **78b**),[78] 4,7-bis(2-selenophenyl)-2,1,3-benzothiadiazole (PFO-SeBT, **79a**) and 4,7-bis(2-selenophenyl)-2,1,3-benzoselenadiazole (PFO-SeBSe, **79b**).[79] For all these materials, the EL peak was shifted from the orange or red spectral range to the NIR range with an increase in the content of guest units in the copolymer molecule from 0.5% to 30%. This effect is explained by migration of excitons generated under electric excitation from the MOPV or FO units luminescing in the visible range to the IR-emitting heterocyclic moieties, and their high polarizability decreases the energies of the excited states of the entire molecule.[80] Among a large number of OLED devices fabricated with these copolymers, the highest efficiency ($\eta_{ext}^{EL} = 0.31\%$ at $\lambda_{max} = 715$ nm) was exhibited by PMOPV-DBTV1 [**78a**(1%)] containing 1% of 4,7-bis(2-thienyl)-2,1,3-benzothiadiazolevinylene units, while the longest emission wavelength $\lambda_{max} = 800$ nm at $\eta_{ext}^{EL} = 0.02\%$ was found for copolymer PMOPV-TBSV30 [**78b**(30%)] containing 30% of 4,7-bis(2-thienyl)-2,1,3-benzoselenadiazolevinylene units. Since the LED efficiency in these cases depends on the host : guest ratio in the copolymer, Table 2 summarizes the characteristics of the most efficient NIR-emitting samples and structures exhibiting the longest wavelengths of EL. The spectra of LEDs based on the organic derivatives considered in this Section are shown in Fig. 2.

The data in Table 2 and Fig. 2 demonstrate that, among the organic derivatives exhibiting EL, the highest emission intensity (19 mW cm^{-2}) has been achieved for the doped

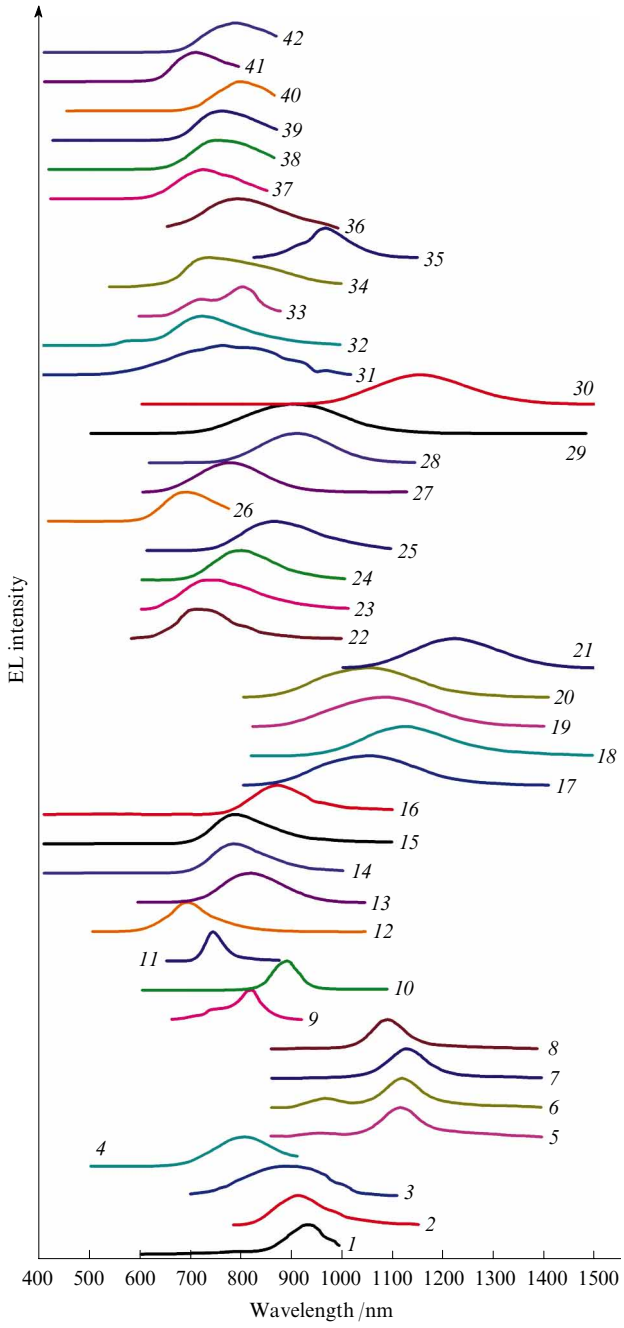


Figure 2. Electroluminescence spectra of organic compounds in the range 600 – 1500 nm.
(*1*) **47a** (H_2Pc), (*2*) **47b** (Tetra-H_2Pc), (*3*) **47c** (MPPc), (*4*) **49** (LDS821), (*5*) **50a** (IR1050), (*6*) **50b** (IR1051), (*7*) **51** (IR1061), (*8*) **50c** (SO447), (*9*) **52** (TCC), (*10*) **54** (ADS830AT), (*11*) **55** (M), (*12*) **57** (BEDOT-TQMe$_2$), (*13*) **58** (BEDOT-BBT), (*14*) **59a**, (*15*) **59b**, (*16*) **59c**, (*17*) **60a**, (*18*) **61b**, (*19*) **60b**, (*20*) **60c**, (*21*) **61a**, (*22*) **62a**, (*23*) **62b**, (*24*) **63a**, (*25*) **63b**, (*26*) **64** (PTZ-BZP), (*27*) **66**, (*28*) **65**, (*29*) **67**, (*30*) **68**, (*31*) **69**, (*32*) **70** (EE-BTD-EE), (*33*) **72** (POPT), (*34*) **73**, (*35*) **74**, (*36*) **75** (PTPTB), (*37*) **77a**(30%) (PMOPV-BTV30), (*38*) **77b**(30%) (PMOPV-BSeV30), (*39*) **78a**(30%) (PMOPV-DBTV30), (*40*) **78b**(30%) (PMOPV-TBSV30), (*41*) **79a**(3%) (PFO-SeBT30), (*42*) **79b**(15%) (PFO-SeBSe15).

LED containing donor – acceptor conjugated oligomer BEDOT-TQMe$_2$ (**57**) and emitting in the near-boundary range ($\lambda_{max} = 692$ nm),[59] while the longest wavelength of

EL at 1220 nm is observed for the OLED device based on D – π – A – π – D compound **61a**.[64]

III.2. d-Metal complexes

Studies of the EL properties of organic complexes of main group metals and d-metals are limited to Zn, Cu, In, Os, Pd, Pt and Ir derivatives. Among them, Pt^{II} compounds have been best studied since they are promising phosphors not only for NIR-emitting OLED devices but also for use in biomedicine.[81] To improve the conductivity and suppress the possibility of triplet – triplet annihilation, as well as to control the number of generated excimers acting as traps for excitons and luminescence centres, the complexes in most cases are used as dopants (2% – 10%) into charge-conducting matrices. As ligands for these metals, porphyrin, phthalocyanine and 1,3-bis(4-pyridyl)benzene derivatives are most often used.

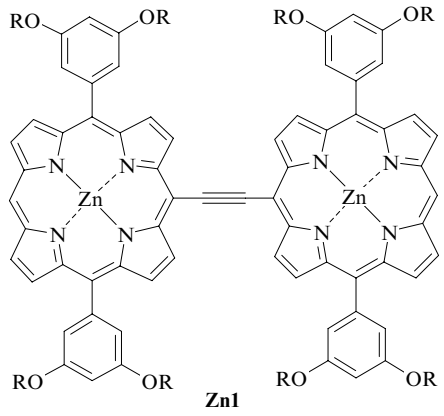
For zinc, bi- (**Zn1**) and trinuclear (**Zn2**) metalloporphyrins with acetylene bridges have been synthesized.[82] In OLED cells, the complexes have been used as dopants into polymers PVK (**14**) and MEH-PPV (**71**). It has been found that the EL intensity (λ_{max} = 720 nm for **Zn1** and 820 nm for **Zn2**) strongly depends on the complex concentration in the matrix. The best results (η_{ext}^{EL} = 0.3%) have been achieved at a concentration of $\leqslant$0.5% for double-layer LEDs ITO/PEDOT/PVK:PBD:**Zn1**(**Zn2**)/Ca/Ag [ITO/**11**/**14**:**17**:**Zn1**(**Zn2**)/Ca/Ag].

Owing to good hole-transport properties and the HOMO energy close to the ITO potential, the unsubstituted copper phthalocyanine (CuPc, **Cu1**) is often applied to the anode as a hole injection layer. However, this compound and its diverse derivatives in host – guest systems exhibit electrophosphorescence with the longest wavelength among the other phosphors based on d-metal complexes. The OLED device with the emission layer CBP:**Cu1** (**35**:**Cu1**) generated weak emission at ~1100 nm.[83] Optimization of the device by introducing an extra electron-blocking layer had no effect on the luminescence spectrum and did not improve the luminescence intensity, which did not exceed 0.006%.[84]

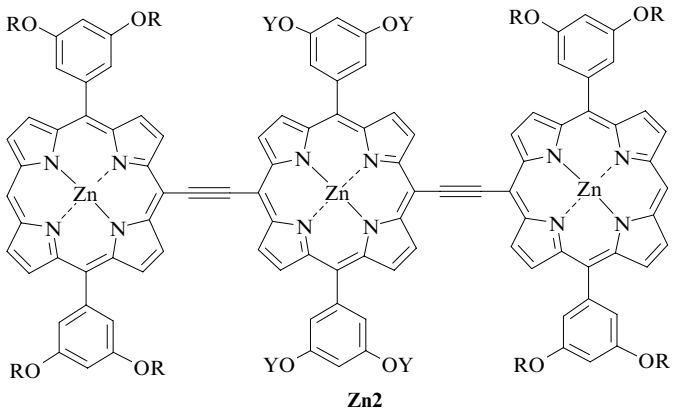
Copper-containing electrophosphor **Cu2** was obtained with the use of substituted phthalocyanine.[85] When introduced into the Alq_3 matrix in a double-layer OLED device, this compound showed EL as a broad band with a maximum at 1098 nm. Other characteristics of this device have not been reported. LEDs based on complex **Cu3** (Ref. 86) and copper decafluorophthalocyanine (**Cu4**) showed luminescence at nearly the same wavelength.[87] It is assumed that, in all systems containing copper phthalocyanine complexes, electron – hole recombination occurs directly on the dopant molecules and luminescence is due to the $^3T_1 \rightarrow {}^1S_0$ transition from the triplet level.

When searching for ways to enhance NIR emission of copper complexes, Yan *et al.*[88] introduced the iridium complex $Ir(piq)_2acac$ (piq is 1-phenylisoquinoline) into the luminescent CBP:**Cu1** layer. As expected by the authors, the luminescence intensity of complex **Cu1** was significantly increased. At the optimal codopant concentration (12% **Cu1** and 10% iridium complex), the EL intensity was increased 15-fold, whereas the luminescence band of the iridium component nearly vanished, which is evidence in favour of full excitation energy transfer from iridium to the

Structures Zn1, Zn2, Cu2, Cu3, In1

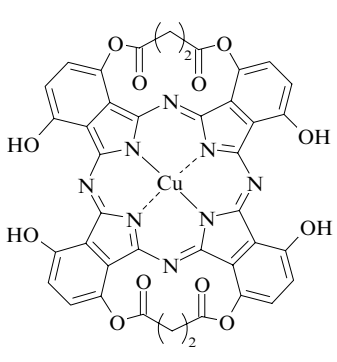


Zn1

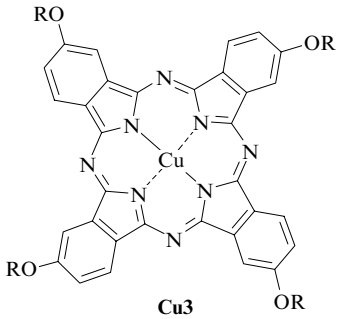


Zn2

R = $(CH_2)_2Bu^t$, Y = $(CH_2CH_2O)_3Me$

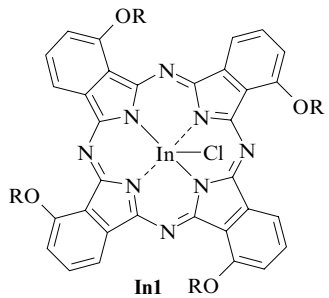


Cu2



Cu3

R = 2-Pr^i-5-MeC_6H_3



In1

R = 2-Bu^t-5-MeC_6H_3

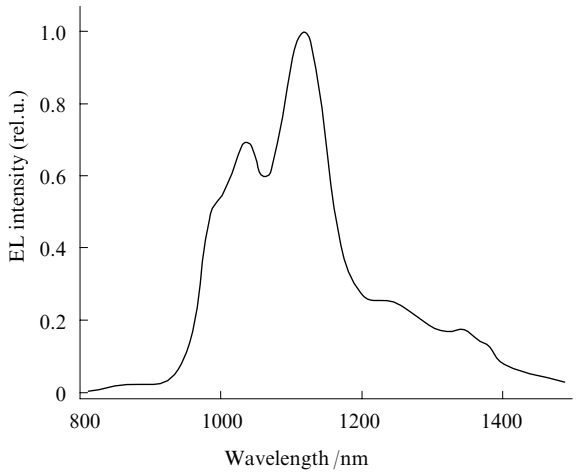


Figure 3. Electroluminescence spectrum of the ITO/TPD/Bath:**Cu1**/Yb(dbm)$_3$(Bath)/TPBI/Li/Al [ITO/**5**/Bath:**Cu1**/Yb(dbm)$_3$(Bath)/**13**/Li/Al] OLED.[89]

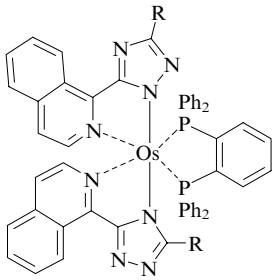
copper compound. As a development of this idea, the same researchers[89] designed the OLED cell containing an ytterbium β-diketonate Yb(dbm)$_3$(Bath) (dbm is dibenzoylmethanate) layer between the emission layer Bath:**Cu1** and the hole-blocking layers TPBI (**13**).[89] Studying the device has demonstrated that, at the optimal ratio between the Cu and Yb complexes, the EL intensity increases 50-fold and the emission band width increases fourfold. The EL spectrum (Fig. 3) shows the band of both dopants. It is assumed that the Yb complex transfers the excitation energy (generated from electron – hole recombination on the ligands) to the MLCT state of the Cu complex, partially retaining its own luminescence activity. It should be, however, noted that, in the device configuration used, the Yb complex is not a codopant of the Bath:**Cu1** layer, and, hence, the possibility of intermolecular interaction is limited by the interface surface. It is of interest that other lanthanide complexes with the same ligands do not exhibit the sensitizing effect with respect to **Cu1**.

The only Group 13 metal complex that has NIR EL is indium chloride phthalocyanine **In1**.[90] The compound was used as a dopant (50%) into the Alq_3 matrix. As a monolayer, this complex did not show emission.

Like visible electrophosphors, the vast majority of NIR emitters based on d-metal complexes are platinum and iridium derivatives. Among rare representatives of other metals are osmium and palladium compounds. The former of them have been synthesized by Taiwanese researchers[91] with the use of 5-(1-isoquinolyl)-1,2,4-triazole anionic ligands and neutral phosphines, for example, complexes with bis(diphenylphosphine)benzene (**Os1a**,**b**). Other complexes have different phosphine ligands; however, LEDs based on them have similar characteristics responding only slightly to a change in material of the electron-transport layer. A specific feature of devices based on osmium complexes is a low turn-on voltage — 1.7 – 3.2 V.

Later, the same researchers,[92] in an attempt to enhance the EL efficiency, have synthesized analogous complexes with bipyrazole and bipyridine or phenanthroline as the ligands. The luminescence intensity and quantum yield of OLED devices based on these compounds were actually higher (53.9 mW cm^{-2} at 11.4 V and 1.54%, respectively), but the emission wavelength shifted to the visible range to 690 nm.

Structures Os1a,b



R = Ph (**a**), Bu^t (**b**)

Os1a,**b**

Currently, phthalocyanine complex **Pd1** is likely the only palladium compound tested as an emitter in a LED cell.[84] The characteristics of this compound are inferior to those of Cu and Pt analogues; in addition, the EL spectrum shows strong bands of the phthalocyanine ligand and the matrix in the visible range.

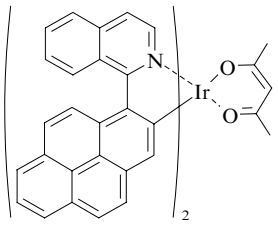
The other NIR-emitting electrophosphors containing d metals are platinum and iridium compounds. LEDs based on these complexes generate moderate emission in the range 690 – 870 nm at 10 – 15 V.

Iridium complexes are widely used as emission materials in OLED devices emitting in the entire visible range; however, EL with a wavelength > 700 nm is known only for a few compounds. The first NIR-emitting LED based on an Ir complex was fabricated using the PVK:PBD:**Ir1** (**14**:**17**:**Ir1**) system.[93] The luminescence spectrum contained only one narrow band (λ_{max} = 720 nm) with and maximal intensity of 280 μW cm^{-2} at a dopant concentration of 5%. Similar characteristics have been shown by cationic complexes with 2-phenylbenzoquinoline (**Ir2**), 3-methyl-2-phenylbenzoquinoxaline (**Ir3**)[94] and diphenylphthalazine (**Ir4**)[95] ligands and by their neutral analogue **Ir5**.[96] It should be noted that the emission layer based on complex **Ir5** was fabricated using an unusual matrix — bis(salicylidene-*o*-aminophenolato)bis(8-hydroxyquinolinato)digallium [Ga_2(saph)$_2q_2$]. The highest-ever NIR emission intensity, 4.6 mW cm^{-2} at 13 V, was recorded for the LED based on neutral compound **Ir6**.[97] This compound and other iridium emitters are distinguished by the enhanced stability, as compared with other metal complexes, of the emission efficiency and spectrum with respect to an increase in applied voltage and current density.

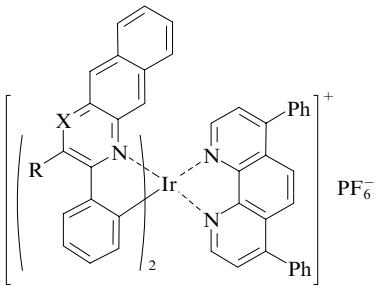
Iridium complexes with boron-substituted oligothiophene ligands **Ir7** and **Ir8** in the doped LED device ITO/PEDOT:PSS/CBP:**Ir7**(**Ir8**)/BCP/Alq_3/LiF/Al [ITO/**11**:**12**/**35**:**Ir7**(**Ir8**)/**31**/**1**/LiF/Al] give a complex luminescence spectrum composed of two bands (~540 and ~750 nm) and a shoulder (~830 nm).[98] With increasing complex concentration in the CBP matrix, the NIR band intensity increases, while the visible band intensity decreases. The optimal concentration ensuring the maximal efficiency of long-wavelength bands is 2%.

Among other long-wavelength iridium-containing emitters, noteworthy is the Ir(ppy)$_2$q complex incorporating two 2-phenylpyridyl and one 8-hydroxyquinoline ligands. In a doped four-layer device, this complex showed weak EL as a broad band centred at ~640 nm, but the long-wavelength tail extended to 800 nm.[99]

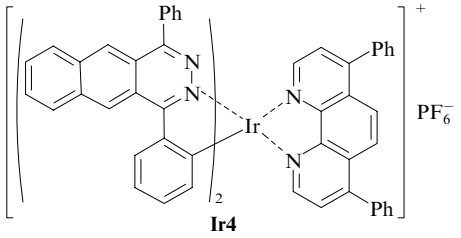
Structures Ir1 – Ir8



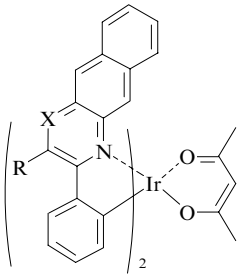
Ir1



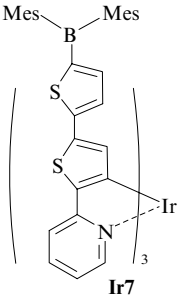
Ir2 (X = CH, R = H), **Ir3** (X = N, R = Me)



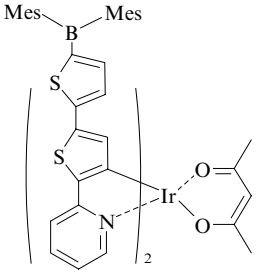
Ir4



Ir5 (X = N, R = Me),
Ir6 (X = CH, R = H)



Ir7

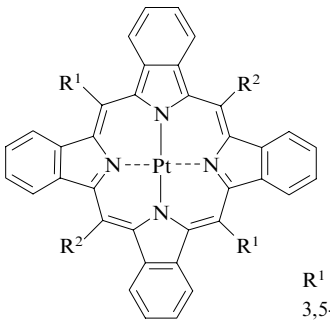


Ir8

Mes = 2,4,6-$Me_3C_6H_2$

The first Pt complex used for fabrication of a NIR-emitting OLED was metalloporphyrin **Pt1**. In a three-layer device, it showed luminescence as a single narrow band at 769 nm with an emission intensity of 720 μW cm^{-2} and an efficiency of 6%.[100] The use of BCP (**31**) instead of Alq_3 (**1**) as a host led to a slight shift of the band (to 772 nm) and to an increase in η_{ext}^{EL} to 8%.[101] Later, researchers from the University of Florida[102] achieved an intensity of 3400 μW cm^{-2} for the same compound and the same device structure.

Structures Pt1 – Pt3

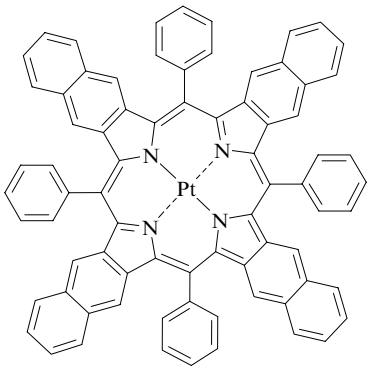


Pt1 – **Pt3**

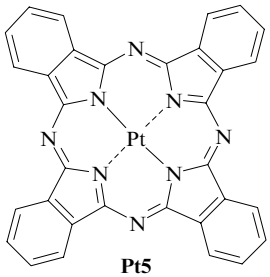
$R^1 = R^2$ = Ph (**Pt1**),
3,5-$Bu^t_2C_6H_3$ (**Pt2**);
R^1 = H, R^2 = 3,5-$Bu^t_2C_6H_3$ (**Pt3**)

A series of other di- and tetra-substituted Pt^{II} porphyrins have been synthesized. One of the complexes (**Pt2**) demonstrated the highest radiant emittance and external quantum efficiency among platinum phosphors.[102] All the synthesized compounds were incorporated into solution-processed polymer light emitting diodes (PLEDs). Tests have demonstrated that these devices generate analogous emission (λ_{max} 771 – 790 nm), but afford lower radiance and efficiency. For the best of them (**Pt3**), the intensity was 3 mW cm^{-2}. Extension of the conjugated system in complex **Pt1** by substituting a naphthalene fragment for the benzene ring conjugated with the pyrrole ring (complex **Pt4**) did not improve the performance of the device but shifted the emission band toward longer wavelengths to 883 nm.[103]

Structures Pt4, Pt5



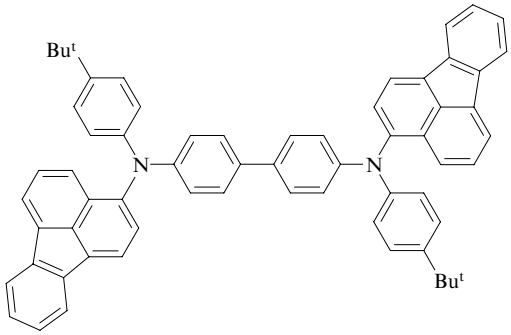
Pt4



Pt5

Phthalocyanine complex **Pt5** in the YSE matrix [yellow single emitter, *N*,*N*′-bis(4-*tert*-butylphenyl)-*N*,*N*′-bis(3-fluoranthenyl)biphenyl-4,4′-diamine (**80**)], like its analogues **Cu1** and **Pd1**, exhibited NIR emission but of considerably higher efficiency — up to 0.3%.[84] In addition, the spectrum of the OLED based on **Pt5** did not show luminescence bands of the ligands and matrix, which was evidence of more complete energy transfer to the emission triplet level.

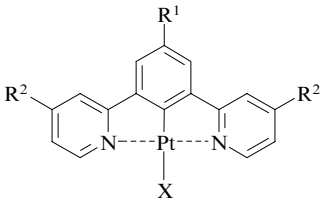
Structure 80



80 (YSE)

NIR-emitting platinum complexes **Pt6** – **Pt14** have been synthesized using NCN-tridentate 2,5-dipyridylphenyl ligands.[104–109] Electrophosphorescence of these compounds is manifested as a broad band (a width at half maximum of 150 – 250 nm) peaking in the range 700 – 970 nm. The simplest of them — complex **Pt6** — incorporated in an undoped device exhibited strong phosphorescence (15.9 mW cm^{-2}) at λ_{max} = 720 nm.[107] The highest emission forward output (25 mW cm^{-2}) reported for a NIR-emitting electrophosphor has been achieved for substituted dipyridylphenyl complex **Pt9**.[108] In this case, a new cathode substrate material — PbO_2 — was used, which, as believed by the authors, was responsible for the high efficiency of electron injection into organic layers. It should be noted that a device based on **Pt9** gives emission at the edge of the visible range (λ_{max} = 700 nm) and is perceived as red, although ~50% of its emission occurs in the NIR range.

Structures Pt6 – Pt14



Pt6 – Pt14

Compound	R^1	R^2	X
Pt6	H	H	Cl
Pt7	F	H	Cl
Pt8	Me	H	Cl
Pt9	MeOC(O)	H	Cl
Pt10	Mes	H	Cl
Pt11	4-$Ph_2NC_6H_4CH{=}CH$	H	Cl
Pt12	4-$Ph_2NC_6H_4C{\equiv}C$	H	Cl
Pt13	Mes	H	NCS
Pt14	H	CF_3	Cl

Studying the electroluminescence of mesityl-containing complexes **Pt10** and **Pt13**, Williams and co-workers [104] have revealed that the substitution of isothiocyanate for chloride leads to the red shift of the emission band maximum from 685 to 855 nm. Comparison of the EL spectra of both complexes in monolayers and in matrices, as well as PL in solutions and films, with single-crystal X-ray diffraction data enabled the conclusion that a considerable difference in spectral characteristics is caused by the different Pt···Pt distances in solid samples. In the chloride, this distance is 4.4 Å; at the same time, in the isothiocyanate analogue, this distance is 3.3 Å owing to the parallel orientations of molecules, which favours the Pt···Pt interaction and formation of associates with a higher HOMO energy. This is responsible for the narrower LUMO – HOMO gap and, as a result, the longer wavelength emission.

The same authors [105] have demonstrated that dipyridylphenyl platinum compounds, as distinct from most of the other complexes emitting only in host – guest systems, exhibit strong EL, being incorporated in undoped OLED devices. Moreover, as shown for complexes **Pt11** and **Pt12**, the incorporation of phosphors into the TCTA (**23**) or CBP (**35**) matrix leads to a considerable luminescence shift to the visible range.[109] The introduction of a fluorine atom into a phenyl moiety (complex **Pt7**) or CF_3 groups into pyridine

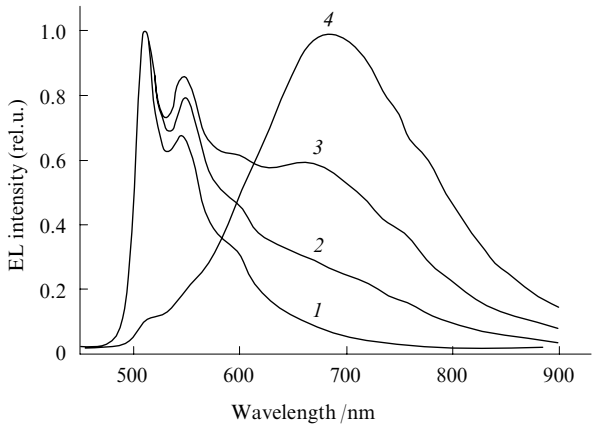
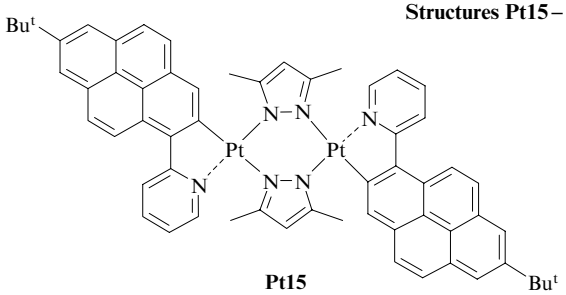


Figure 4. Electroluminescence spectra of the single-layer device ITO/PVK:PBD:**Pt13**/Ba/Al (ITO/**14**:**17**:**Pt13**/Ba/Al) at different concentrations of the complex.[106]
(*1*) 10%, (*2*) 25%, (*3*) 40%, (*4*) 50%.

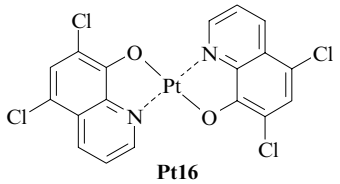
rings (complex **Pt14**) leads to the shift of the EL band to the visible range. However, the ligand that does not contain trifluoromethyl groups but contains the fluorine atom in the 4-position of the phenyl moiety (**Pt7**) is responsible for the NIR emission at λ_{max} = 700 nm, which was assigned, as in most of planar platinum complexes, to excimer luminescence.[106] The change in the complex concentration in the functional layer leads to the intensity redistribution of the luminescence bands of the matrix (at about 440 nm) excimers in the EL spectra, which makes it possible to use these compounds in design of white-light LEDs (Fig. 4).[106]

Studying binuclear pyridylpyrrene complex **Pt15** has shown that extension of the conjugated aromatic system does not increase the NIR emission of the LED and does

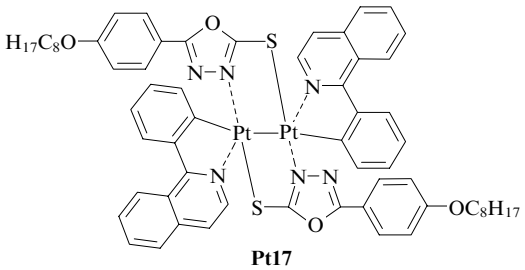
Structures Pt15 – Pt17



Pt15



Pt16



Pt17

not improve its characteristics.[110] An analogous complex without Bu^t substituents gave rise to the same EL spectrum but of lower intensity. In both cases, the spectra of devices showed the matrix luminescence band at 445 nm, which became weaker with increasing dopant concentration and completely disappeared at a concentration of 8%, which was evidence of complete excitation energy transfer to the complex.

Attempts to produce NIR-emitting platinum complexes by using the well-known sensitizing 8-hydroxyquinoline ligands were unsuccessful.[111] Even the best of them — complex **Pt16** — in the doped CBP:**Pt16** (**35**:**Pt16**) (5%) layer produced weak luminescence as a band at 695 nm with a shoulder at ~750 nm. Similar characteristics were determined for an LED with a polymeric emissive layer doped with complex **Pt17**.[112]

To synthesize NIR-emitting electrophosphors suitable for solution-processing fabrication of OLED devices, Bronstein and co-workers[113] synthesized polymeric host – guest systems in which a Pt^{II} porphyrin complex was built into (and covalently bound) a diphenylanthracene chain. A LED cell based on such a material showed weak and poorly reproducible emission as two bands at 666 and 737 nm. It is worth noting the PL spectrum of a solution and film of the same composition did not show the long-wavelength band.

Characteristics of the most efficient OLED devices based on d-metal complexes are summarized in Table 3.

Table 3. Operating characteristics of OLED devices based on organic d-metal complexes emitting in the range > 750 nm.

Device	V_0/V	λ_{max}/nm	R/mW cm^{-2}	η_{ext}^{EL} (%)	Ref.
PEDOT/PVK:PBD:**Zn1**(**Zn2**)/Ca/Ag [**11**/**14**:**17**:**Zn1**(**Zn2**)/Ca/Ag]	4	820	–	0.1	82
NPD/CBP:**Cu1**/BCP/Alq_3/Al (**9**/**35**:**Cu1**/**31**/**1**/Al)	–	1100	–	–	83
NPD/Alq_3:**Cu2**/Al (**9**/**1**:**Cu2**/Al)	–	1098	–	–	85
NPD/CBP:**Cu3**/BCP/Alq_3/Al (**9**/**35**:**Cu3**/**31**/**1**/Al)	–	1100	–	–	86
NPB / TPBI:**Cu4**/BCP/Alq_3/Al (**9** /**13**:**Cu4**/**31**/**1**/Al)	–	1106	–	0.001	87
MTDATA/TPD/CBP:**Cu1**:Ir(piq)$_2$acac/TPBI/LiF/Al [**6**/**5**/**35**:**Cu1**:Ir(piq)$_2$acac/**13**/LiF/Al]	–	1112	–	0.1	88
TPD/Bath:**Cu1**/Yb(dbm)$_3$(Bath)/TPBI/LiF/Al [**5**/Bath:**Cu1**/Yb(dbm)$_3$(Bath)/**13**/LiF/Al]	–	1150	–	–	89
NPB/Alq_3:**In1**/Alq_3/Al (**9**/**1**:**In1**/**1**/Al)	–	880	–	–	90
α-NPD/Alq_3:**Os1**/Alq_3/LiF/Al (**9**/**1**:**Os1**/**1**/LiF/Al)	2.4	814	0.065 (17)	1.5	91
MEO-TPD:F_4-TCNQ/Spiro-TAD/YSE:**Pd1**/TPBI/Bath:Cs/Al (MEO-TPD:F_4-TCNQ/Spiro-TAD/**80**:**Pd1**/**13**/Bath:Cs/Al)	1.8	1025	–	0.03	84
PEDOT/PVK:PBD:**Ir1**/LiF/Al (**11**/**14**:**17**:**Ir1**/LiF /Al)	–	720	0.28 (18)	0.1	93
PEDOT:PSS/PVK:PBD:**Ir2**/TPBI/Cs_2CO_3/Al (**11**:**12**/**14**:**17**:**Ir2**/**13**/Cs_2CO_3/Al)	14	753	0.095 (16)	0.30	94
PEDOT:PSS/PVK:PBD:**Ir4**/TPBI/Cs_2CO_3/Al (**11**:**12**/**14**:**17**:**Ir4**/**13**/Cs_2CO_3/Al)	14	715, 788	1.112 (20)	0.50	95
NPD/Ga_2(saph)$_2$q$_2$:**Ir5**/Bath/Mg:Ag [**9**/Ga_2(saph)$_2$q$_2$:**Ir5**/Bath/Mg:Ag]	4.5	780, 850	1.8 (15)	2.2	96
NPB/Alq_3:**Ir6**/Bath/Mg:Ag (**9**/**1**:**Ir6**/Bath/Mg:Ag)	10	720	4.6 (13)	1.07	97
PEDOT:PSS/CBP:**Ir7**/BCP/Alq_3/LiF/Al (**11**:**12**/**35**:**Ir7**/**31**/**1**/LiF/Al)	9.4	533, 737, 825	283 [a] (17.8)	0.189	98
NPD/Alq_3:**Pt1**/Alq_3/LiF/Al (**9**/**1**:**Pt1**/**1**/LiF/Al)	–	769	0.75 (12)	6.3	100
NPD/Alq_3:**Pt1**/Bath/LiF/Al (**9**/**1**:**Pt1**/Bath/LiF/Al)	–	773	3.4 (15)	8.0	102
NPD/Alq_3:**Pt2**/Bath/LiF/Al (**9**/**1**:**Pt2**/Bath/LiF/Al)	–	773	4.4 (14)	9.2	102
PEDOT:PSS/PVK:PBD:**Pt3**/Ca/Al (**11**:**12**/**14**:**17**:**Pt3**/Ca/Al)	18	774	3.0 (25)	3.02	102
α-NPD/CBP:**Pt4**/Bath/Bath:Cs/LiF/Ca/Al (**9**/**35**:**Pt4**/Bath/Bath:Cs/LiF/Ca/Al)	2.0	883	1.8 (12)	3.3	103
MEO-TPD:F_4-TCNQ/Spiro-TAD/YSE:**Pt5**/TPBI/Bath:Cs/Al (MEO-TPD:F_4-TCNQ/Spiro-TAD/**80**:**Pt5**/**13**/Bath:Cs/Al)	1.8	966	–	0.3	84
TPD:PC/CBP/**Pt6**/OXA/Ca/Al (**5**:PC/**35**/**Pt6**/**33**/Ca/Al)	–	720	15.9 (100)	8.5	107
TPD:PC/CBP/**Pt9**/OXA/PbO_2/Ca/Al (**5**:PC/**35**/**Pt9**/**33**/PbO_2/Ca/Al)	7	700	25 (15)	14.5	108
Mo_2O_x/TCTA/**Pt11**/TPBI/LiF/Al (Mo_2O_x/**23**/**Pt11**/**13**/LiF/Al)	5	800	10.0 (9)	1.2	109
TPD:PC/TCTA/**Pt13**/TAZ/LiF/Al (**5**:PC/**23**/**Pt13**/**15**/LiF/Al)	–	855	–	1.0	104
TPD:PC/TCTA/**Pt14**/TAZ/LiF/Al (**5**:PC/**23**/**Pt14**/**15**/LiF/Al)	16	780	0.5	0.3	105
PEDOT:PSS/PVK/PVK:PBD:**Pt7**/Ba/Al (**11**:**12**/**14**/**14**:**17**:**Pt7**/Ba/Al)	12	700	0.755	0.28	106
PEDOT:PSS/PVK:OXD-7:**Pt15**/Ba/Al (**11**:**12**/**14**:**33**:**Pt15**/Ba/Al)	8.1	695, 753	0.019 (8)	0.15	110
PEDOT:PSS/PVK:PFO-PBD:**Pt17**/Ba/Al (**11**:**12**/**14**:PFO-**17**:**Pt17**/Ba/Al)	9.5	712	3.23 (120)	9.94	112

Note. MEO-TPD is *N*,*N*,*N*′,*N*′-tetrakis(4-methoxyphenyl)benzidine, F_4-TCNQ is 2,3,5,6-tetrafluoro-7,7,8,8-tetracyanoquinodimethane, Spiro-TAD is 2,2′,7,7′-tetrakis(*N*,*N*-diphenylamino)-9,9-spirobifluorene, PC is bisphenol A polycarbonate, PFO is poly(9,9-dioctylfluorene).
[a] In cd m^{-2}.

III.3. Rare earth complexes

Based on photophysical properties, Group 3 metals can be divided into two groups. One of the them includes Sc, Y, and La, which do not have f electrons, and Lu, which has the completely filled f-subshell. Their luminescent properties do not differ from those of d metals and are mainly determined by the energy of frontier molecular orbitals. For Sc, the ligands have been found that ensured high EL intensity but only in the visible range.[114] For these metals, NIR-emitting compounds have not been synthesized so far. The other elements of the same group (Ce, Pr, Nd, Pm, Sm, Eu, Gd, Tb, Dy, Ho, Er, Tm, and Yb) have a partially filled 4f-subshell so that electronic transitions between sublevels of different energy inside this subshell can occur, which is accompanied by absorption or emission of electromagnetic radiation. In this case, emission is called metal-centred, and the wavelength is determined by the energy gap width between the ground and excited states of f electrons. All lanthanides, except Yb, have several metastable levels to which an f-electron can be transferred after excitation; however, relaxation from only some of them is accompanied by emission. In Fig. 5, these levels (resonance levels) are shown by green lines. The levels lying below line I give IR emission, the levels located between lines I and II are responsible for luminescence in the visible range, and those lying above line II produce UV emission. It is easily seen that Pr, Nd, Sm, Ho, Er, Tm and Yb have resonance levels corresponding to IR luminescence. Indeed, under photo- or electroexcitation, organic complexes of these metals can generate metal-centred IR luminescence; its wavelength is determined by the level energy, and its intensity depends to a considerable extent on the nature of sensitizing ligands. Because of efficient shielding of 4f electrons by 5s and 5p electrons and the fact that transitions inside one system are forbidden by the parity selection rule, direct absorption of excitation energy by Ln^{3+} ions is very low. However, the ligands bonded to the metal allow one to partially overcome these limitations and enhance emission. A simplified scheme

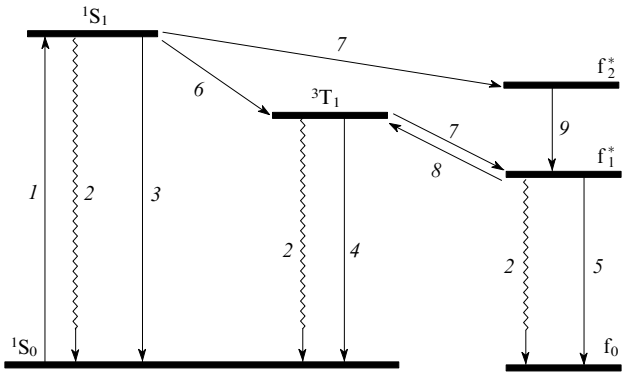


Figure 6. Scheme of energy transitions for a luminescing lanthanide complex (Jablonski — Crosby diagram).
S_0 is ground state, ^1S is singlet level, ^3T is triplet level, f_1^*, f_2^* are levels of excited f electrons, (*1*) excitation, (*2*) nonradiative relaxation, (*3*) fluorescence, (*4*) phosphorescence, (*5*) Ln^{3+} luminescence, (*6*) intersystem crossing, (*7*) intramolecular energy transfer, (*8*) back energy transfer, (*9*) internal conversion.

of the energy transitions in a luminescing molecule in this case can be presented by the diagram in Fig. 6.

It has been experimentally found that sensitization of an Ln^{3+} ion is most efficient when the difference in energy between the triplet level of the ligand and the resonance level of the metal is within 2500 – 4000 cm^{-1}. This empirical rule dictates to an extent the selection of organic ligands for lanthanide phosphors.

Lanthanide NIR phosphors have been addressed in numerous original papers and reviews (see, for example, Ref. 115), which is explained by their advantages (narrow emission lines, stability of spectra for complexes with different ligand environment, large lifetime) as compared with organic materials and d-metal complexes. However, almost all reviews deal only with photoluminescence. Only a few reviews have focused on the problems of electrolumines-

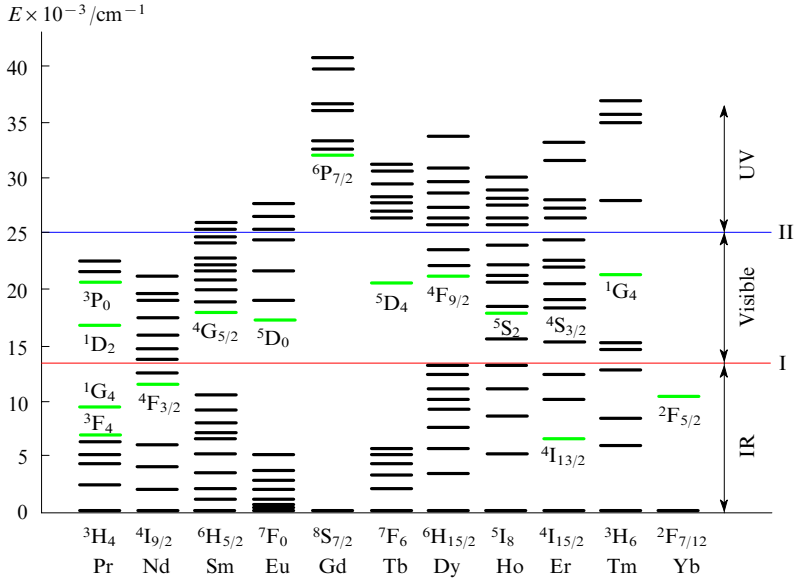


Figure 5. Energy diagram of the 4f levels of Ln^{3+} ions (except Ce, Lu and radioactive Pm).

cence of lanthanide complexes with organic ligands,[116–118] and the latest of them was published more than five years ago. Complexes of rare earth metals exhibiting EL are represented by structures **Ln1** – **Ln35** (when a particular compound is described, Ln is replaced by the symbol of the corresponding metal, for example, **Pr1**, *etc.*).

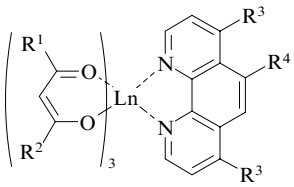
The first of the NIR-emitting lanthanides — praseodymium — is poorly studied since it exhibits weak photo- and electroluminescence, which makes its organic derivatives less attractive as potential materials for optoelectronics and biomedicine. Only few of the theoretically possible f – f transitions of praseodymium are active. The EL spectrum of complex **Pr1**, the first one incorporated in an OLED, showed five bands at 608, 890, 1015, 1065 and 1065 nm assigned to, respectively, the $^1D_2 \rightarrow {}^1H_6$, $^3F_2$, $^3F_3$, $^3F_4$ and $^1G_4$ transitions.[119] In addition, the spectrum showed a broad band of exciplexes in the range 450 – 700 nm. Only the luminance in the visible range was reported (50 cd m^{-2}), but it was underlined that the NIR emission was weaker.

Recently, we have found that deprotonated pentafluorophenol,[120] 2-[benzoxa(thia)zol-2-yl]phenol[121] and 3-[benzoxa(thia)zol-2-yl]-2-naphtol[122] efficiently sensitize the NIR emission of Nd, Er, Tm and Yb; however, the EL spectra of Pr complexes show only one shortest wavelength band due to the $^1D_2 \rightarrow {}^3H_6$ transition in the visible range at about 600 nm and(or) ligand bands. This specific feature is inconsistent with the rule of the optimal gap between the metal resonance level and the ligand triplet level and cannot be adequately explained.

The most popular anionic ligand for synthesis of luminescing coordination compound is presumably 8-hydroxyquinoline, which forms air-stable and vacuum-sublimable complexes with good charge-transport and, often luminescent properties. In a series of lanthanide hydroxyquinolinates, the neodymium derivative Ndq_3 (**Nd2**) was one of the first complexes for which the molecular structure and EL properties were studied.[123] A double-layer diode based on this complex demonstrated the NIR emission inherent in Nd^{3+} ion as three bands arising from the $^4F_{3/2} \rightarrow {}^4I_{9/2}$, $^4I_{11/2}$ and $^4I_{13/2}$ transitions (bands at 900, 1060 and 1320 nm, respectively). The compound exists as two isomeric forms (meridional and facial), but this fact has no effect on the EL spectrum. The use of 8-hydroxy-5,7-dichloroquinoline in the reaction with $NdCl_3(H_2O)_6$ led to a ionic complex containing four hydroxyquinoline ligands at the neodymium atom.[124] However, despite the X-ray crystallography characterization, the structure and composition of the product reported in this work are not quite clear. Nevertheless, the authors determined the PL and EL properties of this material in the PVK:Nd complex system. The EL spectrum has not been reported, but it has been noted that the ITO/PEDOT:PSS/PVK:Nd complex/Ca/Al (ITO/**11**:**12**/**14**:Nd complex/Ca/Al) diode gives NIR emission with the intensity 2.0 nW mm^{-2} at a voltage of 20 V and $\eta_{ext}^{EL} = 0.003\%$.

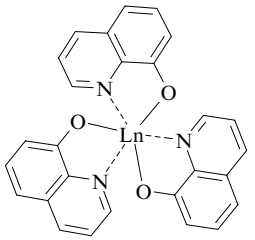
The equally widely used ligands for electroluminescent complexes are β-diketonates. Unsubstituted and substituted derivatives of this group of phosphors are similar in physicochemical properties and availability to 8-hydroxyquinolinates. Like for the latter, the introduction of donor or acceptor substituents that affect the triplet level energy makes it possible to adjust the luminescence colour and intensity of the device. As Yanagida and co-workers have shown,[125] neodymium dibenzoylmethanate **Nd1** in an undoped diode produces characteristic luminescence with the bands at 890, 1070 and 1350 nm. The operating characteristics of this device have not been reported, but it has been noted that the spectrum contains stronger bands in the visible range assigned to Alq_3, which served as an electron-transport material. To remove this undesirable component of the spectrum, the same authors used BCP (**31**) instead of

Structures Ln1 – Ln6, Ln17 – Ln22, Ln24, Ln28

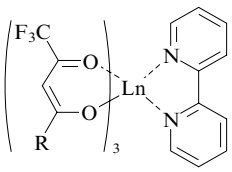


Ln1, **Ln17** – **Ln21**, **Ln24**, **Ln28**

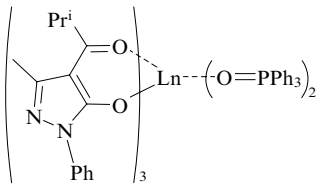
Compound	R^1	R^2	R^3	R^4	Ln
Ln1	Ph	Ph	Ph	H	Pr, Nd, Sm, Ho, Er, Tm, Yb
Ln17	Ph	Ph	H	H	Sm, Er, Tm
Ln18	Me	Me	H	H	Er, Tm
Ln19	CF_3	Me	Ph	H	Er
Ln20	CF_3	Bu^t	H	NO_2	Er
Ln21	CF_3	Me	H	NO_2	Er
Ln24	Me	Me	Ph	H	Tm
Ln28	2-Naph	2-Naph	H	H	Yb



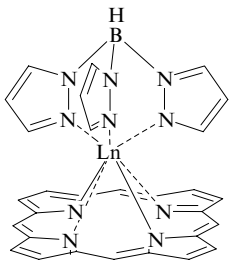
Ln2 (Ln = Nd, Er, Tm, Yb)



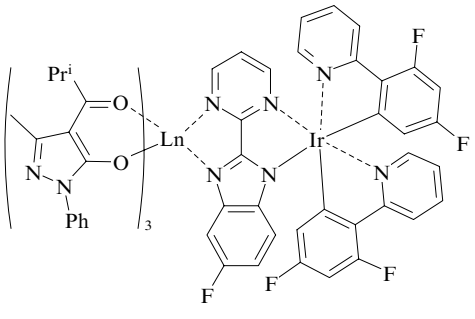
Ln3 (R = CF_3; Ln = Nd, Er, Yb), **Ln22** (R = 2-Naph; Ln = Er)



Ln4 (Ln = Nd, Er, Yb)

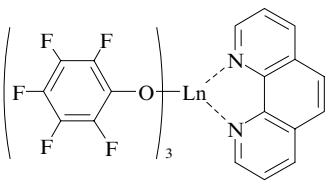


Ln5 (Ln = Nd, Ho, Er, Yb)

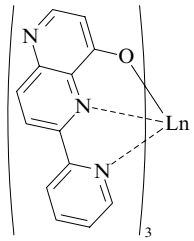


Ln6 (Ln = Nd)

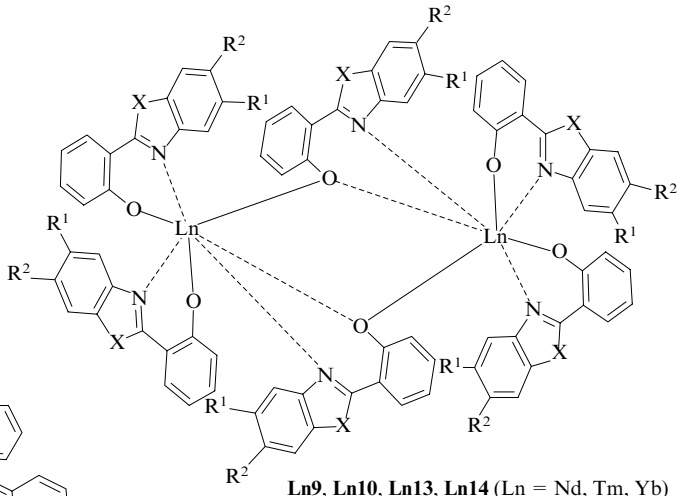
Structures Ln7 – Ln16, Ln23, Ln25 – Ln27, Ln29 – Ln35



Ln7 (Ln = Nd, Yb)

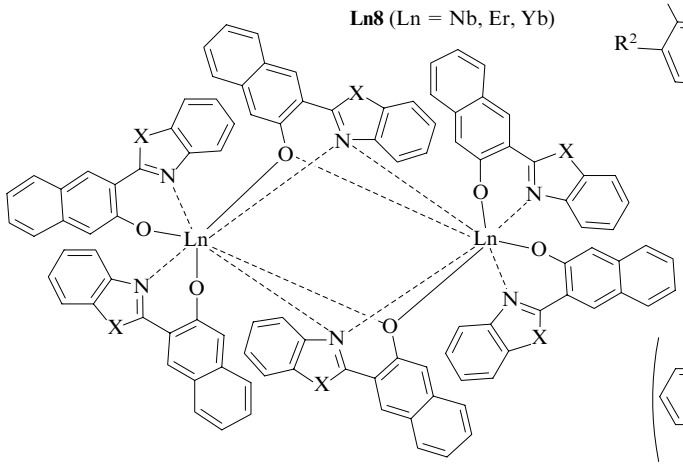


Ln8 (Ln = Nb, Er, Yb)

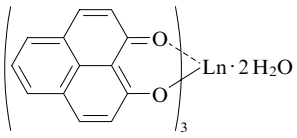


Ln9, **Ln10**, **Ln13**, **Ln14** (Ln = Nd, Tm, Yb)

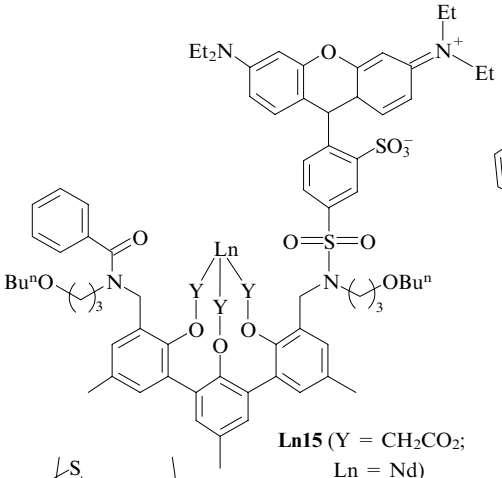
Compound	X	R^1	R^2
Ln9	O	H	H
Ln10	S	H	H
Ln13	O	Me	H
Ln14	O	H	Me



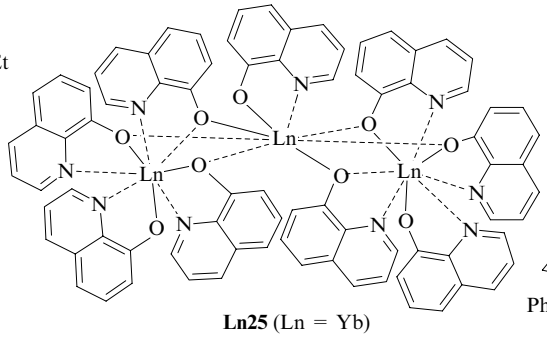
Ln11 (X = O; Ln = Nd, Tm,Yb); **Ln12** (X = S; Ln = Nd, Tm, Yb)



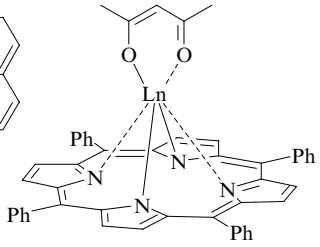
Ln16 (Ln = Nd)



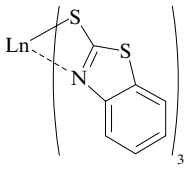
Ln15 (Y = CH_2CO_2; Ln = Nd)



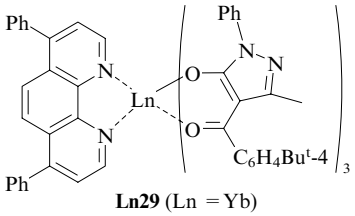
Ln25 (Ln = Yb)



Ln26 (Ln = Yb)



Ln23 (Ln = Tm)



Ln29 (Ln = Yb)

YbL_4Li

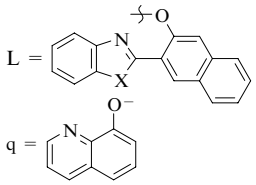
Ln31 (X = O),
Ln32 (X = S)

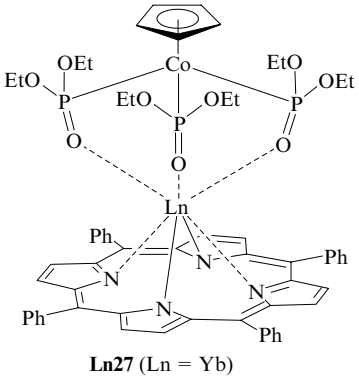
$Yb_2L_4q_2$

Ln34 (X = S)

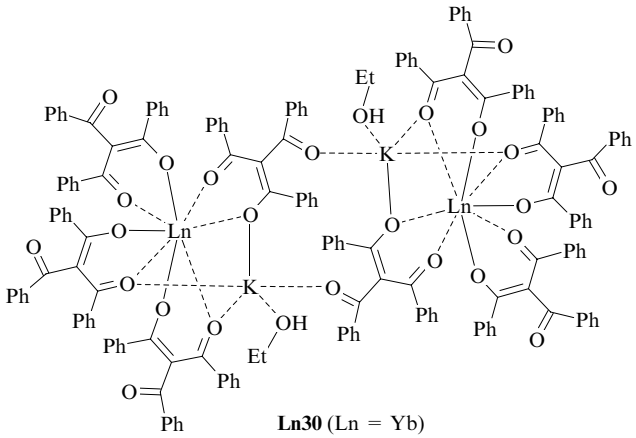
$Yb_2L_2q_4$

Ln35 (X = S)

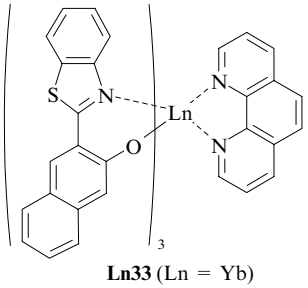




Ln27 (Ln = Yb)



Ln30 (Ln = Yb)



Ln33 (Ln = Yb)

the Alq_3 layer.[126] The Alq_3 band at about 500 nm in an ITO/TPD/**Nd1**/BCP/Mg:Ag/Ag (ITO/**5**/**Nd1**/**31**/Mg:Ag/Ag) LED naturally disappeared, but short-wavelength bands at 400 and 550 nm appeared, which were assigned to the luminescence of TPD (**5**) and exciplexes at the TPD/**Nd1** interface. Indirect evaluation of the metal-centred EL intensity gave a very low value — 7×10^{-5}%. The use of trifluoromethyl-substituted diketonate ligands and neutral dipyridyl (complex **Nd3**) did not disturb the luminescence spectrum of the device, but somewhat enhanced the luminescence intensity.[127]

Complex **Nd1** was used in combination with erbium analogues **Er1** for creating a NIR-emitting OLED with a tuneable wavelength.[128] Study of an ITO/TPD/**Nd1**/**Er1**/Mg:Ag diode has shown that its emission spectrum is a superposition of the emission spectra of Nd^{3+} (major band of the $^4F_{3/2} \rightarrow {}^4I_{11/2}$ transition at 1064 nm) and Er^{3+} ions (major band of the $^4I_{13/2} \rightarrow {}^4I_{15/2}$ transition at 1540 nm). At a **Nd1** layer thickness of 1 nm and an **Er1** layer thickness of 60 nm, the erbium band intensity was more than tenfold higher than the neodymium band intensity; however, an increase in the thickness of the **Nd1** layer to 5 nm led to a sharp change in the intensity ratio: the neodymium band at 1064 nm became dominating. The increase in the voltage on the electrode also led to the redistribution of the Nd and Er luminescence intensities. This effect is explained by the shift of the recombination band from the TPD/**Nd1** interface into the bulk of the neodymium complex layer.

Terbium acylpyrazolonate complexes are known to be the most efficient in a series of lanthanide phosphors.[118] It is believed that the high sensitizing ability of pyrazolonate ligands, which are β-diketone derivatives, is caused by the optimal proportion between the triplet energy of the ligands (21 460 cm^{-1}) and the resonance level of Tb^{3+} (20 430 cm^{-1}), although Dy^{3+} pyrazolonates, which have a close resonance level (20 830 cm^{-1}), do not exhibit strong luminescence. With respect to Nd^{3+}, pyrazolonate groups also do not exhibit good sensitizing properties. The NIR emission of the LED based on complex **Nd4** did not exceed 0.21 μW cm^{-2} at 16.5 V.[129]

Studying the EL properties of NIR-emitting lanthanide porphyrin complexes, has shown that neodymium compound **Nd5** gives rise to a characteristic three-band spectrum (880, 1060 and 1300 nm), which has a lower intensity than the spectrum of the Yb analogue, but higher than the spectra of the Ho and Er compounds.[130]

Organic d-metal complexes are often successfully used as sensitizing ligands for lanthanides emitting in the visible range.[131] The same approach has been used for enhancing the neodymium luminescence in complex **Nd6**, in which neodyminum acylpyrazolonate is coordinated to a neutral iridium complex.[132] The reported molecular structure of **Nd6** has not been strictly proven. It is assumed that such a structure forms through the codeposition of equimolar amounts of neodymium and iridium compounds evaporated in vacuum from separate evaporators. No matter what the actual structure of this material is, tests of the OLED device with a Nd-Ir layers have confirmed the high sensitizing effect of the iridium complex. The reference LED of identical composition, but not containing iridium showed 20-fold lower luminescence intensity and external quantum yield. The authors believe that electron–hole recombination and exciton formation occurs on the Ir complex, and after that the excitation energy is transferred to neodymium, thus enhancing emission.

As mentioned above, to decrease the number of CH groups — well-known luminescence quenchers — in a phosphor molecule, the authors of review[120] have synthesized a series of pentafluorophenyl complexes $Ln(OC_6F_5)_3(phen)$ (phen is 1,10-phenanthroline) and studied their EL properties. An OLED based on neodymium phenolate **Nd7** showed, in addition to the ligand luminescence band, characteristic metal-centred luminescence bands with an integral intensity of 18 μW cm^{-2}, which is inferior to fluorinated diketonate **Nd3** and complex **Nd8** containing a tridentate 8-hydroxy-2-(2-pyridyl)-1,5-naphthyridine ligand.[133] Significantly higher EL characteristics were exhibited by nonfluorinated **Nd9** with a benzoxazolyl substituent in the benzene ring.[121] X-ray crystallographic analysis of this and similar benzoxa(thia)zolyl-substituted phenolates and naphtholates demonstrated a dimeric molecular structure, which persisted in the course of evaporation–deposition processes accompanying the fabrication of a diode cell. The power efficiency for the diode based on complex **Nd9** was as large as 0.82 mW W^{-1}. The replacement of the oxygen atom in the benzoxazole ring by sulfur (complex **Nd10**) leads to a 3–8-fold decrease in all characteristics; however, the EL spectrum remains almost unaltered (Fig. 7).

Extention of π-conjugated systems in benzoxa(thia)zolylphenol ligands *via* the substitution of a naphthol group for the phenol group (complexes **Nd11** and **Nd12**) led to a considerable increase in the efficiency of metal-centred EL in thio analogue **Nd12** as compared with benzoxazole derivative **Nd11**.[122] The dimeric structure of the products upon such a substitution persisted. The maximum intensity of NIR emission intensity achieved on an undoped device ITO/TPD/**Nd12**/Bath/Yb was as high as 80 μW cm^{-2}. The EL intensities of complexes **Nd9**–**Nd12**, which can be arranged in the row **Nd12** > **Nd9** > **Nd10** > **Nd11**, are consistent well with the rule of optimal energy gap between the triplet level of the ligand and the resonance level of the metal. The $^3T_1$ levels for the benzoxazolylphenol and

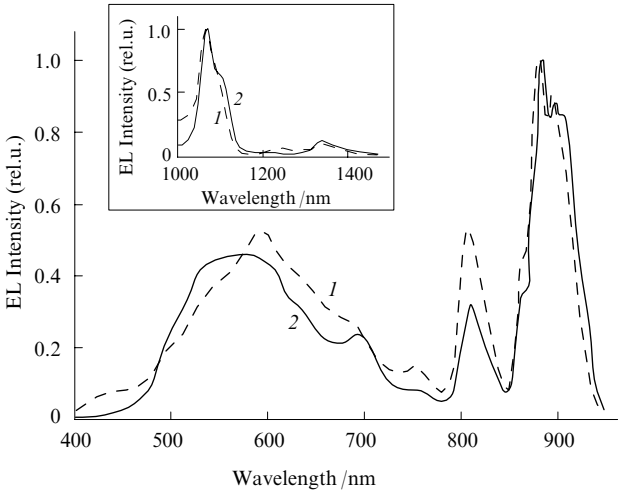
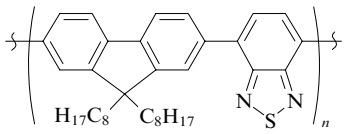


Figure 7. Electroluminescence spectra of ITO/TPD/**Nd9**(**Nd10**)/Bath/Yb (TPD = **5**).[121]
(*1*) **Nd9**, (*2*) **Nd10**.

benzothiazolylphenol ligands and their naphthol derivatives were found to be 19 050, 17 440, 18 600 and 16 050 cm^{-1}, respectively;[114] *i.e.*, the gap width between these levels and the radiative level of Nd^{3+} ($^4F_{3/2}$, 11 335 cm^{-1})[10] increases in the same order, beginning with the gap width for complex **Nd12** (4715 cm^{-1}), which is closest to the optimal value. The introduction of methyl substituents in the 5- or 6-position of the benzoxazole moiety (complexes **Nd13**, **Nd14**) had little effect on the triplet level energies and, hence, on the EL characteristics of OLEDs based on these complexes.[134] The EL efficiency of compound **Nd13** turned out to be the same as for the nonmetallated analogue; among the coordination neodymium electrophosphors, complex **Nd14** exhibited the highest-ever NIR luminescence efficiency — 85 μW cm^{-2}. The spectra of all devices show, in addition to the neodymium bands at 810, 900, 1060 and 1350 nm, broad ligand luminescence bands at about 540 nm, overlapping with the $^2G_{7/2}$, $^4G_{5/2} \rightarrow {}^4I_{9/2}$ transition bands.

As one of the first neodymium phosphors for creation of a doped polymeric EL device, complex **Nd15** with a ligand containing the lissamine moiety.[135] In the F8BT (**81**) matrix in the ITO/PEDOT:PSS/F8BT:**Nd15**/Ca/Al (ITO/**11**:**12**/**81**:**Nd15**/Ca/Al) diode, the compound exhibited very weak Nd^{3+} luminescence as one band at 800 nm. The equally weak (0.85 μW cm^{-2}) metal-centred emission was generated by a doped device based on phenalenone complex **Nd16** with the polymeric PVK matrix.[136] The EL spectrum was recorded only in the 1000 – 1200 nm range where only one band at 1065 nm was observed.

Structure 81

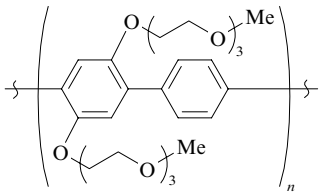


81 (F8BT)

Of a large number of possible f – f transitions, the EL spectra of samarium complexes showed, as a rule, only the bands in the visible range. However, in some cases with a favourable proportion of the triplet level energy of the ligands and the metal resonance bands, the spectra show NIR luminescence band, in addition to the bands in the visible range. In particular, samarium dibenzoylmethanate **Sm1** in a four-layer OLED device showed nine bands in the range 700 – 1400 nm (transitions $^4G_{5/2} \rightarrow {}^6H_{11/2}$, $^6H_{13/2}$, $^6F_{1/2}$, $^6F_{3/2}$, $^6H_{15/2}$, $^6F_{5/2}$, $^6F_{11/2}$ and Stark splitting of the $^6F_{7/2}$ and $^6F_{9/2}$ bands) and three bands in the visible range characteristic of Sm^{3+} (567, 609 and 649 nm) corresponding to the $^4G_{5/2} \rightarrow {}^6H_{5/2}$, $^6H_{7/2}$, $^6H_{9/2}$ transitions.[137] Later, analogous dibenzoylmethanate **Sm17** with the unsubstituted phenanthroline ligand was synthesized. The LED based on this phosphor generated stronger emission in the IR range.[138]

The theoretical luminescence spectrum of Ho^{3+} ion shows two bands in the visible range [at 545 ($^5S_2 \rightarrow {}^5I_8$) and 660 nm ($^5F_5 \rightarrow {}^5I_8$)] and three bands in the NIR range [980 ($^5F_5 \rightarrow {}^5I_7$), 1200 ($^5I_6 \rightarrow {}^5I_8$), 1500 nm ($^5F_5 \rightarrow {}^5I_6$)]. However, the complete set of the bands in the PL and EL spectra of holmium complexes has been observed very rarely. In particular, holmium derivatives with 8-hydroxyquinolinate,[139] benzoxazolyl- and benzothiazolylphenolate,[121] as well as with benzoxazolyl- and benzothiazolylnaphtholate[122] ligands, exhibit metal-centred EL as a single band at 660 nm. Only two NIR-emitting LEDs with a holmium-containing emissive layer have been mentioned in the literature: ITO/TPD/**Ho1**/Mg:Ag (Ref. 140) and ITO/PEDOT:PSS/PPP-OR11:**Ho5**/Ca/Al [PPP-OR11 is substituted poly(*p*-phenylene) **82**].[130, 141] Studying the EL properties of dibenzoylmethanate complex **Ho1** with neutral bathophenanthroline ligand showed that, in addition to the band of exciplexes (λ_{max} = 560 nm) formed through interaction of emitter and TPD (**5**) molecules, the complex gives rise to four emission bands peaking at 660, 980, 1200 and 1500 nm (Fig. 8). The presence of the band at 1500 nm corresponding to the $^5F_5 \rightarrow {}^5I_6$ transition, despite the low efficiency of the sample, makes it possible to predict potential application of holmium compounds in optical communication systems. Heteroligand compound **Ho5** with hydridotris(1-pyrazolyl)borate and porphyrin ligands introduced into the PPP-OR11 matrix exhibited weak emission at 1200 nm.

Structure 82



82 (PPP-OR11)

Erbium compound have always attracted special attention since the luminescence spectrum of Er^{3+} ion shows two bands in the NIR range at 1530 ($^4I_{13/2} \rightarrow {}^4I_{15/2}$) and 2940 nm ($^4I_{11/2} \rightarrow {}^4I_{13/2}$). The former is in the range of fibre optic communication lines, and the latter is promising for biomedical applications of Er compounds.[142 – 145] The first report on erbium electrophosphor Erq_3 (**Er2**) generating, in an ITO/TPD/**Er2**/Al OLED cell, luminescence at 1524 nm (Fig. 9), has served as an impetus for an active search for coordination erbium-containing emitters. The most widely studied class of electroluminescent erbium compounds are β-diketonates with the neutral phenanthroline [complexes **Er18** (Ref. 146) and **Er17** (Ref. 147)], bath-

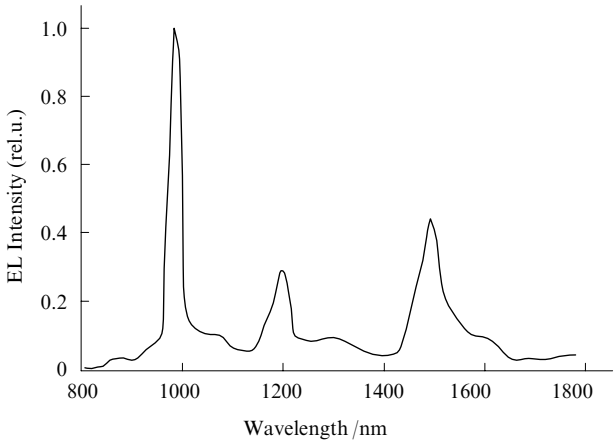


Figure 8. Electroluminescence spectrum of ITO/TPD/**Ho1**/Mg:Ag (ITO/**5**/**Ho1**/Mg:Ag) OLED.[140]

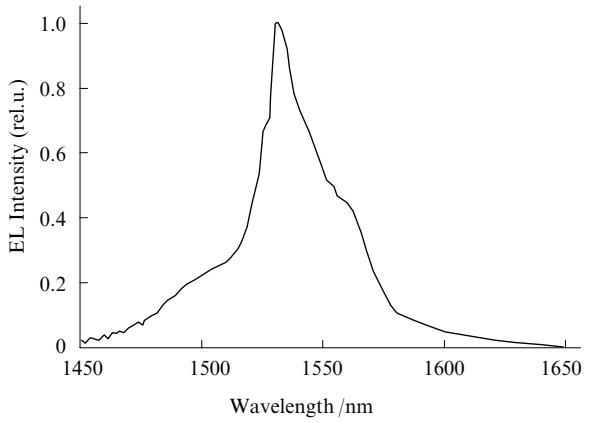


Figure 9. Electroluminescence spectrum of a device based on complex **Er2**.[144]

ophenanthroline [**Er1** (Refs 126, 128 148) and **Er19** (Ref. 149)], 5-nitrophenanthroline [**Er20** (Refs 150, 151) and **Er21** (Ref. 149)] and bipyridine [**Er22** (Refs 150, 152) and **Er3** (Ref. 127)] ligands. It has been shown that complex **Er1** can be used for design of a LED with a voltage-modulated IR spectrum,[128] mentioned above, and codeposition of this compound with the iridium phosphor $Ir(ppy)_3$ onto a substrate leads to a fourfold increase in the erbium band intensity in the EL spectrum as compared with an undoped device caused by energy transfer from the ^{3}MLCT level of $Ir(ppy)_3$ to the $^3T_1$ level of the dibenzoylmethanate ligand.[148] 1,1,1-Trifluoropentane-2,4-dione (complex **Er19**) and 1,1,1-trifluoro-5,5-dimethylhexane-2,4-dione (**Er20**) derivatives with nitro-substituted phenanthroline in OLED cells are characterized by more complete photoexcitation energy transfer from the organic environment to the Er^{3+} ion and less active metal-centred emission as compared with analogous complexes with the Bath ligand, which evidently imparts better charge-transport properties to these compounds.[149, 151] The highest emission intensity (0.93 μW cm^{-2}at 12.5 V) was demonstrated by a device with dibenzoylmethanate **Er17** in the Bath matrix and uncommon composition of the electrodes p-Si/SiO_2/NPB/Bath:**Er17**/Bath/Bath:Cs_2CO_3/Sm/Au (NPB = **9**),[147] whereas the EL efficiency 0.0011%, the highest among erbium-containing OLED devices, was revealed for an OLED with complex **Er3** based on hexafluoroacetylacetonate.[127]

The only erbium β-diketonate compound with an acylpyrazolone ligand emitting under electroexcitation (transition $^4I_{13/2} \rightarrow {}^4I_{15/2}$) is complex **Er4**.[153] A multilayer LED based on this material generates emission with λ_{max} = 1538 nm, its maximum intensity being no higher than 0.21 μW cm^{-2} at 19 V. Erbium derivatives with N,O-chelating ligands analogous to neodymium compounds **Nd9**–**Nd12** also exhibit weak IR electroluminescence.[121, 122] The shift of the triplet level of the organic environment with respect to the hypersensitive resonance level of the metal $^2H_{11/2}$ ($\sim$19 200 cm^{-1}) caused by the replacement of the oxygen atom by the sulfur atom in the heterocyclic moiety or extension of the π-conjugated system of the ligands leads to a decrease in emission efficiency of the lanthanide ion in OLED devices up to its complete disappearance for methyl-substituted (benzoxazolyl)naphtholates.[134] An interesting feature of substituted phenolates **Er3** and **Er4** it their ability to generate short-wavelength emission under electroexcitation, corresponding to the upconversion f–f transitions $^2H_{11/2} \rightarrow {}^4I_{15/2}$ (527 nm) and $^4S_{3/2} \rightarrow {}^4I_{15/2}$ (548 nm), which is not observed under photoexcitation of the compounds.[121] The only explanation of such spectral changes can be the difference in the mechanisms of photo- and electroexcitation of lanthanide complexes. The possibility of IR electroluminescence at 1570 nm in a doped polymeric OLED cell with an active layer made of porphyrin derivative **Er5** (Ref. 141) and PPP-OR11 (**82**) has been demonstrated only at the qualitative level, which allows us to assume a low efficiency of metal centre sensitization by a similar ligand. A relatively high metal-centred emission intensity (0.46 μW cm^{-2}) was achieved for ITO/NPB/CBP/**Er8**/BCP/LiF/Al (ITO/**9**/**35**/**Er8**/**31**/LiF/Al) with 8-hydroxy-2-pyridylnaphthyridine complex;[133] however, the EL efficiency of this compound (0.0004%) turned out to be more than twice as low as the efficiency found for complex **Er3**.

A less popular, but nevertheless fruitful, strategy for design of IR OLED devices is the introduction of inorganic materials into organic matrices. In particular, Cheng *et al.*[154] observed a fourfold increase in the intensity of the band at λ_{max} = 1530 nm in the EL spectrum of a LED with a doped active layer Alq_3:ErF_3 as compared with the cell based on complex **Er17**.

Although the energy diagram of Tm^{3+} ion shows a large number of levels, there are only three emission transitions in OLED devices: $^1G_4 \rightarrow {}^3H_6$, $^3H_4 \rightarrow {}^3H_6$ and $^3H_4 \rightarrow {}^3F_4$, which corresponds to emission in the visible range at 480 nm and NIR range at 800 and 1400 nm. However, all three bands have not been simultaneously observed in the PL and EL spectra of the compounds studied so far. In particular, the ITO/TPD/**Tm2**/Yb OLED based on thulium 8-hydroxyquinolinate complex shows only weak emission at λ_{max} = 795 nm.[139] An analogous spectrum of metal-centred luminescence was observed when studying the EL properties of compound **Tm23** with thiobenzothiazole ligands[155] and benzoxazolyl- and benzothiazolyl derivatives **Tm9**, **Tm10**,[121] **Tm11**, **Tm12**,[122] **Tm13** and **Tm14**;[134] the highest IR emission intensity (8 W cm^{-2} at 19 V) is generated by benzothiazolylnaphtholate **Tm12** in an ITO/TPD/**Tm12**/Bath/Yb cell. LEDs based on dibenzoylmethanate derivatives $Tm(dbm)_3$(phen) (**Tm17**) and $Tm(dbm)_3$(Bath) (**Tm1**)[156] exhibit a narrow band peaking at 803 nm and a broad emission band at 1450 nm (Fig. 10), whereas analogous acetylacetonate complexes **Tm18** and **Tm24** (Refs 156 and 157) show weak IR luminescence at 800 nm and blue emission at 480 nm. Comparison of the luminescent properties of compound with β-diketonate ligands has shown that, in thulium phosphors, anionic ligands have a stronger effect on metal-centred luminescence than neutral coordinatively bonded ligands.

Among lanthanide ions, Yb^{3+} is unique since it has only one resonance level lying 10 200 cm^{-1} higher than the ground state. This feature is responsible for the presence of only one metal-centred emission band in the luminescence spectra of Yb complexes; it is observed at 976–980 nm and corresponds to the $^2F_{5/2} \rightarrow {}^2F_{7/2}$ transition. In addition to a narrow peak, the PL and EL spectra, as a rule, show also a broad band or several poorly resolved bands corresponding to optical transitions of electron between the Stark sublevels of the ion. The shape of these bands depends on the ligand field symmetry of a particular

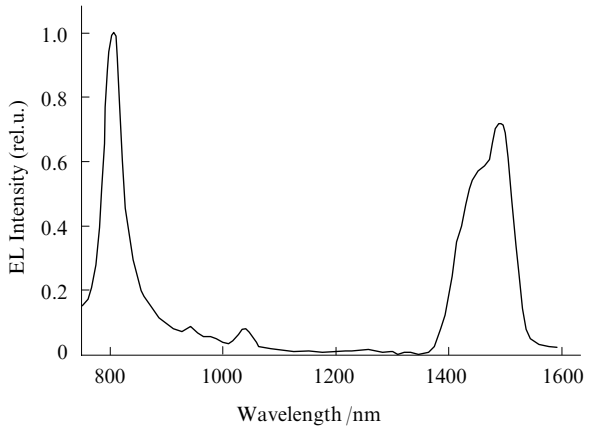


Figure 10. Electroluminescence spectrum of LED ITO/TPD/**Tm9**/Mg:Ag.[156]

organic metal complex. The electroluminescence of an ytterbium complex (8-hydroxyquinolinate **Yb2**) was first reported by Khreis *et al.*[158] The ITO/TPD/**Yb2**/Al device thry designed showed emission at 980 nm (Fig. 11) with an efficiency of 0.01%. The authors have assumed that the compound is a monomeric molecule similar in structure to the known Alq_3 complex. However, it has been recently established that ytterbium hydroxyquinolinate has a trinuclear structure in which the metal atoms are surrounded by five terminal and four bridging ligands.[159] According to laser desorption – ionization time-of-flight mass spectrometry, the complex retains its structure in the course of evaporation – deposition onto a substrate in vacuum, which is an important characteristics of electroluminescent materials used for fabrication of OLED devices. The LED with the optimized ITO/TPD/**Yb25**/Bath/Yb structure showed IR emission with a maximum intensity of 50 μW cm^{-2} at 15.5 V.

It has been found for polymeric OLED cells based on tetraphenylporphyrin compounds with one acetylacetonate (complex **Yb26**)[141, 160] or tris(pyrazolyl)borate ligand (**Yb5**),[130, 141] as well as with a cobalt cyclopentadienyltris(diethylphosphinate) moiety (**Yb27**),[130, 161] that the use of conjugated polymer PPP-OR11 (**82**) as a matrix containing 2 mol.% of an IR phosphor, leads to a fivefold increase in the efficiency of metal-centred luminescence (λ_{max} = 977 nm) as compared with a device based on the MEH-PPV (**71**) matrix owing to more complete Förster electroexcitation energy transfer from the PPP-OR11 units to the guest molecules.[160] An increase in the concentration of complexes **Yb26, Yb5** and **Yb27** in an emission layer up to 67 mol.% enhances the EL efficiency and charge mobility in a nanostructure whatever the matrix material [PPP-OR11 (**82**), poly(methyl methacrylate (PMMA), poly(butyl methacrylate) (PBMA), polystyrene (PS), poly(bisphenol A carbonate) (PC)].[130] Thus, major conductors of charge carriers in the active layer of the OLEDs under consideration are ytterbium porphyrin complexes. Maximum IR emission intensity (11 μW cm^{-2} at 10 V) and efficiency (0.013%) were achieved for ITO/PEDOT:PSS/PPP-OR11:**Yb5**(15 mol.%)/Ca/Al [ITO/**11**:**12**/**82**:**Yb5**(15 mol.%)/Ca/Al].[130] Much better EL characteristics (R_{max} = 86 μW cm^{-2}, η^{EL}_{ext} = 0.14%) were found for a model OLED ITO/NPB/CBP/**Yb8**/BCP/LiF/Al (ITO/**9**/**35**/**Yb8**/**31**/LiF/Al) with a compound analogous in structure to **Nd8** and **Er8**.[133]

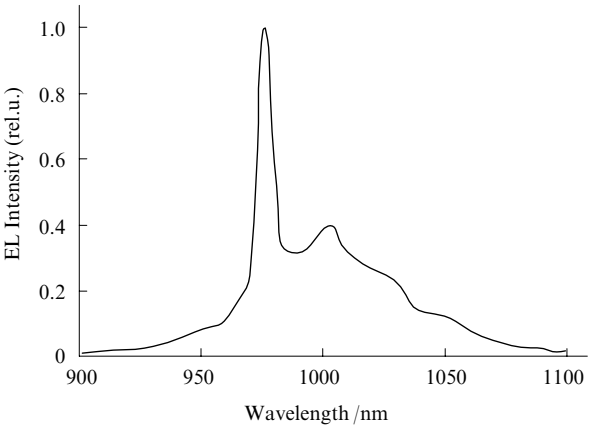


Figure 11. Electroluminescence spectrum of the OLED cell ITO/TPD/**Yb2**/Al.[158]

Studying dibenzoylmethanates **Yb1** (Refs 126 and 162) and **Yb28** (Ref. 161) has shown that, in addition to efficient luminescence at λ_{max} = 985 nm, they are characterized by good charge-conducting properties, which makes it possible to use these materials not only as the emission layer but also the electron-transport layer in LEDs.[162] A large difference in energy (10 400 cm^{-1}) between the $^3T_1$ level of anionic ligand (20 600 cm^{-1}) and the $^2F_{5/2}$ resonance level of ytterbium ion (10 200 cm^{-1}), as well as the absence of spectral overlap of the ligand emission and metal centre absorption in complex **Yb1** (Ref. 126) are not favourable for successful intramolecular excitation energy transfer *via* the Dexter and Förster mechanisms. The authors assume that there are two possible explanations of sensitization of Yb^{3+} emission: (1) filling of the $^2F_{5/2}$ state of the Yb^{3+} ion *via* energy transfer from high-energy vibrational sublevels of the $^1S_0$ state of the ligand,[163] and (2) realization of an alternative redox mechanism of luminescence excitation, suggested by Horrocks *et al.*[164] and then studied by Ala-Kleme *et al.*[165] The replacement of phenyl substituents in complex **Yb1** by naphthyl substituents results in a decrease in the HOMO – LUMO optical gap for complex **Yb28**, which is responsible for the 10-fold increase in EL intensity in the PPP-OR11 matrix owing to more complete excitation energy transfer caused by the better overlap of the emission spectrum of the polymer and the absorption spectrum of **Yb28** than in the case of **Yb1**.[161] Like complex **Yb1**, two acylpyrazolonate derivatives **Yb4** and **Yb29** (Ref. 166) were used as, respectively, a luminescent and charge-conducting material for ITO/**Yb4**/**Yb29**/LiF/Al OLED. The sample exhibited low EL intensity and efficiency: 1.4 μW cm^{-2} and 0.027%. The highest EL characteristics among the known ytterbium β-diketonates were observed for hexafluoroacetylacetonate **Yb3** with neutral bipyridine ligand. The OLED device based on this complex generated strong IR emission — 93 μW cm^{-2} at 16 V.

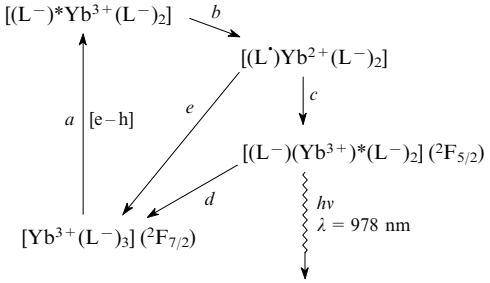
Analysis of luminescent characteristics of ytterbium diketonate derivatives shows that a neutral molecule, not containing H_2O molecules (luminescence quenchers) in the coordination sphere of the metal, is often formed by neutral ligands, which, on the one hand, stabilize the complex, and, on the other hand, can reduce the f – f luminescence lifetime

because of the lowering of symmetry of the electrostatic ligand field at the point of the Ln^{3+} ion and the presence of additional quenchers (CH groups). To synthesize a nine-coordinate complex with three equivalent anionic ligands, Massi and co-workers[167] carried out the reaction of $YbCl_3\,6\,H_2O$ with 2-benzoyl-1,3-diphenylpropane-1,3-dione (L) in ethanol in the presence of KOH. However, product **Yb30** isolated from the reaction mixture turned out to be the tetranuclear complex $[Yb(K\ HOEt)L_4]_2$. The compound demonstrated long-lifetime metal-centred emission (47 s) with a PL quantum yield of 3.9%. Its luminescence intensity in the OLED cell at 12.9 V was 390 μW cm^{-2}, which was more than four times higher than the characteristics for complex **Yb3**. The same objective (the decrease in the number of CH groups) was pursued in the synthesis of pentafluorophenolate complex **Yb7**.[120] The compound exhibited moderate IR luminescence intensity.

Ytterbium, along with Nd, Sm, Eu, Dy and Tm, is a rare earth metal that has, in addition to the stable oxidation state 3+, a metastable divalent state. The stability of organic derivatives of Ln^{2+} decreases,[168] while the Ln^{3+}/Ln^{2+} electrode potential (E_p) increases in the row Eu (−0.35 V) > Yb (−1.15 V) > Sm (−1.55 V) > Tm (−2.30 V) > Dy (−2.50 V) > Nd (−2.60 V).[169] Since PL and EL of metal complexes are sometimes realized through the charge transfer excitation state, which implies partial electron density transfer from the ligand orbitals to the metal orbitals (LMCT) or from the metal orbitals to the ligand orbitals (MLCT), it can be concluded that the redox properties of a lanthanide have an effect on the luminescence efficiency of complexes. The optimal proportion between the redox potentials of the metal and ligand enables complete and reversible electron transfer from the metal to the ligand, *i.e.*, reversible Ln^{3+}/Ln^{2+} reduction. For the first time, such a possibility was emphasized by Horroks *et al.*,[164] who suggested the redox excitation mechanism, involving reversible electron transfer Trp − Ln, in order to explain PL of Yb^{3+} ions and the lack of luminescence of Eu^{3+} ions in complexes with parvalbumin [tryptophan-containing (Trp) protein]. Neutral tryptophan absorbs a photon and is converted into the excited state Trp*, which is able to reduce Eu^{3+} and Yb^{3+} ions. The resulting system contains the radical cation $Trp^{+\bullet}$ and Ln^{2+} ion. In the case of europium, the system energy is lower than the excited emission state energy (Eu^{3+})*, so that excited europium cation does not form and subsequent relaxation of the system into the ground state $[Trp - Eu^{3+}]$ is a nonradiative process. The energy of the ytterbium system $[Trp^{+\bullet} - Yb^{2+}]$ is higher than the emission level ($^2F_{5/2}$) energy of trivalent Yb^{3+} ion, which makes possible the formation of excited ion (Yb^{3+})*, which exhibits metal-centred luminescence in the course of relaxation.

The redox mechanism of excitation of ytterbium ions, suggested by Horroks and later developed by other researchers,[170, 171] was used in our study for explaining the lack of europium luminescence and the high EL intensity of ytterbium in complexes with 3-(2-benzoxazolyl)phenol (**Yb9**),[121] 3-(2-benzothiazolyl)phenol (**Yb10**),[121] 3-(2-benzoxazolyl)-2-naphthol (**Yb11**, **Yb31**),[122, 172] 3-(2-benzothiazolyl)-2-naphthol (**Yb12**, **Yb32-Yb35**),[122, 172, 173] 3-(5-methyl-2-benzoxazolyl)-2-naphthol (**Yb13**)[134] and 3-(6-methyl-2-benzoxazolyl)-2-naphthol (**Yb14**).[134] All these compounds exhibited enhanced metal-centred emission as compared with their Nd, Tm and Er analogues. The strongest EL (889 μW cm^{-2} at 19.2 V) in a model LED ITO/TPD/Yb complex/Bath/Yb was shown by naphtholate **Yb12**.[122] The maximum external quantum efficiency of the LED was as high as 1.6%. This result exceeds more than twofold the intensity and almost tenfold the emission efficiency of β-diketonate **Yb30**, which is the best among the other ytterbium electrophosphors. The revealed 'hyper-emission' of the ytterbium ion in complex **Yb12** cannot be explained in the framework of the classical scheme — excitation energy transfer from the ligand to the metal centre by the Dexter or Förster mechanism, since the energy gap $E(^3T_1)$ — $E(^2F_{5/2})$ 5850 cm^{-1} is considerably larger than the optimal one; in addition, the spectra do not show the overlap of ligand emission and Yb^{3+} absorption. Conversely, the alternative redox mechanism of Yb^{3+} excitation, similar to the above Horroks mechanism, is consistent well with the data obtained. It is assumed that ytterbium luminescence in the phenolates and naphtholates is caused by reversible intramolecular electron transfer and involves several stages (Scheme 1).

Scheme 1



At the first stage (stage *a*), electron – hole recombination ([e – h]) occurs on the ligand, which leads to the formation of the excited anionic ligand exhibiting higher reduction ability as compared with the nonexcited ligand. The second stage (*b*) — electron transfer from the excited ligand to the Yb^{3+} ion to give the free radical ligand $L^{\bullet}$ coordinated to the Yb^{2+} cation. At stage *c*, back electron transfer occurs from the Yb^{2+} ion to radical $L^{\bullet}$ to give anionic ligand L^- and excited cation (Yb^{3+})*. Stage *d* is radiative relaxation of (Yb^{3+})* to the ground state $^2F_{7/2}$ to give the initial complex $Yb(L^-)_3$. In addition, a parallel process is possible — back electron transfer from the Yb^{2+} ion to the $L^{\bullet}$ radical without formation of the excited cation (Yb^{3+})* and nonradiative transition of the system to the initial state $Yb(L^-)_3$. Since the scheme describes the process as ytterbium chemiluminescence, parity selection rule and shielding of the 4f electrons by the 5s and 5p electrons cannot prevent the efficient population of the excited $^2F_{5/2}$ level of the Yb^{3+} ion, which is responsible for its strong luminescence. In agreement with this mechanism, europium complexes do not show metal-centred emission, since the energy of the excited (Eu^{3+})* ion is considerably higher than the energy of the $[L^{\bullet} - Eu^{2+}]$ system, which rules out the possibility of population of the luminescent levels of Eu^{3+}.

To prove the suggested energy scheme of luminescence, ytterbium complexes with naphtholate ligands containing the methyl substituent in the 5- or 6-position of the benzoxazole moiety have been synthesized.[134] Tests of these compounds in three-layer OLED devices have shown

that the introduction of the methyl group in these positions of the benzoxazole moiety has almost no effect on the charge-transport properties of materials but influences the metal-centred emission intensity. In particular, the intensity of ytterbium luminescence in complex **Yb13** is three times lower than that in unsubstituted analogue **Yb12**; the triplet level energies of the 3-(2-benzothiazolyl)-2-naphtholate (16 050 cm^{-1}) and 3-(5-methyl-2-benzoxazolyl)-2-naphtholate (16 800 cm^{-1}) ligands are very close to each other. This fact is not explained in the framework of the classical scheme of Yb^{3+} excitation, but it is consistent with the suggested redox mechanism.

The characteristics of the most efficient devices based on rare earth complexes are summarized in Table 4.

Comparison of the characteristics of IR electrophosphors enables the conclusion that neat organic compounds are less efficient than metal complex emitters; it is likely that the characteristics of organic compounds will not compare with metal complex emitters in the future, despite actually infinite possibilities to modify organic molecules. Conversely, the potential of emission materials based on d and f transition metals seems to be far from being exhausted in both emission efficiency and maximum wavelength. The validity of the prediction is supported by the existence of theoretically possible long-wavelength f–f transition for Er^{3+} ions ($^4I_{11/2} \rightarrow {}^4I_{13/2}$, 2.9 m; $^4I_{9/2} \rightarrow {}^4I_{11/2}$, 4.5 m; $^4F_{9/2} \rightarrow {}^4I_{9/2}$, 3.5 m). However, for such metal-centred emission to be realized, ligands are required that have a very high sensitization efficiency, which are not currently available.

IV. Conclusion

The reviewed data demonstrate that organic compounds, organometallic and coordination complexes can be successfully used for design of LEDs emitting in the UV and NIR

Table 4. Operating characteristics of IR-emitting OLED devices based on lanthanide complexes.

Device	V_0/V	λ_{max}/nm	R_{max}/μW cm^{-2}	η_{ext}^{EL} (%)	Ref.
TPD/TPD:**Pr1**/**Pr1**/Mg:Ag	7.5	608, 890, 1015, 1065, 1065	50[a] (15)	–	119
TPD/**Nd2**/Al	13	900, 1060, 1320	–	–	123
CuPc/**Nd3**/BCP/Alq_3/LiF/Al	–	880, 1060, 1350	28 (16)	0.022	127
NPB/**Nd4**/BCP/Alq_3/LiF/Al	8.1	890, 1060, 1336	0.21 (16.5)	–	129
NPB/**Nd6**/BCP/Alq_3/Mg:Ag	14	900, 1060, 1350	6.1 (18)	0.3	132
TPD/**Nd7**/Yb	7.5	580, 808, 900, 1064	18 (20)	0.14	120
NPB/CBP:**Nd8**/LiF/Al	–	880, 1064, 1330	25	0.019	133
TPD/**Nd9**/Bath/Yb	8	601, 807, 882, 1069	74 (17)	–	121
TPD/**Nd12**/Bath/Yb	6.5	1347, 586, 810, 885, 1060	80 (18.5)	0.03	122
TPD/**Nd14**/Bath/Yb	5	550, 820, 910, 1060, 1340	85 (22)	0.04	134
TPD/TPD:**Sm1**/**Sm1**/Bath/Mg:Ag	4.5	713, 797, 887, 909, 932, 953, 1010, 1036, 1148, 1183, 1406	–	–	137
TPD/**Ho1**/Mg:Ag	9	570, 660, 980, 1200, 1500	–	–	140
TPD/**Er1**/BCP/Mg:Ag/Ag	18	400, 530, 545, 1540	–	0.0001	126
TPD/**Er2**/Al	12	600, 1524	–	–	144
PEDOT:PSS/**Er19**/Ca/Al	4	1530	–	–	149
CuPc/CBP:**Er3**/BCP/Alq_3/LiF/Al	9	1530	0.50 (17)	0.0011	127
NPB/**Er4**/BCP/Alq_3/LiF/Al	12	1538	0.21 (19)	–	153
NPB/CBP/**Er8**/BCP/LiF/Al	9	1530	0.46 (16)	0.0004	133
TPD/**Tm2**/Yb	–	525, 795	–	–	139
TPD/**Tm23**/Yb	–	795	–	–	155
TPD/**Tm11**/Bath/Yb	6.8	530, 795	3.6 (18)	–	122
TPD/**Tm12**/Bath/Yb	6.1	590, 800	8 (19)	0.001	122
TPD/**Tm13**/Bath/Yb	5	522, 795	5.8 (22)	0.0032	134
TPD/**Tm14**/Bath/Yb	4.5	522, 795	7 (22)	0.0043	134
TPD/**Tm17**/Mg:Ag	–	803, 1450	–	–	156
TPD/**Yb2**/Bath/Yb	9.5	530, 979	50 (15.5)	–	159
PEDOT:PSS/PPP-OR11:**Yb5**/Ca/Al	4	977	11 (10)	0.013	130
NPB/CBP/**Yb8**/BCP/LiF/Al	5	976	86 (16)	0.14	133
ITO/**Yb4**/**Yb29**/LiF/Al	6.7	980	1.47 (17.8)	0.027	166
CuPc/CBP:**Yb3**/BCP/Alq_3/LiF/Al	4	983	93 (16)	0.18	127
mCP/mCP:**Yb30**/TPBi/LiF/Al	6	980	390 (12.9)	0.17	167
TPD/**Yb7**/Yb	6	580, 979	90 (18.5)	1.2	120
TPD/**Yb9**/Bath/Yb	8	982	154 (18)	–	121
TPD/**Yb10**/Bath/Yb	6	982	286 (18)	–	121
TPD/**Yb11**/Bath/Yb	9.3	530, 978	316 (19.8)	0.6	122
TPD/**Yb12**/Bath/Yb	5.7	580, 978	889 (19.2)	1.6	122
TPD/**Yb13**/Bath/Yb	4.5	522, 979	315 (22)	–	134
TPD/**Yb14**/Bath/Yb	4.5	522, 979	320 (22)	–	134

Note. TPD = **5**, BCP = **31**, NPB = **9**, PEDOT = **11**, PSS = **12**, CBP = **35**, PPP-OR11 = **82**. [a] In cd m^{-2}.

ranges. In their technical characteristics, devices are not inferior to solid analogues, and in some of parameters, they are better. The most efficient organic electrophosphors make it possible to design LED cells generating UV emission with an intensity of 5 mW cm^{-2} at 393 nm.[29] The shortest wavelength emission with $\lambda_{max} = 352$ nm was obtained on a device with the organic emitter 1,3-bis[2-(4-*tert*-butylphenyl)-1,3,4-oxadiazol-5-yl]benzene (OXD-7, **33**).[24] The best characteristics for NIR-emitting devices (25 mW cm^{-2} at 15 V, quantum yield 14.5%) were achieved with the use of platinum dipyridylphenyl complex **Pt9**.[108] However, the wavelength in this case (700 nm) was at the edge of the visible range. The brightest NIR emitter ($\lambda_{max} = 720$ nm) — analogous platinum complex **Pt8** with the methyl substituent in the phenyl ring — exhibited the intensity 15.9 mW cm^{-2}, but at a very high voltage (100 V).[107] The maximum emission wavelength for organic compounds and d-metal complexes in OLED devices of different configuration does not exceed 1100 nm. By this characteristic, the first place is held by lanthanide complexes, in particular, neodymium [1350 nm (Ref. 127)], holmium [1500 nm (Ref. 140)] and erbium [1538 nm (Ref. 153)] derivatives; however, their luminescence intensity does not exceed 20 – 80 μW cm^{-2}.

Despite significant progress achieved in the area of organic UV- and NIR-emitting LEDs, there are issues that should be solved to make these devices attractive for producers and consumers. Among these issues are EL intensity, stability and service life of devices, extension of the wavelength range toward deep UV and far IR ranges. Noteworthy is also the problem of development of simple and convenient methods for synthesis of electroluminescent materials, which can emerge in launching of large-scale production of organic UV and NIT emitters. Relevant studies are underway in many research centres.

The preparation of this review was supported by funding from the Russian Science Foundation (Project No. 14-13-01158).

References

1. C W Tang, S A VanSlyke *Appl. Phys. Lett.* **51** 913 (1987)
2. *Highly Efficient OLEDs with Phosphorescent Materials* (Ed. H Yersin) (Weinheim: Wiley-VCH, 2008)
3. *Lanthanide Luminescence. Photophysical, Analytical and Biological Aspects* Vol. 7 (Eds P Hänninen, H Härmä) (Heidelberg: Springer, 2011)
4. *Luminescence: from Theory to Applications* (Ed. C Ronda) (Weinheim: Wiley-VCH, 2008)
5. J Kalinowski *Organic Light-Emitting Diodes. Principles, Characteristics, and Processes* (New York: Marcel Dekker, 2005)
6. *Organic Light Emitting Diode* (Ed. M Mazzeo) (Rijeka: Sciyo, 2010)
7. M N Bochkarev, A G Vitukhnovskii, M A Katkova *Organicheskie Svetoizluchayushchie Diody (OLED)* [Organic Light Emitting Diodes (OLED)] (Nizhny Novgorod: DEKOM, 2011)
8. J-C G Bünzli, S V Eliseeva *J. Rare Earths* **28** 824 (2010)
9. R T Wegh, A Meijerink, R-J Lamminmäki, J Hölsä *J. Lumin.* **87 – 89** 1002 (2000)
10. C-K Duan, P A Tanner *J. Phys. Chem. A* **114** 6055 (2010)
11. W A Barnett, M L H Wise, E C Jones *J. Microsc.* **105** 299 (1975)
12. S F Varol, S Sayin, S Eymur, Z Merdan, D Ünal *Org. Electron.* **31** 25 (2016)
13. D B Romero, F Nüesch, T Benazzi, D Adès, A Siove, L Zuppiroli *Adv. Mater.* **9** 1158 (1997)
14. K Okumoto, Y Shirota *Appl. Phys. Lett.* **79** 1231 (2001)
15. A M-C Ng, A B Djurišić, K-H Tam, K W Cheng, W-K Chan, H L Tam, K -W Cheah, A W Lu, J Chan, A D Rakić *Opt. Commun.* **281** 2498 (2008)
16. J Kido, K Hongawa, K Okuyama, K Nagai *Appl. Phys. Lett.* **63** 2627 (1993)
17. J Huang, H Zhang, W Tian, J Hou, Y Ma, J Shen, S Liu *Synth. Met.* **87** 105 (1997)
18. Q Zhang, J Li, K Shizu, S Huang, S Hirata, H Miyazaki, C Adachi *J. Am. Chem. Soc.* **134** 14706 (2012)
19. T-C Chao, Y-T Lin, C-Y Yang, T S Hung, H-C Chou, C-C Wu, K-T Wong *Adv. Mater.* **17** 992 (2005)
20. K-T Wong, Y-L Liao, Y-T Lin, H-C Su, C-C Wu *Org. Lett.* **7** 5131 (2005)
21. H Etori, X L Jin, T Yasuda, S Mataka, T Tsutsui *Synth. Met.* **156** 1090 (2006)
22. N Cocherel, C Poriel, L Vignau, J-F Bergamini, J Rault-Berthelot *Org. Lett.* **12** 452 (2010)
23. K H Lee, Y S Kwon, J Y Lee, S Kang, K S Yook, S O Jeon, J Y Lee, S S Yoon *Chem. – Eur. J.* **17** 12994 (2011)
24. D G (Dan)Patel, Y-y Ohnishi, Y Yang, S-H Eom, R T Farley, K R Graham, J Xue, S Hirata, K S Schanze, J R Reynolds *J. Polym. Sci., Part B: Polym. Phys.* **49** 557 (2011)
25. H H Kang, M S Kang, D H Oh, D H Lee, D-C Shin, S-K Kwon, Y-H Kim *J. Appl. Polym. Sci.* **121** 43 (2011)
26. L Zou, V Savvate'ev, J Booher, C-H Kim, J Shinar *Appl. Phys. Lett.* **79** 2282 (2001)
27. R Liu, Y Cai, J-M Park, K-M Ho, J Shinar, R Shinar *Adv. Funct. Mater.* **21** 4744 (2011)
28. Y Park, S Kim, J-H Lee, D H Jung, C-C Wu, J Park *Org. Electron.* **11** 864 (2010)
29. Y Yang, P Cohn, S-H Eom, K A Abboud, R K Castellano, J Xue *J. Mater. Chem. C* **1** 2867 (2013)
30. Q-D Liu, J Lu, J Ding, M Day, Y Tao, P Barrios, J Stupak, K Chan, J Li, Y Chi *Adv. Funct. Mater.* **17** 1028 (2007)
31. A Fujii, K Yoshimoto, M Yoshida, Y Ohmori, K Yoshino *Jpn. J. Appl. Phys., Part 2* **34** L1365 (1995)
32. H Suzuki *J. Lumin.* **72 – 74** 1005 (1997)
33. S Hoshino, H Suzuki, M Fujiki, M Morita, N Matsumoto *Synth. Met.* **89** 221 (1997)
34. Y Xu, T Fujino, H Naito, K Oka, T Dohmaru *Chem. Lett.* 299 (1998)
35. H Suzuki, S Hoshino, C-H Yuan, M Fujiki, S Toyoda, N Matsumoto *Thin Solid Films* **331** 64 (1998)
36. S Hoshino, K Ebata, K Furukawa *J. Appl. Phys.* **87** 1968 (2000)
37. R J Holmes, S R Forrest, T Sajoto, A Tamayo, P I Djurovich, M E Thompson, J Brooks, Y-J Tung, B W D'Andrade, M S Weaver, R C Kwong, J J Brown *Appl. Phys. Lett.* **87** 243507 (2005)
38. N S Poluektov, Yu V Zelyukova, E A Zhikhareva, V T Mishchenko *Zh. Prikl. Spektrosk.* **17** 67 (1972)
39. A Strasser, A Vogler *Inorg. Chim. Acta* **357** 2345 (2004)
40. T Yu, W Su, W Li, R Hua, B Chu, B Li *Solid-State Electron.* **51** 894 (2007)
41. C P Shipley, S Capecchi, O V Salata, M Etchells, P J Dobson, V Christou *Adv. Mater.* **11** 533 (1999)
42. D M Kuzyaev, T V Balashova, M E Burin, G K Fukin, R V Rumyantcev, A P Pushkarev, V A Ilichev, I D Grishin, D L Vorozhtsov, M N Bochkarev *Dalton Trans.* **45** 3464 (2016)
43. D M Kuzyaev, R V Rumyantsev, G K Fukin, M N Bochkarev *Russ. Chem. Bull., Int. Ed.* **63** 848 (2014)

44. K Dedeian, J Shi, N Shepherd, E Forsythe, D C Morton *Inorg. Chem.* **44** 4445 (2005)
45. S Achilefu, R B Dorshow, J E Bugaj, R Rajagopalan *Invest. Radiol.* **35** 479 (2000)
46. A Fujii, M Yoshida, Y Ohmori, K Yoshino *Jpn. J. Appl. Phys., Part 2* **35** L37 (1996)
47. A Fujii, Y Ohmori, K Yoshino *IEEE Trans. Electron Devices* **44** 1204 (1997)
48. Z Fan, C Cheng, S Yu, K Ye, R Sheng, D Xia, C Ma, X Wang, Y Chang, G Du *Opt. Mater.* **31** 889 (2009)
49. Q Bai, C Zhang, C Cheng, W Li, J Wang, G Du *Chin. J. Chem.* **30** 689 (2012)
50. H Suzuki *Appl. Phys. Lett.* **76** 1543 (2000)
51. H Suzuki *Appl. Phys. Lett.* **80** 3256 (2002)
52. H Suzuki, K Ogura, N Matsumoto, P Prosposito, S Schutzmann *Mol. Cryst. Liq. Cryst.* **444** 51 (2006)
53. E I Maltsev, D A Lypenko, V V Bobinkin, A R Tameev, S V Kirillov, B I Shapiro, H F M Schoo, A V Vannikov *Appl. Phys. Lett.* **81** 3088 (2002)
54. Y Xuan, G Qian, Z Wang, D Ma *Thin Solid Films* **516** 7891 (2008)
55. B Stender, S F Völker, C Lambert, J Pflaum *Adv. Mater.* **25** 2943 (2013)
56. T Förster *Discuss. Faraday Soc.* **27** 7 (1959)
57. B-J Jung, C-B Yoon, H-K Shim, L-M Do, T Zyung *Adv. Funct. Mater.* **11** 430 (2001)
58. C-T Chen *Chem. Mater.* **16** 4389 (2004)
59. Y Yang, R T Farley, T T Steckler, S-H Eom, J R Reynolds, K S Schanze, J Xue *Appl. Phys. Lett.* **93** 163305 (2008)
60. Y Yang, R T Farley, T T Steckler, S-H Eom, J R Reynolds, K S Schanze, J Xue *J. Appl. Phys.* **106** 044509 (2009)
61. G Qian, Z Zhong, M Luo, D Yu, Z Zhang, D Ma, Z Y Wang *J. Phys. Chem. C* **113** 1589 (2009)
62. V Bulović, A Shoustikov, M A Baldo, E Bose, V G Kozlov, M E Thompson, S R Forrest *Chem. Phys. Lett.* **287** 455 (1998)
63. G Qian, B Dai, M Luo, D Yu, J Zhan, Z Zhang, D Ma, Z Y Wang *Chem. Mater.* **20** 6208 (2008)
64. G Qian, Z Zhong, M Luo, D Yu, Z Zhang, Z Y Wang, D Ma *Adv. Mater.* **21** 111 (2009)
65. X Du, J Qi, Z Zhang, D Ma, Z Y Wang *Chem. Mater.* **24** 2178 (2012)
66. L Yao, S Zhang, R Wang, W Li, F Shen, B Yang, Y Ma *Angew. Chem., Int. Ed.* **53** 2119 (2014)
67. M T Sharbati, F Panahi, A Gharavi *IEEE Photon. Technol. Lett.* **22** 1695 (2010)
68. M T Sharbati, F Emami *Opt. Express* **19** 3619 (2011)
69. M T Sharbati, F Panahi, A Shourvarzi, S Khademi, F Emami *Optik* **124** 52 (2013)
70. J Y Lee, K S Kim, B J Mhin *J. Chem. Phys.* **115** 9484 (2001)
71. S Ellinger, K R Graham, P Shi, R T Farley, T T Steckler, R N Brookins, P Taranekar, J Mei, L A Padilha, T R Ensley, H Hu, S Webster, D J Hagan, E W Van Stryland, K S Schanze, J R Reynolds *Chem. Mater.* **23** 3805 (2011)
72. M Berggren, G Gustafsson, O Inganäs, M R Andersson, O Wennerström, T Hjertberg *Appl. Phys. Lett.* **65** 1489 (1994)
73. D R Baigent, P J Hamer, R H Friend, S C Moratti, A B Holmes *Synth. Met.* **71** 2175 (1995)
74. M Chen, E Perzon, M R Andersson, S Marcinkevicius, S K M Jönsson, M Fahlman, M Berggren *Appl. Phys. Lett.* **84** 3570 (2004)
75. C J Brabec, C Winder, N S Sariciftci, J C Hummelen, A Dhanabalan, P A van Hal, R A J Janssen *Adv. Funct. Mater.* **12** 709 (2002)
76. X Li, Y Zhang, R Yang, J Huang, W Yang, Y Cao *J. Polym. Sci., Part A: Polym. Chem.* **43** 2325 (2005)
77. X Li, W Zeng, Y Xia, W Yang, Y Cao *J. Appl. Polym. Sci.* **102** 4321 (2006)
78. X Li, W Zeng, Y Zhang, Q Hou, W Yang, Y Cao *Eur. Polym. J.* **41** 2923 (2005)
79. R Yang, R Tian, J Yan, Y Zhang, J Yang, Q Hou, W Yang, C Zhang, Y Cao *Macromolecules* **38** 244 (2005)
80. R Yang, R Tian, Q Hou, W Yang, Y Cao *Macromolecules* **36** 7453 (2003)
81. K Li, G S M Tong, Q Wan, G Cheng, W-Y Tong, W-H Ang, W-L Kwong, C-M Che *Chem. Sci.* **7** 1653 (2016)
82. J C Ostrowski, K Susumu, M R Robinson, M J Therien, G C Bazan *Adv. Mater.* **15** 1296 (2003)
83. C-H Cheng, Z-Q Fan, S-K Yu, W-H Jiang, X Wang, G-T Du, Y-C Chang, C-Y Ma *Appl. Phys. Lett.* **88** 213505 (2006)
84. T C Rosenow, K Walzer, K Leo *J. Appl. Phys.* **103** 043105 (2008)
85. D-c Xia, W-c Li *Synth. Met.* **209** 549 (2015)
86. W He, C-H Chen, S-K Yu, Z-Q Fan, X-G Du, G-T Du *Russ. J. Inorg. Chem.* **54** 407 (2009)
87. Z Fan, C Cheng, S Yu, K Ye, D Xia, Q Bai, H Guan, G Du *Chin. Opt. Lett.* **7** 413 (2009)
88. F Yan, W Li, B Chu, H Liu, G Zhang, Z Su, J Zhu, L Han, T Li, Y Chen, C H Cheng, Z Q Fan, G T Du *Org. Electron.* **10** 1408 (2009)
89. F Yan, W L Li, B Chu, T L Li, W M Su, Z S Su, J Z Zhu, D F Yang, G Zhang, D F Bi, L L Han, C H Cheng, Z Q Fan, S K Yu, G T Du, T Tsuboi *Appl. Phys. Lett.* **91** 203512 (2007)
90. S Yu, C Ma, C Cheng, X Wang, D Ji, Z Fan, D Xia, W He, Y Chang, G Du *Dyes Pigm.* **76** 492 (2008)
91. T-C Lee, J-Y Hung, Y Chi, Y-M Cheng, G-H Lee, P-T Chou, C-C Chen, C-H Chang, C-C Wu *Adv. Funct. Mater.* **19** 2639 (2009)
92. J-L Liao, Y Chi, C-C Yeh, H-C Kao, C-H Chang, M A Fox, P J Low, G-H Lee *J. Mater. Chem. C* **3** 4910 (2015)
93. E L Williams, J Li, G E Jabbour *Appl. Phys. Lett.* **89** 083506 (2006)
94. R Tao, J Qiao, G Zhang, L Duan, L Wang, Y Qiu *J. Phys. Chem. C* **116** 11658 (2012)
95. L Xin, J Xue, G Lei, J Qiao *RSC Adv.* **5** 42354 (2015)
96. R Tao, J Qiao, G Zhang, L Duan, C Chen, L Wang, Y Qiu *J. Mater. Chem. C* **1** 6446 (2013)
97. J Qiao, L Duan, L Tang, L He, L Wang, Y Qiu *J. Mater. Chem.* **19** 6573 (2009)
98. C-L Ho, B Yao, B Zhang, K-L Wong, W-Y Wong, Z Xie, L Wang, Z Lin *J. Organomet. Chem.* **730** 144 (2013)
99. C Yi, C-J Yang, J Liu, M Xu, J-H Wang, Q-Y Cao, X-C Gao *Inorg. Chim. Acta* **360** 3493 (2007)
100. C Borek, K Hanson, P I Djurovich, M E Thompson, K Aznavour, R Bau, Y Sun, S R Forrest, J Brooks, L Michalski, J Brown *Angew. Chem., Int. Ed.* **46** 1109 (2007)
101. Y Sun, C Borek, K Hanson, P I Djurovich, M E Thompson, J Brooks, J J Brown, S R Forrest *Appl. Phys. Lett.* **90** 213503 (2007)
102. K R Graham, Y Yang, J R Sommer, A H Shelton, K S Schanze, J Xue, J R Reynolds *Chem. Mater.* **23** 5305 (2011)
103. J R Sommer, R T Farley, K R Graham, Y Yang, J R Reynolds, J Xue, K S Schanze *ACS Appl. Mater. Interfaces* **1** 274 (2009)
104. E Rossi, A Colombo, C Dragonetti, D Roberto, F Demartin, M Cocchi, P Brulatti, V Fattorie, J A G Williams *Chem. Commun.* **48** 3182 (2012)
105. E Rossi, L Murphy, P L Brothwood, A Colombo, C Dragonetti, D Roberto, R Ugo, M Cocchi, J A G Williams *J. Mater. Chem.* **21** 15501 (2011)
106. W Mróz, C Botta, U Giovanella, E Rossi, A Colombo, C Dragonetti, D Roberto, R Ugo, A Valore, J A G Williams *J. Mater. Chem.* **21** 8653 (2011)

107. M Cocchi, D Virgili, V Fattori, J A G Williams, J Kalinowski *Appl. Phys. Lett.* **90** 023506 (2007)
108. M Cocchi, J Kalinowski, D Virgili, J A G Williams *Appl. Phys. Lett.* **92** 113302 (2008)
109. F Nisic, A Colombo, C Dragonetti, D Roberto, A Valore, J M Malicka, M Cocchi, G R Freemane, J A G Williams *J. Mater. Chem. C* **2** 1791 (2014)
110. N Su, F Meng, J Chen, Y Wang, H Tan, S Su, W Zhu *Dyes Pigm.* **128** 68 (2016)
111. H-F Xiang, Z-X Xu, V A L Roy, B-P Yan, S-C Chan, C-M Che, P T Lai *Appl. Phys. Lett.* **92** 163305 (2008)
112. X Wu, Y Liu, Y Wang, L Wang, H Tan, M Zhu, W Zhu, Y Cao *Org. Electron.* **13** 932 (2012)
113. D M E Freeman, A Minotto, W Duffy, K J Fallon, I McCulloch, F Cacialli, H Bronstein *Polym. Chem.* **7** 722 (2016)
114. M E Burin, D M Kuzyaev, M A Lopatin, A P Pushkarev, V A Ilichev, D L Vorozhtsov, A V Dmitriev, D A Lypenko, E I Maltsev, M N Bochkarev *Synth. Met.* **164** 55 (2013)
115. S Comby, J-C G Bünzli, in *Handbook on the Physics and Chemistry of Rare Earths* Vol. 37 (Eds K A Gschneidner Jr, J-C G Bünzli, V K Pecharsky) (North-Holland, 2007) p. 217
116. M A Katkova, A G Vitukhnovskii, M N Bochkarev *Russ. Chem. Rev.* **74** 1089 (2005)
117. M N Bochkarev, M A Katkova, in *Handbook of Light Emitting and Schottky Diode Research* (Ed. N P Chen) (New York: Nova Science Publishers, 2009) p. 1
118. M A Katkova, M N Bochkarev *Dalton Trans.* **39** 6599 (2010)
119. Z Hong, C Liang, R Li, F Zang, D Fan, W Li, L S Hung S T Lee *Appl. Phys. Lett.* **79** 1942 (2001)
120. A P Pushkarev, V A Ilichev, A A Maleev, A A Fagin, A N Konev, A F Shestakov, R V Rumyantzev, G K Fukin, M N Bochkarev *J. Mater. Chem. C* **2** 1532 (2014)
121. M A Katkova, A P Pushkarev, T V Balashova, A N Konev, G K Fukin, S Yu Ketkov, M N Bochkarev *J. Mater. Chem.* **21** 16611 (2011)
122. A P Pushkarev, V A Ilichev, T V Balashova, D L Vorozhtsov, M E Burin, D M Kuzyaev, G K Fukin, B A Andreev, D I Kryzhkov, A N Yablonskiy, M N Bochkarev *Russ. Chem. Bull., Int. Ed.* **62** 392 (2013) [*Izv. Akad. Nauk, Ser. Khim.* 395 (2013)]
123. O M Khreis, R J Curry, M Somerton, W P Gillin *J. Appl. Phys.* **88** 777 (2000)
124. A O'Riordan, R Van Deun, E Mairiaux, S Moynihan, P Fias, P Nockemann, K Binnemans, G Redmond *Thin Solid Films* **516** 5098 (2008)
125. Y Kawamura, Y Wada, Y Hasegawa, M Iwamuro, T Kitamura, S Yanagida *Appl. Phys. Lett.* **74** 3245 (1999)
126. Y Kawamura, Y Wada, S Yanagida *Jpn. J. Appl. Phys., Part 1* **40** 350 (2001)
127. Z Ahmed, K Iftikhar *Polyhedron* **85** 570 (2015)
128. F Zang, T-C Sum, F Zhu, Z-R Hong, X Sun, W L Li, C H A Huan *J. Lightwave Technol.* **27** 1522 (2009)
129. Z Li, J Yu, L Zhou, R Deng, H Zhang *Inorg. Chem. Commun.* **12** 151 (2009)
130. B S Harrison, T J Foley, A S Knefely, J K Mwaura, G B Cunningham, T -S Kang, M Bouguettaya, J M Boncella, J R Reynolds, K S Schanze *Chem. Mater.* **16** 2938 (2004)
131. L-J Xu, G-T Xu, Z-N Chen *Coord. Chem. Rev.* **273** – **274** 47 (2014)
132. Z-Q Chen, F Ding, Z-Q Bian, C-H Huang *Org. Electron.* **11** 369 (2010)
133. H Wei, G Yu, Z Zhao, Z Liu, Z Bian, C Huang *Dalton Trans.* **42** 8951 (2013)
134. T V Balashova, N A Belova, M E Burin, D M Kuzyaev, R V Rumyantcev, G K Fukin, A P Pushkarev, V A Ilichev, A F Shestakov, I D Grishin, M N Bochkarev *RSC Adv.* **4** 35505 (2014)
135. L H Slooff, A Polman, F Cacialli, R H Friend, G A Hebbink, F C J M van Veggel, D N Reinhoudt *Appl. Phys. Lett.* **78** 2122 (2001)
136. A O'Riordan, E O'Connor, S Moynihan, P Nockemann, P Fias, R Van Deun, D Cupertino, P Mackie, G Redmond *Thin Solid Films* **497** 299 (2006)
137. B Chu, W L Li, Z R Hong, F X Zang, H Z Wei, D Y Wang, M T Li, C S Lee, S T Lee *J. Phys. D: Appl. Phys.* **39** 4549 (2006)
138. R Deng, L Zhou, M Song, Z Hao, H Zhang *Sci. Adv. Mater.* **5** 1556 (2013)
139. M A Katkova, V A Ilichev, A N Konev, M N Bochkarev *Russ. Chem. Bull., Int. Ed.* **57** 2281 (2008)
140. F X Zang, W L Li, Z R Hong, H Z Wei, M T Li, X Y Sun, C S Lee *Appl. Phys. Lett.* **84** 5115 (2004)
141. K S Schanze, J R Reynolds, J M Boncella, B S Harrison, T J Foley, M Bouguettaya, T-S Kang *Synth. Met.* **137** 1013 (2003)
142. M Pollnau, R Spring, C Ghisler, S Wittwer, W Luthy, H P Weber *IEEE J. Quantum Electron.* **32** 657 (1996)
143. R J Curry, W P Gillin *Appl. Phys. Lett.* **75** 1380 (1999)
144. R J Curry, W P Gillin *Synth. Met.* **111** – **112** 35 (2000)
145. R J Curry, W P Gillin, A P Knights, R Gwilliam *Opt. Mater.* **17** 161 (2001)
146. R G Sun, Y Z Wang, Q B Zheng, H J Zhang, A J Epstein *J. Appl. Phys.* **87** 7589 (2000)
147. F Wei, Y Z Li, G Z Ran, G G Qin *Opt. Express* **18** 13542 (2010)
148. D Zhang, W Li, B Chu, X Li, L Han, J Zhu, T Li, D Bi, D Yang, F Yan, H Liu, D Wang *Appl. Phys. Lett.* **92** 093501 (2008)
149. P Martín-Ramos, C Coya, V Lavín, I R Martín, M Ramos Silva, P S Pereira Silva, M García-Vélez, A L Álvarez, J Martín-Gil *Dalton Trans.* **43** 18087 (2014)
150. C Coya, A L Álvarez, M García-Vélez, P Martín-Ramos, M Ramos-Silva, C Zaldo, P Chamorro-Posada, J Martín-Gil *Ópt. Pura Apl.* **46** 257 (2013)
151. P Martín-Ramos, M Ramos Silva, C Coya, C Zaldo, A L Álvarez, S Álvarez-García, A M Matos Beja, J Martín-Gil *J. Mater. Chem. C* **1** 2725 (2013)
152. P Martín-Ramos, C Coya, A L Álvarez, M Ramos Silva, C Zaldo, J A Paixão, P Chamorro-Posada, J Martín-Gil *J. Phys. Chem. C* **117** 10020 (2013)
153. Z Li, J Yu, L Zhou, H Zhang, R Deng, Z Guo *Org. Electron.* **9** 487 (2008)
154. C H Cheng, J Wang, Z J Du, S H Shi, Z Q Fan, D F Geng, R S Shen, Y M Luo, G T Du *J. Lumin.* **130** 2293 (2010)
155. M A Katkova, V A Ilichev, A N Konev, I I Pestova, G K Fukin, M N Bochkarev *Org. Electron.* **10** 623 (2009)
156. F X Zang, Z R Hong, W L Li, M T Li, X Y Sun *Appl. Phys. Lett.* **84** 2679 (2004)
157. Z Hong, W Li, D Zhao, C Liang, X Liu, J Peng, D Zhao *Synth. Met.* **104** 165 (1999)
158. O M Khreis, W P Gillin, M Somerton, R J Curry *Org. Electron.* **2** 45 (2001)
159. E V Baranov, G K Fukin, T V Balashova, A P Pushkarev, I D Grishin, M N Bochkarev *Dalton Trans.* **42** 15699 (2013)
160. B S Harrison, T J Foley, M Bouguettaya, J M Boncella, J R Reynolds, K S Schanze, J Shim, P H Holloway, G Padmanaban, S Ramakrishnan *Appl. Phys. Lett.* **79** 3770 (2001)
161. T-S Kang, B S Harrison, M Bouguettaya, T J Foley, J M Boncella, K S Schanze, J R Reynolds *Adv. Funct. Mater.* **13** 205 (2003)
162. Z R Hong, C J Liang, R G Li, D Zhao, D Fan, W L Li *Thin Solid Films* **391** 122 (2001)
163. G A Crosby, M Kasha *Spectrochim. Acta* **10** 377 (1958)
164. W D Horrocks, J P Bolender, W D Smith, R M Supkowski *J. Am. Chem. Soc.* **119** 5972 (1997)

165. T Ala-Kleme, K Haapakka, M Latva *Anal. Chim. Acta* **395** 205 (1999)
166. Z Li, H Zhang, J Yu *Thin Solid Films* **520** 3663 (2012)
167. B L Reid, S Stagni, J M Malicka, M Cocchi, G S Hanan, M I Ogden, M Massi *Chem. Commun*. **50** 11580 (2014)
168. M N Bochkarev *Coord. Chem. Rev*. **248** 835 (2004)
169. N B Mikheev, L N Auerman, I A Rumer, A N Kamenskaya, M Z Kazakevich *Russ. Chem. Rev*. **61** 990 (1992)
170. A Beeby, S Faulkner, J A G Williams *J. Chem. Soc., Dalton Trans*. 1918 (2002)
171. T Lazarides, M A H Alamiry, H Adams, S J A Pope, S Faulkner, J A Weinstein, M D Ward *Dalton Trans*. 1484 (2007)
172. M E Burin, T V Balashova, D L Vorozhtsov, A P Pushkarev, M A Samsonov, G K Fukin, M N Bochkarev *Russ. J. Coord. Chem*. **39** 667 (2013) [*Koord. Khim*. **39** 554 (2013)]
173. A P Pushkarev, V A Ilichev, T V Balashova, A N Yablonskiy, B A Andreev, M N Bochkarev *Synth. Met*. **203** 117 (2015)